2018

Crossing Three Deep Valleys: The Sedimentology, Geomorphology and Palaeo-environments of Thirlmere Lakes, N.S.W

E J. Barber

Crossing Three Deep Valleys: The Sedimentology, Geomorphology and Palaeo-environments of Thirlmere Lakes, N.S.W

Abstract

The Thirlmere Lakes are a series of five freshwater lakes that reside in ancient, uplifted river meander situated on the eastern margins of the Greater Blue Mountains World Heritage Area near Picton, NSW. These lakes are important ecologically and recreationally, and are generally viewed as being perennially inundated. In the last few decades, however, there has been an observable drying trend in the lakes. This offers an important question; is the recent water loss unprecedented or is it part of natural variability experienced by the lakes? This honours thesis aimed to assess past hydrological variability within one of the Thirlmere Lakes, Lake Couridjah, in order to put the recent trend of water loss into a longer-term context of how the lakes respond to change.

This aim was achieved by broadly investigating the palaeo-environments within Lake Couridjah, through examining the sedimentary characteristics and stratigraphic relationships in and between Lake Couridjah and the neighbouring Lake Baraba. This included examining the age, grain size, organic content, elemental composition and carbon isotopes of the sediments. The results of these analyses were then synchronously compared along with other palaeo-environmental research from south eastern Australia.

The results of this study found that within the past ~100 ka, Lake Couridjah has experienced significant hydrological change. However, throughout the Holocene (~12 - 0 ka), there was a marked shift into sustained lacustrine conditions resulting in near constant peat formation in Lake Couridjah. While there is some evidence for lake drying during the Holocene, these events are only minimal and do not show complete drying of the whole lake. Furthermore, this study found that lakes Couridjah and Baraba appear to have experienced different hydrological and sedimentological processes through time, which suggests that despite their close proximity, these lakes can operate as independent water bodies. These findings highlight Thirlmere Lakes are unique within the Sydney Basin, as well as a potentially important palaeo-environmental archive for south eastern Australia.

Degree Type

Thesis

Degree Name

BSci Int Hons

Department

School of Earth & Environmental Sciences

Advisor(s)

Tim Cohen

Keywords

Thirlmere Lakes, Stratigraphy, Sedimentology, Palaeoclimatology

UNIVERSITY OF WOLLONGONG

Crossing Three Deep Valleys:
The Sedimentology, Geomorphology and Palaeo-environments of Thirlmere Lakes, N.S.W

A thesis submitted in (partial) fulfilment of the requirements for the award of the degree of

INTERNATIONAL BACHELOR OF SCIENCE

from

The University of Wollongong

By

Emily Joan Barber

School of Earth & Environmental Sciences, Faculty of Science, Medicine and Health

May, 2018

The information in this thesis is entirely the result of investigations conducted by the author, unless otherwise acknowledged, and has not been submitted in part, or otherwise, for any other degree or qualification.

Emily Barber

9th May 2018

Cover image: Lake Werri Berri in bloom, taken by the author December 2016

ACKNOWLEDGMENTS

I would like to sincerely thank my two supervisors; Tim Cohen and Sam Marx.

Tim – thank you for your continued support and encouragement. Your readiness and enthusiasm for the project from the very beginning is greatly appreciated.

Sam – thank you for all your insightful feedback, willingness to help and encouragement.

Thank you both for your constant guidance and wisdom, as well as showing me the ropes of research and sparking my interest in palaeo-environmental studies.

Also, thank you to Brent Peterson for your resourcefulness and support in the field; your many hours extracting cores and wading through turbid lake water is greatly appreciated.

Patricia Gadd, from ANSTO, thank you sincerely for your quick delivery of the ITRAX data despite problems with the core scanner. Jonathan Tyler, University of Adelaide, thank you for assistance with the stable isotope dataset and insightful thoughts.

From SEES, thank you to Marina McGlinn for your constant support and 'check-ins'. Brian Jones, thank you for your help throughout the year.

A special thanks to my parents and siblings for their continued love and support. Mum, thank you for your help with formatting and presentation, you saved me many frustrating hours of work. Dad, thanks for your efforts with the field work.

To all my friends who have been there but have not received a special mention, thanks for your support and understanding.

Lastly, Lloyd – thank you for your love and encouragement and for being with me every step of the way. Your generous hours spent in the field, proof reading and assistant bringing the thesis together are greatly appreciated. Thank you for being my point of stability, I love you, and I couldn't have done it without you.

ABSTRACT

The Thirlmere Lakes are a series of five freshwater lakes that reside in ancient, uplifted river meander situated on the eastern margins of the Greater Blue Mountains World Heritage Area near Picton, NSW. These lakes are important ecologically and recreationally, and are generally viewed as being perennially inundated. In the last few decades, however, there has been an observable drying trend in the lakes. This offers an important question; is the recent water loss unprecedented or is it part of natural variability experienced by the lakes? This honours thesis aimed to assess past hydrological variability within one of the Thirlmere Lakes, Lake Couridjah, in order to put the recent trend of water loss into a longer-term context of how the lakes respond to change.

This aim was achieved by broadly investigating the palaeo-environments within Lake Couridjah, through examining the sedimentary characteristics and stratigraphic relationships in and between Lake Couridjah and the neighbouring Lake Baraba. This included examining the age, grain size, organic content, elemental composition and carbon isotopes of the sediments. The results of these analyses were then synchronously compared along with other palaeo-environmental research from south eastern Australia.

The results of this study found that within the past ~100 ka, Lake Couridjah has experienced significant hydrological change. However, throughout the Holocene (~12 - 0 ka), there was a marked shift into sustained lacustrine conditions resulting in near constant peat formation in Lake Couridjah. While there is some evidence for lake drying during the Holocene, these events are only minimal and do not show complete drying of the whole lake. Furthermore, this study found that lakes Couridjah and Baraba appear to have experienced different hydrological and sedimentological processes through time, which suggests that despite their close proximity, these lakes can operate as independent water bodies. These findings highlight Thirlmere Lakes are unique within the Sydney Basin, as well as a potentially important palaeo-environmental archive for south eastern Australia.

TABLE OF CONTENTS

ACKNOWLEDGMENTS……i

ABSTRACT……ii

TABLE OF CONTENTS……iii

LIST OF FIGURES……vii

LIST OF TABLES……ix

1. INTRODUCTION……1

1.1 Context……1

1.2 Aims and Objectives……3

1.3 Thesis Outline and Scope……4

2. LITERATURE REVIEW……5

2.1 Lake Geomorphology and Sedimentology……5

2.1.1 Lake Dynamics……5

2.1.2 Lake Sediments……7

2.2 Peat forming environments: peatlands and upland swamps ……9

2.2.1 Peatlands……9

2.2.2 Upland Swamps……13

2.2.3 Lake and Peatland Evolution……15

2.3 Lakes as Palaeo-environmental Archives……17

2.3.1 Stable carbon ($\delta^{13}C$) and nitrogen ($\delta^{15}N$) isotopes from lake sediments……18

2.3.2 Late Quaternary environmental change in southeast Australia……20

3. REGIONAL SETTING……23

3.1 Study Area……23

3.2 Geology of the Thirlmere Lakes……24

3.2.1 Evolution of the lake sequence……25

3.3 Modern Catchment Geomorphology and Sedimentology……25

3.3.1 Alluvial fans……25

3.3.2 Stratigraphy……27

3.3.3 Sedimentation rates……29

3.4 Climate and Hydrology……30

3.4.1 Lake hydrology……30

3.4.2 The effect of sills on lake hydrology……31

3.4.3 Limnology of the Thirlmere Lakes……32

3.4.4 Rainfall variability and its impact on lake levels……33

3.4.5 Groundwater……34

3.5 Flora and Fauna……35

4. METHODS……38

4.1 Field Methods……38

4.1.1 Site selection and sub-surface data collection……38

4.2 Laboratory Analyses……42

4.2.1 Subsampling……42

4.2.2 Loss-on-Ignition (LOI) analysis……42

4.2.3 Methods of grain size determination in lacustrine sediments……43

4.2.4 Elemental composition……44

4.2.5 Stable δ13C and δ15N isotopes, %C, %N and C: N……44

4.2.6 Accelerated Mass Spectrometry (AMS) Carbon-14 dating……45

5. RESULTS……46

5.1 Core Descriptions and Sedimentology……46

5.1.1 Primary cores……48

5.1.2 Secondary cores……59

5.1.3 Alluvial fan surface sediments……61

5.2 Radiocarbon Dating……62

5.3 Lake Couridjah Trace Element Geochemistry……63

5.3.1 Catchment erosion proxies……63

5.3.2 Changing hydrological and chemical conditions inferred from elemental data…67

5.4 Stable carbon ($\delta^{13}C$) and nitrogen ($\delta^{15}N$) isotopes from Lake Couridjah……69

5.4.1 Stable carbon ($\delta^{13}C$) and nitrogen ($\delta^{15}N$) isotopes from modern soil and living vegetation ……73

6. DISCUSSION……75

6.1 δ13C values and C:N ratios……75

6.1.1 Sources of organic matter……78

6.1.2 Decomposition……78

6.1.3 Water stress/availability……79

6.1.4 Summary……80

6.2 Chronology and Stratigraphic Relationships……80

6.2.1 Sill and lake stratigraphy……82

6.2.2 Chronostratigraphy……82

6.3 Facies Interpretation……84

6.3.1 Primary Unit 1: Sill Deposits……85

6.3.2 Primary Unit 2: Lacustrine Deposits ……..86

6.4 Stratigraphy and groundwater and its implications for connectivity between Lake Couridjah and Lake Baraba……90

6.5 Palaeo-environments and South-east Australian Context……92

6.6 Limitations……95

7. CONCLUSION……97

7.1 Summary……97

7.2 Future Research……99

REFERENCES……101

APPENDIX A – Lake level and rainfall graphs

APPENDIX B – Core logs, grain size data and particle size distribution

APPENDIX C – LOI analysis

APPENDIX D – Radiocarbon dating reports

APPENDIX E – Stable C and N isotope data

APPENDIX F – ITRAX data

LIST OF FIGURES

Figure 2.1	Moore's (1995) classification of peatlands	12
Figure 2.2	Distribution of THPSS across NSW	14
Figure 3.1	The position of Thirlmere Lakes within the Sydney Basin	23
Figure 3.2	Geology of Thirlmere Lakes	24
Figure 3.3	The location of the alluvial fans impinging on the valley of Thirlmere Lakes	26
Figure 3.4	Deep borehole stratigraphy of the Thirlmere Lakes	29
Figure 3.5	Lake classification. From Bowler (1981)	31
Figure 3.6	Relationship between lake levels and rainfall. From Schadler and Kingsford (2016)	33
Figure 3.7	Groundwater schematic of the Thirlmere Lakes system	35
Figure 3.8	Schematic of general vegetation assemblage on lake margins at Thirlmere Lakes.	36
Figure 3.9	View of *Lepironia Articulata* from Lake Werri Berri eastern shore	37
Figure 4.1	Exact locations of all cores obtained during this study	38
Figure 4.2	Positions of surface sample collection across the LC-LB transect	39
Figure 4.3	Set-up used for the extraction of LC2 (Lake Couridjah core)	41
Figure 5.1	Stratigraphic findings of all cores in this study	47
Figure 5.2	Sedimentary details of the core LC2.	48
Figure 5.3	Grain size results for pre-treatment A and pre-treatment B	49
Figure 5.4	Particle size distribution for 0.3 m depth and core photo (LC2)	50
Figure 5.5	Particle size distribution for 2.95 m depth and core photo (LC2)	51
Figure 5.6	Particle size distribution for 6.68 m depth and core photo (LC2)	53

Figure 5.7	Sedimentary details of the core LC1.	54
Figure 5.8	Particle size distribution for 1 m depth and core photo (LC1)	55
Figure 5.9	Particle size distribution for 3.8 m depth and core photo (LC1)	56
Figure 5.10	Sedimentary details of the HA1 auger hole.	57
Figure 5.11	Particle size distribution for 0.75 m depth and core photo (HA1)	58
Figure 5.12	Particle size distribution for 4.1 m depth and core photo (HA1)	59
Figure 5.13	The upper 4.55 m of the HA2 core.	60
Figure 5.14	Elemental analysis of LC2 including geochemical profiles of Si, Al, Ti, Si:Ti, Ca:Ti, Sr:Ca and Fe:Mn	65
Figure 5.15	Elemental analysis of LC2 including geochemical profiles of Sr:Zr, Sr:Rb and Ba:Zr	66
Figure 5.16	Scatterplots A. $\delta^{15}N$ vs C:N, B. $\delta^{15}C$ vs C:N, C. %N vs %C and D. $\delta^{15}C$ vs $\delta^{15}N$ from Lake Couridjah centre (core LC2)	70
Figure 5.17	Stable isotope data for Lake Couridjah with plotted $\delta^{15}N$, $\delta^{13}C$, C/N, %N and %C against LC2 core depth	71
Figure 6.1	General ranges of δ13C values and C:N ratios for varying organic sources. From Lamb *et al.*, (2006)	75
Figure 6.2	The δ13C values and C:N ratios for the sediments within Lake Couridjah (core LC2), living vegetation and modern soil	77
Figure 6.3	Illustration of the stratigraphic interpretation of the core data	81
Figure 6.4	Age – depth relationship of the core LC2	83

LIST OF TABLES

Table 2.1	Various classifications of peatlands	11
Table 3.1	Key stratigraphical findings from previous studies at Thirlmere Lakes	28
Table 4.1	Details of the cores in this study	42
Table 5.1	Summary of radiocarbon results for Lake Couridjah and the Lake Couridjah – Lake Baraba sill	68
Table 6.1	The approximate ages for the stratigraphic units in the LC2 core	84

1. INTRODUCTION

1.1 Context

Wetlands and lakes are fundamental and indispensable environments, contributing to a broad array of ecosystem services that benefit the wellbeing of both natural and anthropogenic landscapes (Costanza *et al.,* 1997; Ramsar, 2018). Ramsar (2018) broadly define wetlands as landscapes where the existence of water acts as the primary regulator of environmental processes. This includes a large variety of environments ranging from all lake and river types, coastal lagoons and mangroves to swamps, peatlands and even man-made reservoirs. Not only do wetlands function to store and purify freshwater, mitigate floods, recharge groundwater systems and retain nutrients, but they are also highly productive systems, acting as critical habitat refugia for >40% of the world's flora and fauna (Opperman *et al.,* 2010; Hu *et al.,* 2017).

Globally, wetland habitat covers up to 29.83 million km^2, 5 % of which exists in Oceania (Hu *et al.,* 2017). Australia, the driest continent outside of Antarctica, has relatively few (non-coastal) wetlands, many of which are subject to long periods of drying where they do not function as typical wetlands (Whinam *et al.,* 2003; Bridgman and Timms, 2012). Despite this, permanent lake systems exist infrequently along the humid to temperate eastern Australian coastline, and are critical ecologically and hydrologically. For example, Little Llangothlin Lagoon on the New England Tablelands is a valuable freshwater resource and drought refuge for many waterbird species, as well as a cradle for remnant native vegetation amongst cleared agricultural country (Woodward *et al.,* 2014; Ramsar, 2016). Yet, fundamental sites as such are increasingly threatened by anthropogenic forces, such as water extraction, inducing changes in hydrology and increasing the length dry periods (Brinson and Malvarez, 2002).

Within the Sydney Basin, which includes the Greater Blue Mountains World Heritage Area, a number of critical wetlands have been impacted by human activity. For example; peat mining in the late 1990's resulted in the partial collapse of the environmentally significant Wingecarribee swamp, changing the peatland form from extensive and intact to sunken and fragmented with vastly reduced water filtering capacities (Whinam *et al.,* 2003). Wetlands within the Sydney Basin are also being impacted by subsidence associated with longwall mining (Young, 2017). This has resulted in bedrock cracking, which in turn causes water loss

from streams and large tributaries within Cordeaux and Dendrobium coalfields (South32 Annual FY, 2017). Of particular concern are changes to the upland swamps that act as headwater systems for these streams. These have been regarded as “the canaries above the mines”; usually providing the initial evidence of water loss from the system (Young, 2017).

Thirlmere Lakes, a series of five elongated lakes in an upland fluviatile system situated on the eastern margins of the Greater Blue Mountains World Heritage Area, are amongst the most important wetlands within the Sydney Basin. They have been listed in the Directory of Important Wetlands in Australia, meeting five of six directory criteria relating to their hydrological significance and ability to provide a refuge and nursery habitat for animal taxa (Department of the Environment and Energy, 2010). In addition, the lakes are valued recreationally and aesthetically. Thirlmere Lakes are generally regarded as being perennially inundated, although have been seen dry during extreme droughts (OEH, 2012). However, throughout the past few decades there has been an observable drying trend. While this trend may not seem unprecedented due to the lakes past fluctuations, it apparently defies the usual close correlation between the systems surface water levels and regional rainfall patterns (Kingsford and Schadler, 2016). Despite high rainfall throughout 2010 and 2011, Thirlmere Lakes struggled to fully recover its water levels (Kingsford and Schadler, 2016; BOM, 2018). This drying has sparked increasing community concern about the long-term future of the lakes. In particular, concern has been centred on what role longwall coal mining (nearest panel 800 m from the lakes) is playing in affecting the hydrology of Thirlmere Lakes.

A lot of new knowledge is required to holistically understand the Thirlmere Lakes system, and disentangle derived threats from potential ones (OEH, 2016). Despite their significance, little is definitively known about the palaeo-history of Thirlmere Lakes, in particular regard to their hydrology. The recent changes to the lakes offer an important question; is the recent water loss unprecedented or is it part of natural variability experienced by the lakes? Other south eastern Australian lakes display long-term wetting and drying patterns (Harrison, 1993), implying that Thirlmere Lakes would likely experience similar variability. The information regarding Thirlmere Lake’s environmental histories and thresholds is most likely recorded in its lacustrine sediment record. That is, general subsurface sediment characteristics (i.e., grain size, sorting, total organic content and mineralogy) can indicate depositional history and a potential history of wetting and drying. In addition, the unique geologic origin of Thirlmere

Lakes suggests they may have been geomorphically stable since 15 Ma and contain 50 m of unconsolidated fluvial and lacustrine sediment (Vorst, 1974; Timms, 1992). This qualifies the lakes as potentially important palaeo-environmental archives, representing one of the few systems that could reflect Quaternary climate change in temperate south-eastern Australia.

1.2 Aims and Objectives

The aim of this project is to assess past hydrological variability within one of the Thirlmere Lakes, Lake Couridjah, in order to put recent changes into a longer-term context of how the Thirlmere Lakes respond to climate change. This will be achieved by examining sedimentological, geomorphologic and palaeo-environmental characteristics in Lake Couridjah, as well as between Lake Couridjah and the neighbouring Lake Baraba.

Specifically, the objectives of this project are to:

1. Assess palaeo-environments and long-term lake dynamics based on sedimentological data;
2. Investigate the subsurface characteristics and stratigraphic relationships in and between lakes Couridjah and Baraba;
3. Evaluate the geomorphological controls that act to physically separate these lakes.

The anticipated outcomes of this honours thesis will provide a robust palaeo-environmental assessment using the sedimentology, geomorphology and palaeo-environments to elucidate past lake levels and potential drying events. It will also strengthen and build upon previous models of lake-floor sedimentology and stratigraphy, namely the pioneering work and fundamental relationships established by Vorst (1974). Sandy alluvial fans have been viewed as the main geomorphic control of Thirlmere Lakes (Timms, 1992), and this thesis will comment as to what extent and influence these alluvial fans have on the lake sediments.

Increased knowledge surrounding the stratigraphy and sub-surface characteristics of Thirlmere Lakes will help guide future research in understanding sub-surface flow pathways, surface water – groundwater interactions and general groundwater catchment boundaries (OEH, 2016). Overall, anticipated results include: improved stratigraphy, evidence of past drying, a preliminary chronology and a legacy for ongoing research. Increased general

knowledge surrounding the geomorphic and climatic controls of lacustrine environments is another important outcome.

This project was developed in collaboration with the broader NSW Office of Environment and Heritage Thirlmere Lakes Research Project (TLRP), to form the foundation of a three-year research program which will involve groundwater and surface water modelling, isotopic analysis and deep geologic drilling.

1.3 Thesis Outline and Scope

Following this introduction, this thesis presents a broad review of the literature surrounding lake processes, sediments and responses to environmental change. Chapter 3 outlines the study area and presents previous research specific to Thirlmere Lakes. In Chapter 4, the processes of data collection and analysis are detailed. Following this, Chapter 5 presents the results of this study, in terms of core descriptions, radiocarbon dating, elemental analysis and stable C and N isotope results. Chapter 6 then provides a discussion of the acquired results in relation to past research, the broader context of south eastern Australia and the limitations of the study. Chapter 7 provides a conclusion to the study and recommends topics of future research surrounding Thirlmere Lakes.

2. LITERATURE REVIEW

In this chapter, an overview of lake processes and responses to environmental change will be provided, in order to broadly assist in interpretation of subsequent results. This will involve a reviewal of; (a) general lake dynamics and sedimentology, as well as associated geomorphology and climate, (b) peat-forming environments, and (c) palaeo-environmental indicators for change. Examples from within Australia are provided where possible.

2.1 Lake Geomorphology and Sedimentology

Mainland Australia has relatively few lakes, and most are shallow and ephemeral, experiencing completely dry conditions during long-lasting droughts (Bridgman and Timms, 2012). Despite their limited number, Australian lakes have a variety of origins; Timms (1992) categorized Australian lakes based on their formation into tectonic lakes, volcanic lakes, lakes formed by landslides, glacial lakes, fluvial lakes, solution lakes, lakes formed by wind action and coastal lakes. The lack of freshwater lakes in Australia is not just explained by the predominantly arid climate, as many coastal areas are humid with high rainfall (BOM, 2018). The existence and dynamics of lakes is therefore closely related to Australia's geomorphology, including a limited history of glaciation (Chang *et al.*, 2014), and relative tectonic stability.

2.1.1 Lake Dynamics

Lake productivity and hydrology

Lake productivity, that is, the difference between gross primary production (inputs) and total respiration (outputs), influences the physical expression of lakes and is intricately connected to carbon and nutrient cycles (Tranvik *et al.*, 2009; Mitsch *et al.*, 2013). Lake water naturally shows vertical stratification; a process that also affects the productivity of lakes, and is largely controlled by different water densities influenced by the imposing atmospheric temperature and seasonal changes in wind speed (Boehrer and Schultze, 2008; Magee *et al.*, 2017). Lake stratification can be generalised into three distinct layers; the *epilimnion*, a surface zone of increase water temperature, lower density and higher dissolved oxygen due to mixing; the *metalimnion*, an intermediate zone of radical temperature and physiochemical change; and the *hypolimnion*, which has characteristically cooler and denser conditions with depleted dissolved oxygen in deeper water (Boehrer and Schultze, 2008). During warmer periods, lake stratification can become very pronounced, whereas in colder conditions, the density of the

epilimnion decreases relative to the density of the hypolimnion (i.e., it cools) and the lake is generally more mixed.

Water temperatures and stratification are significant regulators of ecological and water quality dynamics within lakes (Magee *et al.*, 2017). Resultantly, primary production and nutrient cycling is greatly mediated by vertical mixing, sometimes more so than external nutrient influxes (Bloesch *et al.*, 1977). Nutrient inputs to lakes can come from precipitation, run-off and N-fixation, and loses can occur due to sedimentation, which decreases the amount of particulate nutrients, and hydrologic outflow, which consists of both particulate nutrients and dissolved nutrients.

Lake dynamics and geomorphology

Lake physiochemical dynamics, such as thermal stratification and mixing regimes, are largely governed by external factors such as the morphology and evolution of lake basins. Topographically closed basin morphologies, such as some crater lakes and other uplifted water bodies, are particularly sensitive to climate forcing as their hydrodynamics are primarily governed by precipitation and evaporation, rather than predominantly groundwater (Barr *et al.*, 2014; Woodward, 2014). Therefore, conditions within lakes are subject to change as these parameters change (Chang *et al.*, 2014). For example, Magee and Wu (2017) found that morphometry (i.e., lake depth and surface area) plays a significant role in lake-wide stratification processes, surface heat flux and resistance to mixing. Heat is more easily transferred through the entire water column in shallow lakes (<3 m depth) and thus they respond more completely to changes in climatic conditions. A large fetch also increases the degree of wind-driven mixing and heat transfer to bottom waters, and so changing conditions such as increased windiness can significantly cool lake water temperatures (Magee and Wu, 2017). Deep lakes are more stratified, particularly during warm periods, which increases anoxia in the bottom waters (Richardson *et al.*, 2017). Consequently, differences in temperature dynamics greatly impacts the biotic expression of lakes. Shallow lakes, due to their superior ability to transfer heat, can at times favour cyanobacterial algal blooms and transition into a more eutrophic state, whereas deeper lakes have a greater presence of stratification which regulates predator-prey interactions through the vertical movement of zooplankton and phytoplankton, thus hosting a more mesotrophic state (Richardson *et al.*, 2017).

In light of the above processes of stratification and mixing, it's not surprising that most mainland Australian lakes, being shallow and ephemeral, are eutrophic to hypereutrophic (Chang *et al.*, 2014). The general eutrophic state of Australian lakes is often further enhanced by fertiliser run-off, where nitrogen and phosphorous nutrients are easily carried into lakes (Burkitt, 2014). Yet, mesotrophic lake conditions in Australia do exist in regions such as the Kosciuszko alpine area and within some crater lakes in Northern Queensland (Chang *et al.*, 2014). This highlights that although Australian lakes are relatively limited in number when compared internationally, they are indeed diverse in their trophic status.

2.1.2 Lake Sediments

Most lakes accumulate sediments through time; the rate of which is broadly governed by local climate, lake morphology and catchment geomorphology (Timms, 1992). Lacustrine sediments can be generally classified, based on the origin of the sediment, into three main categories: autochthonous sediments are sediments native to their location (e.g., carbonate precipitation in a lake), allochthonous sediments refer to sediments physically transported away from the place of their formation (e.g., fluvially-transported clastic material in a lake), and para-autochthonous sediments which resemble mixed characteristics (Rubensdotter and Rosqvist, 2009; Huang *et al.*, 2017). Changes in the ratio of allochthonous and autochthonous sediments in lakes is complex yet offers an understanding of the physical and biological mechanisms behind lake sedimentation (Rubensdotter and Rosqvist, 2009).

Sediment input derived from stream, river or overland inflows can deliver coarse grained, minerogenic sediment into the lake, which disperses and is deposited in accordance with physical parameters such as sediment size, lake depth, water density and wave action (Timms, 1992). Generally, coarse material is deposited close to the lake shoreline and fine terrigenous clays and silts depart from the coarse fraction and settle out in a trend that fines towards the lake centre (Nelson and Lister, 1995). During periods of decreased water levels, coarser grained sediment can travel further towards to the lake centre due to the relative shift in the position of the shoreline. Therefore, low lake levels may be depicted by a coarsening of clastic texture, with fine grained deposits signifying higher lake levels. Sometimes during hyperpycnal inflows when the water entering the lake basin is denser (i.e., colder or laden with fine sediment), a zone of sediment mixing is created at the lake margin and the denser

incoming water flows under the standing water, readily eroding pervious lake margin material and forming turbidite deposits (Timms, 1992; Osleger *et al.*, 2009).

Closed lake systems with few inflowing streams can predominantly exhibit autochthonous organic sediments, closely reflecting the biological character of the lake. That is, organic matter in lakes comprises of a complex mixture biochemicals (i.e., proteins, lipids and carbohydrates) derived from organisms previously living in the lake (Meyers and Ishiwatari, 1993). Therefore, changes in the community structure of lake biota produce variations in the types of organic matter that is deposited as autochthonous lake sediment.

In general, however, the spatial variability of sediment textures throughout lacustrine sediment can be used to infer shoreline proximity, sediment transport dynamics and biological processes operating within the lake (Nelson and Lister, 1995; Mishra *et al.*, 2014).

Peat Formation and Peat Types in Lakes

Peat accumulates when the rates of organic matter deposition exceeds that of microbial decomposition (Hope *et al.*, 2009; Cowley *et al.*, 2016). In lakes, peat is likely to form in shallow basins with high nutrient levels, discontinuous drainage and thus a constant presence of water. This promotes prolonged periods of waterlogging and complete saturation of sediments, which furthers the system's capacity to store organic material (Cowley *et al.*, 2016). Associated anaerobic and acidic conditions hinder the breakdown of plant material, and the relatively porous and light matrix of peat encourages even more water retention (Hope *et al.*, 2009; Fryirs *et al.*, 2014). Consequently, the mechanisms governing the formation of peat in lakes differ greatly to the previously mentioned processes of minerogenic and fine organic material deposition. Obviously, the formation of peat is closely related to peatland environments and not lakes. However, some lake systems, such as Thirlmere Lakes, contain prime peat-forming conditions and thus may exist somewhere on the geomorphic spectrum between a lake and a peatland. Other examples of lacustrine-mire systems with limited drainage and high water tables, such as the Tasik Bera mire in Malaysia, are said to have formed in response to either tectonic activity in the basin, or the accumulation of organic matter damming the outflow point (Phillips and Bustin, 1998).

Peat can be subdivided into different classes based on composition, including fibric peat, hemic peat and sapric peat (The Australian Soil Classification, 2018). Sapric peat is strongly

decomposed with no identifiable intact plant remnants, and remains a dark, oozing mud upon squeezing a sample between fingers (Young, 2017). Hemic peat may contain some recognisable plant matter, and expresses water, laden with mud, when compressed. Fibric peat, however, is characteristic of intact and undecomposed plant material, yielding predominantly clear water. These types of peat differ in their vertical positioning within a peatland; fibric peat is predominantly found in the upper vegetated layers (i.e., in the acrotelm), while hemic and sapric peat exist in the deeper, more anoxic layers (i.e., in the catotelm). The acrotelm and catotelm of peatlands are further discussed in section 2.2.1. Therefore, the portion of fibrous peat typically decreases with depth in peat-forming systems (Hope *et al.*, 2009). However, Hope *et al.*, (2009) remarks that fibrous peat horizons can occur underneath humic ones and Vorst (1974) found a strongly humified peat layer beneath clay and sand at Thirlmere Lakes, both results suggesting that periods of rapid growth of peat can occur within the peatland complex in wet-dry intervals (Kalnina *et al.*, 2014).

2.2 Peat forming environments: peatlands and upland swamps

Environments in which the formation of peat prevails have been studied over many decades. There is great complexity in the literature in terms of classification of peat forming environments, undoubtedly due to their highly variable nature throughout different global systems. For the means of this honours thesis, 'peatland' as well as 'upland swamp' environments will be broadly discussed because of their presence in the literature and relevance to Australian peat forming systems.

2.2.1 Peatlands

Peatlands cover a limited 5% of the Earth's surface and are often perceived as biologically harsh environments due to waterlogging, generally low nutrient levels and acidic conditions in an anaerobic setting (Pemberton, 2005; Fryirs *et al.,* 2014). Nevertheless, not only do they serve as important habitats and regulators of water quality, their ability to slowly accumulate peat provides a significant carbon store as well as a powerful archive for past vegetation and fire regimes (Hope *et al.,* 2012). Indeed, the discovery of a bog body or 'Lindow Man', with intact hair and nails, in the United Kingdom during the 1980's is testimony the high preservation capacity of organic matter in some peatlands (Pemberton, 2005).

There are a number of definitions and classifications of a 'peatland'. Specific classification frameworks have been developed and applied on a case-by-case basis to particular regions. Furthermore, the term 'peatland' and 'mire' are relatively interchangeable, with environments described as bogs, fens, swamps, moors and marshes also falling under the category of 'peatlands' but usually differentiated according to vegetation, hydrology and water chemistry (Moore, 1995; National Wetlands Working Group, 1997; Hope *et al.,* 2009, 2012). Table 2.1 indicates differing classification schemes used for peatlands throughout the world and demonstrates that study area, as well as research aims and context, are highly important in determining which definition has been used (Inisheva, 2006). For example, the distinct Temperate Highland Peat Swamps on Sandstone (THPSS) of south-eastern Australia are not true peat-forming systems when placed in the international context and compared to the vast temperate peatlands of the Northern Hemisphere (Fryirs *et al.,* 2014). That is, the definition of true peat requires 50 - 95% organic substances by an international standard (Inisheva, 2006), yet most Australian peats are characteristically high in minerogenic materials such as sand and clay (Young, 2017). Therefore, that particular case requires a region-specific classification. Figure 2.1 shows Moore's (1995) classification of peatland types based on a precipitation/evaporation ratio and the influence of groundwater in the peatland system. Generally, the consensus is that peatlands are simply organic wetlands that can accumulate peat.

Table 2.1 Various classifications of peatlands

Reference	Classification Description	Study area
Fryirs, 2016	Used the 'River Styles Framework' (see Brierley and Fryirs, 2005). A range of geomorphic indicators are used to assess 'intact' and 'channelized' swamps and their condition (good, moderate, and poor).	Blue Mountains National Park, NSW
Hope *et al.*, 2009, 2012	Peatlands indicate terrestrial sediments in which organic matter exceeds 20% dry weight and with a depth generally greater than 30 cm.	Snowy Mountains, NSW and Australia Capital Territory (ACT)
Inisheva, 2006	Suggests peat types and peat soils should be classified based on floristics and botanical composition of the peat. Degree of decomposition and ash content are also important determinants.	Russia
The National Wetlands Working Group, 1997	Peatlands contain more than 40 cm of peat accumulation on which organic soils develop.	Canada
Moore, 1984, 1995 (Fig. 2.1)	Mires can be classified based on a range of different criteria including floristics, morphology and peat characteristics (see Moore, 1984). However, classification based on hydrological aspects is the most useful; groundwater or *flow-fed* (rheotrophic) and *rain-fed* (ombrotrophic) peatlands.	Europe

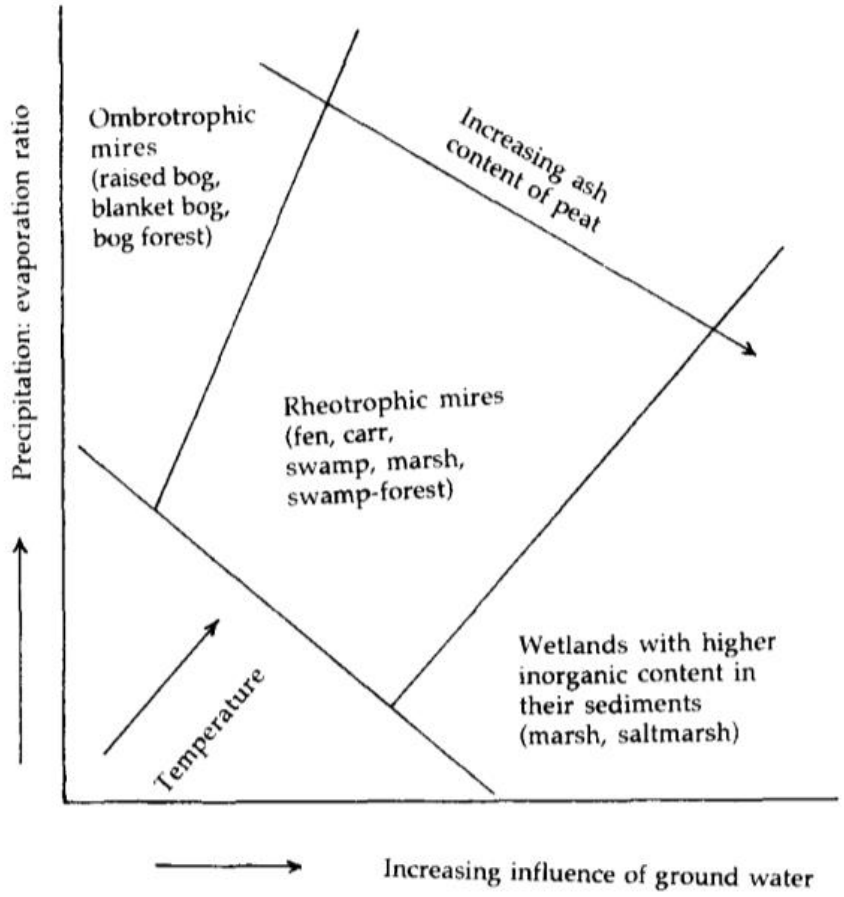

Figure 2.1 - Moore's (1995) classification of peatlands based primarily on hydrology.

Globally, peatland environments are abundant throughout the temperate regions of Canada, Sweden, Finland and Russia, but can occur in any tundra or maritime area throughout the Northern Hemisphere (Pemberton 2005). Many of these peatlands were initiated and developed during the Holocene and since the Last Glacial Maximum (LGM) (Fryirs *et al.,* 2014), and formed in response to the presence of different landforms generated in the LGM such as glaciated landscapes (e.g., hummocky topography), lunette complexes and palaeolakes/small basins, all of which provide the constrained drainage conditions needed for waterlogged peatlands (Pemberton 2005; Kokfelt *et al.,* 2010; Kolaczek *et al.,* 2016).

Peatlands in Australia are rare but quite unique, existing from the wet tropics in the north to the alpine and coastal regions in the south-east. At high altitudes, bogs and fens are found above 1650 m in south-eastern Australia (Brinson and Malvarez, 2002), and the peatlands in Tasmania are thought to be the most prominent in the Southern Hemisphere (Pemberton, 2005).

The hydrology of peatlands is a powerful determinant of peatland form and function and, as aforementioned, is commonly used in the classification of such environments (Fig. 2.1). Hydrological processes are intimately linked with the floristic expression of peatlands, and a dynamic hydrological regime can result in a mosaic of vegetation types and growth rates (Hope *et al.,* 2009). At one end of the scale, peatlands occurring in cool climates that primarily derive their nutrients and water from atmospheric precipitation are termed ombrotophic peatlands. These peatlands usually exhibit slow-growing mosses such as *Sphagnum*. At the other end, if the influence of groundwater predominates and increases nutrient availability, then the peatland is more rheotrophic. Shrubs, grasses and sedges can now establish and co-exist with the moss species (Hope *et al.,* 2009). Holden (2006) describes the simple and widely accepted acrotelm – catotelm layering system for analysing peatlands: an upper actively living layer with high hydraulic conductivity and variable water depths through time (acrotelm), and a lower anaerobic layer with low hydraulic conductivity that is permanently saturated and represents the bulk of the peat deposits in the system (catotelm). As previously mentioned in section 2.1.2, acrotelm and catotelm horizons differ regarding the amount of fibrous peat available, with more decomposed sapric peat occurring at depth in the catotelm. Thus, these layers may be differentiated in the field accordingly. In some Australian peatlands, especially deep acrotelm horizons occur, reflecting substantial drying out and water table fluctuation during droughts (Hope *et al.,* 2009). Peatland vegetation can only survive in the acrotelm due to the aeration, nutrient transfer and microorganisms intrinsic to this layer. The relationships between peatland hydrology (e.g., groundwater – surface water interactions), vegetation and carbon accumulation are intricate and complex and may well be influenced by the plant types growing on the peatland surface (Devito *et al.,* 1996; Holden, 2006; Swanson, 2007; Morris *et al.,* 2011).

2.2.2 Upland swamps

Where the slope permits, some peat-forming environments exist on plateaus, headwater reaches, high-altitude alpine environments and other upland settings within a catchment. These types of environments have been referred to in the literature as ombrogenous mires (meaning 'ombrotrophic': rain-fed) (Bragg and Tallis 2001), alpine mires (McGlone *et al.,* 1997) and headwater blanket peats (Holden and Burt 2002), all of which provide important functions in catchment scale processes such as water regulation and filtration. In south

eastern Australia, dells (Young, 1982) and upland swamps (Freidman and Fryirs, 2015; Fryirs *et al.,* 2016; Young, 2017) occupy many headwater regions, however differ greatly both hydrologically and geomorphologically to the abovementioned environments.

According to Fryirs *et al.,* (2014a), upland swamps (also called Temperature Highland Peat Swamps on Sandstone (THPSS)) are a form of mire that exists upon low-relief plateaus of south-east Australia. THPSS are particularly distinctive throughout the Southern Highlands and Woronora Plateau in NSW and occur across an area of 2000 km^2 in the Blue Mountains, NSW (Young, 1982; Kohlhagen *et al.,* 2013; Fryirs *et al.,* 2014a) (Fig. 2.2). The development of many THPSS was initiated during the Holocene in response to increased rainfall following climate amelioration and occurred on topographical lows throughout the headwater reaches of low order streams (Jenkins and Frazier, 2010). Associated gentle slopes and minimal stream-power encouraged sediment (derived from the underlying sandstone) deposition in the headwater drainage lines. This caused discontinuous drainage and provided conditions for waterlogging to occur, promoting simultaneous organic matter accumulation (Fryirs *et al.,* 2014a; Cowley *et al.,* 2016).

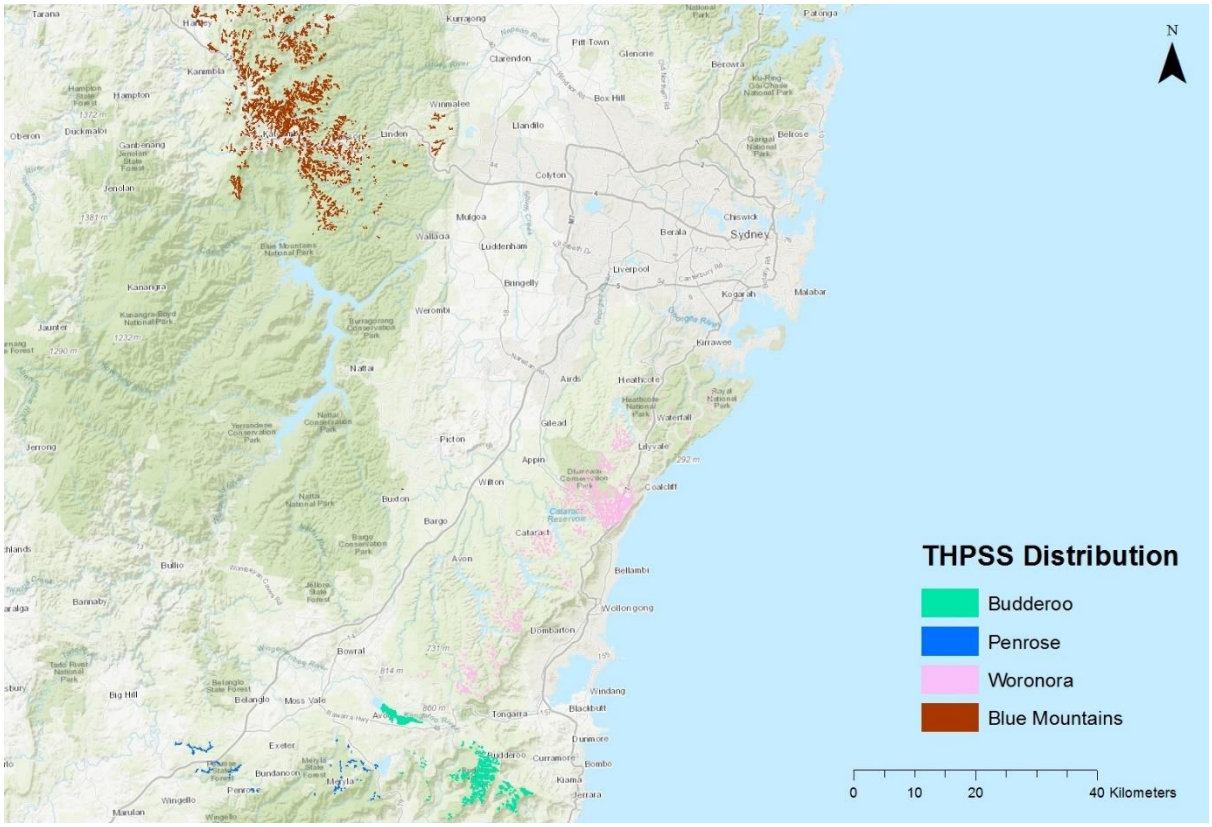

Figure 2.2 - Distribution of Temperate Highland Peat Swamps on Sandstone across NSW. Data was freely available from NSW Office of Environment and Heritage official website.

The underlying impervious sandstone substrate promotes shallow groundwater interactions and lateral flow, increasing THPSS systems sensitivity to water fluctuations (Jenkins and Frazier, 2010). Indeed, while THPSS are similar to Northern Hemisphere fens in terms of water and carbon storage, the underlying sandstone makes them distinct to the south-eastern Australian region (Cowley *et al.,* 2016). There is prominent mineralisation of the peat layers in THPSS, with overall swamp substrate typically containing coarse quartzose sand with peat and usually connected to an overlying peaty mat at the surface (Jenkins and Frazier, 2010).

Floristically, upland swamps of south-eastern Australia are typically composed of low lying vegetation, such as heaths and sedges, fringed by eucalypt woodland (Jenkins and Frazier, 2010). While THPSS are comparatively weak in their peat forming ability, they have been recognised for their high ecological value. In south-eastern Australia, droughts and dry spells can be somewhat mitigated by the swamps ability to absorb, retain and slowly release water (Fryirs *et al.,* 2014a). Likewise, intense rainfall and subsequent catastrophic run-off can be regulated through this 'sponge' phenomenon (Fryirs *et al.,* 2014a). Disturbance-related impacts such as knick-point erosion, channelization and fire can exceed the stability threshold of a particular swamp and thus jeopardise its function as a water regulator and an important habitat (Jenkins and Frazier, 2010; Kohlhagen *et al.,* 2013). As such, upland swamps existing in the Blue Mountains were labelled by the Threatened Species Conservation Act 1995 as a vulnerable ecological community (Kohlhangen *et al.,* 2013).

2.2.3 Lake and Peatland Evolution

Because lakes continually accumulate sediment, they will often gradually transform over time, becoming shallower with a smaller surface area (Timms, 1992; Niska and Kolodziej, 2015). This process of lake in-filling is referred to as 'hydroseral succession' or 'terrestrialisation' and can take hundreds and thousands of years to develop (Heathwaite, 1993; National Wetlands Working Group, 1997).

Lake terrestrialisation, whereby the infilling of lakes results in their conversion to terrestrial environments, is the origin of many bogs and mires throughout the Northern Hemisphere. This typically involves a shift from lacustrine sediment to increasingly organic peat (Tallis, 1973; Balaga, 2007; Kalina *et al.*, 2014). Balaga's (2007) study in eastern Poland used changing elemental composition down core to reveal that sedge-moss and sedge-reed peat developed

atop lacustrine deposits as lake water level decreased. This resulted in a changed shoreline that became dominated in a mosaic of vegetation. Eventually, cotton-grass and sphagnum peat developed reflecting the change from a lake to a peat-bog complex. Terrestrialisation has also occurred in Australian lakes (Moss *et al.*, 2016). Fen complexes on Fraser Island in south east Queensland, developed via the gradual in-filling of deeper lake systems, as noted at many sites by the clear transition of deep-lake (i.e., clay) to shallower-water (i.e., silt) sediments and then establishment of the dominant peat-forming rush *Empodisma minus* (Moss *et al.*, 2016). Furthermore, it has been suggested that for small and steep-sided depressions, or for basins that are perched and heavily influenced by climatic fluctuations, terrestrialisation can often occur due to the presence of a 'schwingmoor' structure, whereby rapidly increasing water levels can flood mire complexes resulting in the uplift of floating peat rafts and islands (Tallis, 1973). The basal layers of the peat raft then settle down into the underlying water and act to progressively in-fill the area (Tallis, 1973).

Another developmental pathway of lakes and peat-forming systems is the process of paludification, involving the expansion and colonisation of peat vegetation beyond basal depressions due to rising water tables (Heathwaite, 1993; Phillips and Bustin, 1998; Crawford *et al.*, 2003). The deposition of coarse hemic peat atop massive rooted clays at sites located high in drainage basins has been noted, suggesting paludification and the initial development of a flooded forest swamp (Phillips and Bustin, 1998). Likewise, paludification processes in Northern Europe are widespread and often closely associated to ecological shifts and the disappearance of forests due to bog expansion (Crawford *et al.*, 2003).

Additionally, the processes of both terrestrialisation and paludification can interact at the same place through time and wetland development can consequently occur differently and at varying rates within the one basin (Balaga, 2007). Thus, a wide variety of lake and peatland forms can arise due to changes in lake shoreline and wetland margin configurations (National Wetlands Working Group, 1997). These changes are tied closely to the inherent morphometric and geological characteristics of basins (Timms, 1992; Niska and Kolodziej, 2015).

2.3 Lakes as Palaeo-environmental Archives

As sediments accumulate in lake environments, a range of palaeo-environmental proxies are contemporaneously preserved. This is vastly dependent on basin morphology, catchment size, hydrological characteristics and position within the landscape (Barr *et al.*, 2014). South-eastern Australia, being proximal to the Pacific and Southern Oceans, has the potential to inform on continental climate variability due to its sensitivity to major climatic events such as the El-Nino Southern Oscillation (ENSO) and the inter-decadal Pacific Oscillation (IPO) (Marx *et al.*, 2011; Petherick *et al.*, 2013; Barr *et al.,* 2014). While there are generally few lake systems along south-eastern Australia to infer palaeoclimatic shifts, previous study sites include; expansive inland saline systems like Lake Eyre and Frome (Cohen *et al.,* 2011; Habeck-Fardy and Nanson, 2014; May *et al.,* 2015). Likewise, the Coorong coastal lakes (Mee *et al.,* 2008) and maar lakes in Western Victoria (e.g., Keilambete, Gnotuk and Bullenmerri lakes) (Jones *et al.,* 2001) contain palaeo-environmental archives for Southern Australia. Lake George is one of the largest freshwater lakes in N.S.W and stores the longest quasi-continuous sedimentary archive of any Australian lake basin (*ca* 4 Ma) (Macphail *et al.*, 2016), so it too is a strong indicator of past climates and environments throughout the Southern Tablelands and surrounding regions.

Palaeo-environmental records from lakes are often developed from a variety of proxies such as charcoal, diatom and pollen analysis, as well as geochemical data like stable isotope (e.g., $\delta^{13}C$ and $\delta^{15}N$) composition and elemental analysis. For example, pollen is widely used as an indicator of vegetation history, and in south-eastern Australia, pollen derived from key taxa such as *Casuarina* and Myrtaceae (i.e. *Eucalyptus*) generally indicate arboreal conditions and forest expansion (Donders *et al.,* 2007; Kershaw *et al.,* 2010). Changes in the abundance and diversity of Myrtaceae pollen types can reflect changing hydrological conditions and environmental states (Thornhill, 2010), such that Black *et al.* (2006) found high Mrytaceae/Casuarinaceae ratios which indicated swamp conditions and the reciprocal indicated a lake environment at one of the Thirlmere lakes; Lake Baraba. The pollen from *Pinus radiata* is a useful indicator for sediments that have accumulated post European occupation (Dodson, 1974; Noakes, 1998; Black *et al.,* 2006). Also, diatoms are the most sensitive proxy to changing water levels and subsequent changes in water chemistry (Barr *et al.*, 2014). Diatoms are a microscopic algae found in most aquatic and marine environments,

and are highly responsive to rapid changes in pH, water salinity, nutrient availability and sedimentary processes due to their short life span (Barr *et al.,* 2014; Proske *et al.,* 2017). Discerning the relative abundances of planktonic (freely moving benthic forms) and epiphytic (adherence to living substrata) diatom communities is important for the inference of macrophyte dynamics through time, changes in lake turbidity, regimes shifts and local hydrology (Reid *et al.,* 2007; Tiffany, 2011; Kattel *et al.,* 2017).

These datasets can be coupled with macrofossil identification and sediment stratigraphy to aid palaeo-environmental interpretation (Kershaw *et al.*, 2010). Crucial to the formation of precise limnological records is the inclusion of geochronological techniques (e.g., Accelerator Mass Spectrometry (AMS) radiocarbon dating and optically stimulated luminescence (OSL) to create age-depth models (Donders *et al.*, 2007; Kershaw *et al.*, 2010).

2.3.1 Stable carbon ($\delta^{13}C$) and nitrogen ($\delta^{15}N$) isotopes from lake sediments

Stable carbon ($\delta^{13}C$) and nitrogen ($\delta^{15}N$) isotope signatures in plants and sediments can serve as useful palaeo-environmental indicators (Ma *et al.*, 2012; Woodward *et al.*, 2017). Isotopes of carbon, ^{13}C and ^{12}C, fractionate during photosynthesis, normally resulting in relative depletion of the heavier ^{13}C (Brugnoli & Farquhar, 2000). This degree of fractionation varies between different photosynthetic pathways (i.e., C3, C4 and CAM), and thus can reflect species composition (Brugnoli & Farquhar, 2000; Ma *et al.*, 2012). Generally, however, C3 terrestrial vegetation have $\delta^{13}C$ values that range from -32 ‰ to -21 ‰ and C:N ratios of >12 (Lamb *et al.*, 2006). C4 plants typically have $\delta^{13}C$ values of approximately -13 ‰ and C:N ratios of >30, while CAM plants, utilising both C3 and C4 photosynthetic pathways, incorporate a wide range of $\delta^{13}C$ values and C:N ratios depending on which pathway is primary (Lamb *et al.*, 2006).

Furthermore, the degree of fractionation reflects the plants metabolism during changing environmental conditions such as varying water availability (Ma *et al.*, 2012). That is, a decrease in precipitation causes a change in the difference between atmospheric and intercellular humidity's in plants, resulting in a decrease of stomatal conductance which consequently enriches the plant $\delta^{13}C$ value (Ma *et al.*, 2012). Isotopic discrimination between nitrogen isotopes, ^{15}N and ^{14}N, can also reflect changing hydrological conditions as high rainfall events cause a larger loss in ^{14}N compared to ^{15}N in soil (Ma *et al.*, 2012). However, in

lakes, isotopes of nitrogen are also commonly used to infer nutrient availability, nitrogen fixation and species composition (Schulze *et al.*, 2014).

C3 plants, such as woody vegetation, typically have a $^{13}C/^{12}C$ ratio of 20‰ less than the atmosphere and are enriched in $\delta^{13}C$ under drought conditions. C4 plants, such as grasses, have a $^{13}C/^{12}C$ ratio of 10‰ less than the atmosphere, are far less sensitive to water-stress and thus will not show the same $\delta^{13}C$ enrichment signatures (Farquhar *et al.*, 1982; Ma *et al.*, 2012).

Relating stable isotope composition in lake sediments to parent vegetation

Just as $\delta^{13}C$ and $\delta^{15}N$ values in surface soil can inform on the stable isotope composition of the parent vegetation (Balesdent *et al.*, 1993; Ma *et al.*, 2009), bulk lake sediment $\delta^{13}C$ and $\delta^{15}N$ can reflect the changing vegetation communities and biotic conditions occurring within the lake water (Woodward *et al.*, 2012). Therefore, $\delta^{13}C$ and $\delta^{15}N$ composition in lake and wetland sediments has been commonly used as a palaeo-environmental tool for changes in vegetation, rainfall and catchment processes (Woodward *et al.*, 2017). Stable isotope composition in lake sediment is influenced by a mix of organic and inorganic components, which is characterized by the material being mainly derived from the lake catchment (allochthonous) or as a result of within-lake productivity (autochthonous) (Woodward *et al.*, 2012). A mainly allochthonous sediment input results in a high carbon-to-nitrogen (C:N) ratio and $\delta^{13}C$ and $\delta^{15}N$ signatures that reflect the values of terrestrial plants in the surrounding area. Lake sediments with low C:N ratios indicate autochthonous material and have more variable $\delta^{13}C$ and $\delta^{15}N$ values, better depicting with-in lake environmental conditions and the fractionation of ^{13}C and ^{15}N by lacustrine biota (Woodward *et al.*, 2012).

Studies conducted in Australia have found that lake-bed material derived from C3 lake macrophytes such as *Eleocharis sphacelata, Nitella* spp., *Myriophyllum* spp. and *Potamogeton* spp. produced C:N ratios of ≥11 and had $\delta^{13}C$ values closely related to these C3 macrophytes, reflecting the autochthonous nature of the sediment and the persistence of standing water (Woodward *et al.*, 2017). Multiple studies agree that stable isotope datasets from soil and lake sediments are useful in determining site-specific $\delta^{13}C$ and $\delta^{15}N$ sources and processes (Balesdent *et al.*, 1993; Woodward *et al.*, 2012).

2.3.2 Late Quaternary environmental change in southeast Australia

Since the mid-Miocene epoch ~12 Ma, the continent of Australia has become increasingly arid, particularly throughout the Quaternary period (Martin, 2006). Quaternary climate oscillations within south-eastern Australia were marked by interglacial and glacial periods that were relatively wet and arid respectively, and correspond to the globally registered Marine Isotope Stages (MIS) (Webb *et al.*, 2014). Generally, MIS 5 (~130 – 74 ka) and 3 (~60 – 24 ka) were characterised by relatively high effective precipitation, increased river activity and lake levels as well as forest expansion, whereas MIS 4 (~74 – 60 ka) and 2 (~24 – 11 ka) were demarked by diminished forests, decreases in lake levels and increased dune building (Harrison, 1993; Kershaw *et al.*, 2007; van Meerbeeck *et al.*, 2009; Webb *et al.*, 2014).

Early Last Glacial period (~35 – 22 ka)

In south eastern Australia, the early glacial period coincides with the end of MIS 3 and the beginning of MIS 2, and was therefore a time of moist conditions with associated high fluvial activity and lake levels that digressed into a cool and dry climate at the onset of the subsequent glacial period (van Meerbeeck *et al.*, 2009; Petherick *et al.*, 2013). From ~35 ka, high effective moisture was noted by increased fluvial activity in the Murray Darling Basin, with bankfull river discharges suggested to be 5 times greater than present (Page *et al.*, 1996), and in Lake George, which showed periods of water depths up to 37 m (Coventry, 1976). Glaciers started occurring in the Snowy Mountains by ~32 ka (the Headley Tarn Advance) (Barrows *et al.*, 2001), and forest taxa started being replaced by herbaceous species as the south eastern Australian climate started to become cool and arid (Petherick *et al.*, 2011).

Last Glacial Maximum (~22 – 18 ka)

The Last Glacial Maximum (LGM) was characterised by enhanced aridity, evapotranspiration and wind, with half the amount of modern precipitation levels occurring in southern Australia (Petherick *et al.*, 2011). At that time, Australia was roughly one-third larger and eustatic sea levels were 120 m lower than present (Black *et al.,* 2006; Petherick *et al.,* 2008). This increased continentality encouraged dust entrainment and dune building in an expanding arid zone (Petherick *et al.,* 2008). Resultantly, southeast Australian lake levels during the LGM were comparatively low (Petherick *et al.,* 2011), and there is consensus that a mostly treeless landscape prevailed above 600 m AHD (Kemp and Hope 2014), with a lower tree line limit of

500 m AHD established at Mountains Lagoon, NSW (Robbie and Martin 2007). While the majority of palynological records indicate open steppe grasslands characterised by species such as *Asteraceae, Poaceae* and *Chenopodiaceae* (Petherick *et al.,* 2011), some indicate the contrary (Black *et al.,* 2006). A pollen record at Lake Baraba, NSW, depicts Casuarinaceae community dominance during the late glacial period, suggesting that this site may have acted as a refugium for arboreal species (Black *et al.,* 2006).

Deglacial period (~18-12 ka)

The subsequent glacial – interglacial transition period generally exhibited increases in temperature and moisture, as indicated by significant retreat of glaciers in the Snowy Mountains (Barrows *et al.*, 2001), and the re-emergence of arboreal species (e.g., Casuarinaceae) indicating warmer conditions (Williams *et al.*, 2006). However, the deglacial period was found to be relatively arid in the Southern Tablelands of NSW (Kemp and Hope, 2014) and lake levels from Lake George were significantly low between 14 – 10 ka (Fitzsimmons and Barrows, 2010).

Holocene (~12 – 0 ka)

The onset of the Holocene (~12 ka) is described as a period of increased temperatures and precipitation with generally stable climates (Kemp and Hope, 2014). Throughout south eastern Australia, the onset of the Holocene is marked in numerous lacustrine records showing an increase in effective moisture. For example, Mountain Lagoon in the Blue Mountains persisted as a swamp until becoming a lake at about 10 ka (Robbie and Martin, 2007), Little Llangothlin Lagoon switched to a positive water balance at 9.3 ka (Woodward, 2014) and Lake George experienced its highest Holocene shorelines between 10 – 8 ka (Fitzsimmons and Barrows, 2010). Furthermore, mires at Barrington Tops started accumulating peat after 8.6 ka (Dodson, 1987) and Lake Baraba, one of the Thirlmere Lakes, started accumulating peats at 8.5 ka (Black *et al.*, 2006), highlighting an increase in swamp vegetation and permanently saturated conditions at these sites.

By the mid-Holocene (~6 ka) south-eastern Australia experienced a reversion back to drier and cooler conditions with more pronounced climatic variability, a trend that is widespread in the literature (e.g., Dodson, 1987; Harrison, 1993; Woodward *et al.*, 2014; Tyler *et al.*, 2015). This change is thought to have come about by the onset of modern climate processes

such as El Nino Southern Oscillation (ENSO) with a dominate El Nino, which can induce pronounced dry periods in south-eastern Australia (Reeves *et al.*, 2013; Woodward *et al.*, 2014).

From the late Holocene (~4 ka) to the present, south eastern Australia has experienced a reasonably variable climate. Lake George has experienced hydrologic variability in the form of intermittent pulses of lake transgression in the last 2.5 ka (Fitzsimmons and Barrows, 2010), and some mires in the Australian Capital Territory contain peats that have been overlain with lenses of sand at ~3.5 ka, after which peat deposits reappear, therefore indicating different catchment-driven responses to a variable climate (Hope *et al.*, 2009).

What remains to be resolved is how lakes systems, such as Thirlmere Lakes, have responded to these changing environmental conditions throughout the Late Quaternary. The following chapter outlines the physiographic context of the Thirlmere lakes region.

3. REGIONAL SETTING

3.1 Study Area

Thirlmere Lakes are located approximately 90 km south-west of Sydney and 40 km north-west of Wollongong, NSW (Fig. 3.1). Forming part of the Warragamba Dam catchment and the Greater Blue Mountains World Heritage area, the small Thirlmere Lakes National Park is of high conservation value due to its unique biology and geological origin (Riley *et al.,* 2012). This freshwater wetland system is comprised of five elongated lakes, including Lake Gandangarra, Werri Berri, Couridjah, Baraba and Nerrigorang (Fig. 3.1). Upstream (i.e., to the north-west) of Lake Gandangarra exists Dry Lake, which is not generally included in the Thirlmere Lakes system because it drains north-east through the Cedar Creek catchment. However, it may be morphologically related to the rest of the lakes (Riley *et al.,* 2012). The Thirlmere Lakes catchment area is small, existing at approximately between 4.5 – 4.7 km^2 (Riley *et al.*, 2012). Catchment elevations vary between 390 m AHD and 298 m AHD, with the lake floor elevations differing between lakes (i.e., difference of 6 m between Lake Nerrigorang and Lake Baraba's lake floors). The lakes occupy a topographic high in the region, with the eastward Cumberland Basin residing at an elevation beneath the beds of the lakes (Riley *et al.,* 2012).

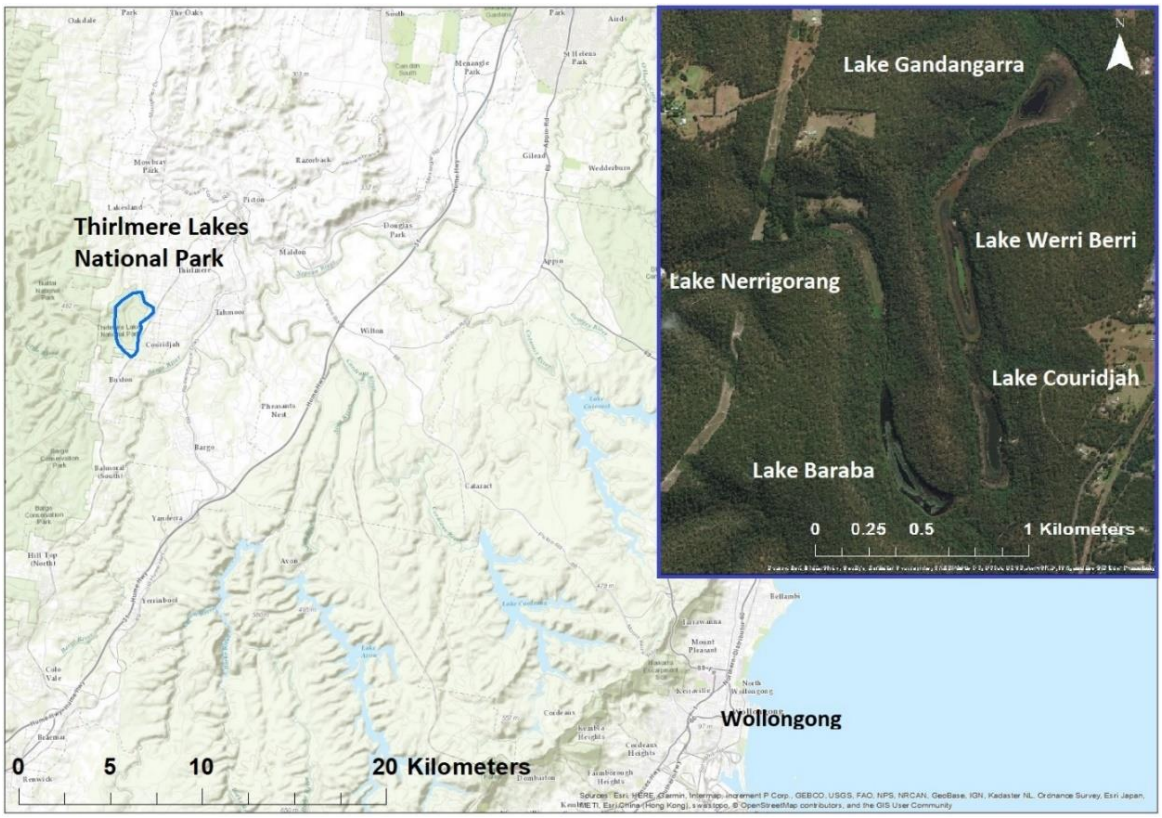

Figure 3.1 The position of Thirlmere Lakes within the Sydney Basin. The insert map shows a satellite image of the five lakes.

3.2 Geology of the Thirlmere Lakes

The geology of Thirlmere Lakes is representative of the southern Sydney basin sequence (Fig. 3.2). Catchment rocks form part of the Triassic Narrabeen Group which is comprised of a number of subgroups and formations (Geoscience Australia, 2017). These include the regionally important Bald Hill Claystone, part of the Clifton subgroup, which is a low permeability stratum that exists >100 m below the lakes (OEH, 2016). The Bald Hill Claystone is then overlain by the Hawkesbury Sandstone, described as a medium to coarse grained fluvially derived quartz sandstone containing minor shale and laminite lenses (Geoscience Australia, 2017). The Hawkesbury Sandstone outcrops directly around, and to the south-west of the Lakes, forming the erosion-resistant ridgelines and steep valley walls of the Thirlmere Lakes system (Fanning, 1982). The Hawkesbury Sandstone then becomes overlain by the Wianamatta Group forming the Razorback Range to the north and north-east of Thirlmere Lakes. The Wianamatta Group comprises mainly of shale, laminite and sandstone and contains subunits of the Ashfield Shale, the Minchinbury Sandstone and the Bringelly Shale (Geoscience Australia, 2017).

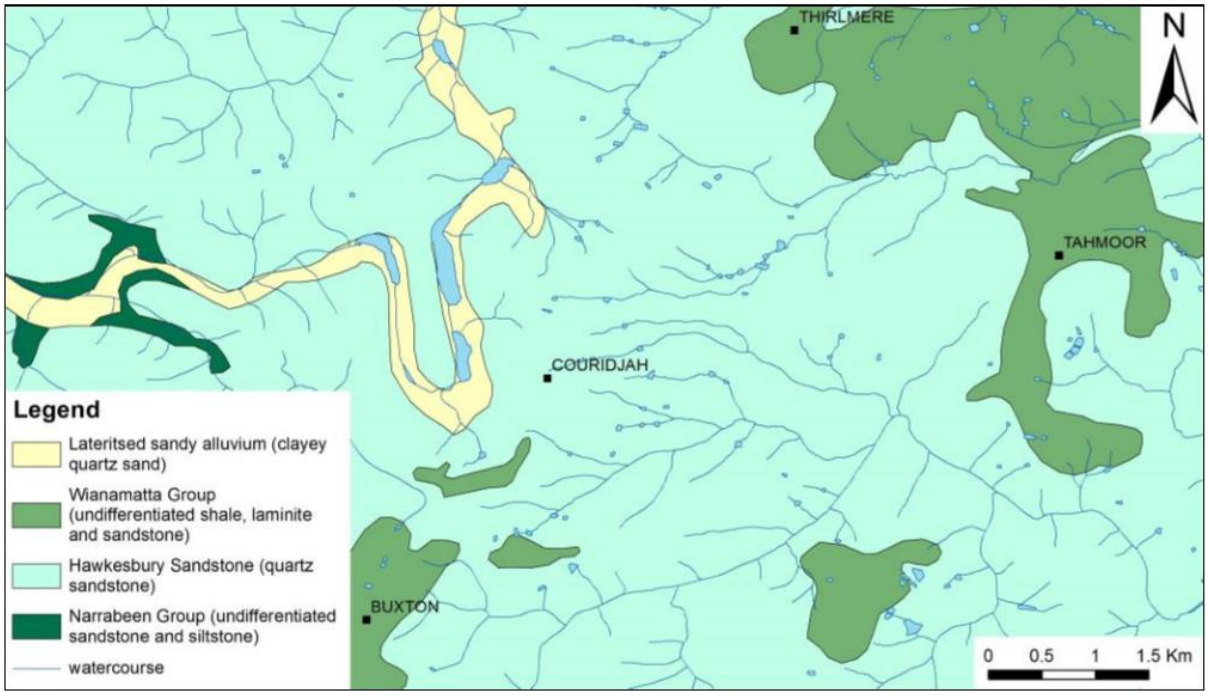

Figure 3.2 Geology of Thirlmere Lakes. From OEH (2016).

3.2.1 Evolution of the lake sequence

Thirlmere Lakes occupy an intriguing and seemingly regionally misplaced-looking valley. The origin of this distinct 'U' shape planform is attributed to the past occurrence of a meandering river that incised into the Hawkesbury Sandstone (Timms, 1992). It is generally accepted that this river was then uplifted and subsequently truncated from its original south-west drainage in response to structural forces associated with the formation of the Lapstone Monocline and Southern Lapstone Structural Complex (Fanning, 1982; Timms, 1992; Noakes, 1998; Black *et al.,* 2006). During the early to mid Cenozoic, east-west contraction occurred in the Thirlmere Lakes area and neighbouring regions causing high-angle, west-over-east reverse faulting (Fergusson *et al.,* 2011). This is expressed presently as a series of fault zones across the Sydney Basin, including the Victoria Park, Bargo and Picton Fault Zones. The Thirlmere Lakes possibly occupy the hanging wall of these reverse faults (Fergusson *et al.,* 2011 see Fig. 2). Sediments within the Thirlmere Lakes system begun accumulating concurrently with the initiation of this uplift (Vorst, 1974), with sedimentation converting what was once a fluvial system into the present lacustrine environment. Ordinarily, lake basins of this age would have undergone terrestrialization by slowly infilling (Timms, 1992). The longevity of Thirlmere Lakes can be ascribed to the erosion-resistant properties (high quartz content) of the Hawkesbury sandstone (Pells Consulting, 2011), combined with low erosion rates.

3.3 Modern Catchment Geomorphology and Sedimentology

3.3.1 Alluvial Fans

Thirlmere Lakes has been described as a fluviatile lake system in an upland, entrenched meander system (Timms, 1992). Their small catchment area results in inflow which when combined with the highly erosion resistant Hawkesbury Sandstone and the densely vegetated lake margins, leads to slow sedimentation rates and highly stable geomorphology (Timms, 1992; Noakes, 1998; Pells Consulting, 2011). Despite this, a series of alluvial fans (Fig. 3.3) have formed on the valley margins from ephemeral tributaries. The sandy material characteristic of the alluvial fans is likely to be remobilised and eventually transported elsewhere on the fans or into the lakes themselves, thereby possibly reflecting multiple depositional phases (Vorst, 1974). Transport of material is likely increased when fires disrupt

the dense, natural vegetation within the catchment, potentially increasing suspended sediment loads in lakes for up to several years (Smith *et al.,* 2012).

The formation of these five alluvial fans has led to the development of the five distinct lakes, where the fans debouch onto the trunk valley floor separating the lakes, making up the Thirlmere Lakes system (Riley *et al.,* 2012). The sediment within the fans is bimodal, consisting of fine to medium sand and silt/clay (Vorst, 1974), reflecting the composition of the Hawkesbury Sandstone source rock, and has moderate to poor drainage (Rose and Martin, 2007). Their occurrence indicates the fans are being deposited quicker than the system's ability to erode this sediment, testimony to the general low-energy state of the system. The fans are generally poorly sorted with no distinct sorting trend down-fan (Vorst, 1974), attributable to the very short transport distance of sediment from the ridges and the sudden drop in carrying capacity of the sheet-flow (Blair and McPherson, 1994).

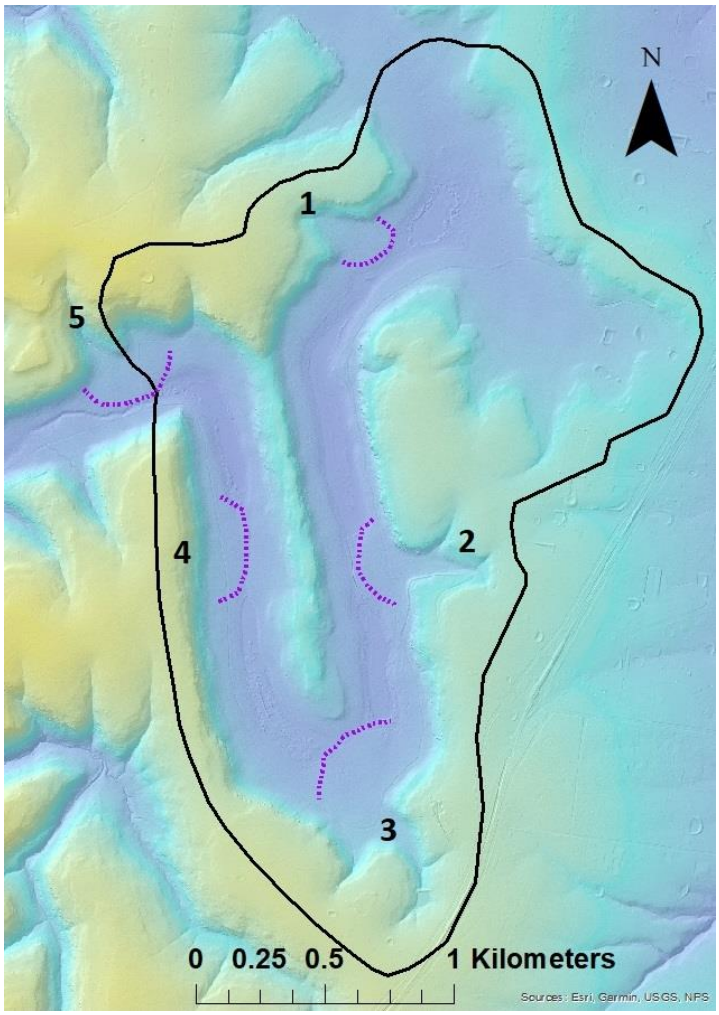

Figure 3.3 The location of the alluvial fans impinging on the valley of Thirlmere Lakes (numbered 1 – 5 from upstream to downstream). The black line represents the catchment boundary of Thirlmere Lakes, which has an area of 4.6 km^2. The dotted purple outline the alluvial fans. The approximate areas of the alluvial fan catchments are as follows; 1 = 0.15 km^2, 2 = 0.24 km^2, 3 = 0.54 km^2, 4 = 0.08 km^2 and 5 = 0.21 km^2.

3.3.2 Stratigraphy

Within the potential >50 m of unconsolidated sediment existing beneath the depots of the Thirlmere Lakes (Vorst, 1974), it is thought that the bottom 30 m are derived from the valley (initial alluvium, weathered sandstone bedrock) and the top 20 m were deposited through lacustrine processes (Timms, 1992). Generally, the Thirlmere Lakes alluvium is described as a clayey quartz sand. Yet, some studies have encountered distinctive stratigraphic layers such as; dark organic grey clays indicating anaerobic lake conditions; alternating yellow and orange clays representing oxidising conditions during lake drying (Black *et al.,* 2006) and a distinct humified peat layer discovered at depth in Vorst's (1974) study (Table 3.1). Furthermore, stages of lake infilling, expressed as clay overlain by peat deposits, have been shown to occur at different depths and times in the Lake Couridjah, Dry Lake and Lake Baraba basins, highlighting the variability in sub-surface sediment and thus distinct differences in the lakes morphological histories (Gergis, 2000; Black *et al.*, 2006; Rose and Martin, 2007) (Table 3.1). Depth to bedrock is poorly constrained but where investigated is also shown to vary, indicating a highly inconsistent weathering profile at the lake margins (Russell, 2012).

Vorst's (1974) thesis was the first and one of the only studies to infer stratigraphical relationships within Thirlmere Lakes unconsolidated sediment. Her four deep boreholes (>18 m depth) named BH1, BH2, BH4 and BH5, were drilled proximal to different lakes (Fig. 3.4). This large distance between each borehole makes the derived stratigraphical interpretations only rough approximations, but nonetheless useful.

Table 3.1 Summary of key stratigraphical findings from previous studies at Thirlmere Lakes, highlighting the variable nature of sub-surface material and depth to bedrock, as well as different ages of lake infilling.

	Location of Core	**Stratigraphic description**	**Depth of dated interval (m), Age (Ka)**	**Environment Interpretation**	**Author, Core ID and max. core depth**
Shallow cores (<5 m)	Lake Couridjah basin	Gradual transition from organic lake mud (peat) into fine-medium grey clay.	2.092 m, 12.4 Ka	Lake infilling.	Gergis (2000), TL L1, 2.628 m
	Dry Lake basin	Transition from brown fibrous peat and black clayey peat into clay.	0.22 m, 0.986 Ka	Lake infilling, change from a lake to a swamp.	Rose and Martin (2007) Pit 1, 1.5 m
Deep cores (>5 m)	Lake Baraba/Lake Nerrigorang sill	Humified peat layer with sponge spicules present.	Between 14.3 - 17.3 m, *no age data*	Open water environment.	Vorst (1974), see Appendix D (B.), BH2, 29.5 m
	Lake Baraba basin	Clayey peat (modern) to alternating organic and yellow clay	4.1 m, 8.5 Ka	Lake infilling, change from a lake to a swamp.	Black *et al.,* (2006), unspecified Core ID, 6.35 m
	Lake Couridjah eastern margin	Colluvium to bedrock (Hawkesbury sandstone)	24 m; 37 m, *no age data*	Bedrock boundary.	Russell (2012), GW075409/1, 24 m; GW075409/2, 100 m
	Lake Gandangarra near road intersection.	Alluvium to bedrock (Hawkesbury sandstone)	28 m, *no age data*	Bedrock boundary.	Russell (2012), GW075411, 28 m
	Lake Nerrigorang northern margin	Alluvium to bedrock (Hawkesbury sandstone)	18 m, no age data	Bedrock boundary.	Russell (2012), GW075410, 17 m

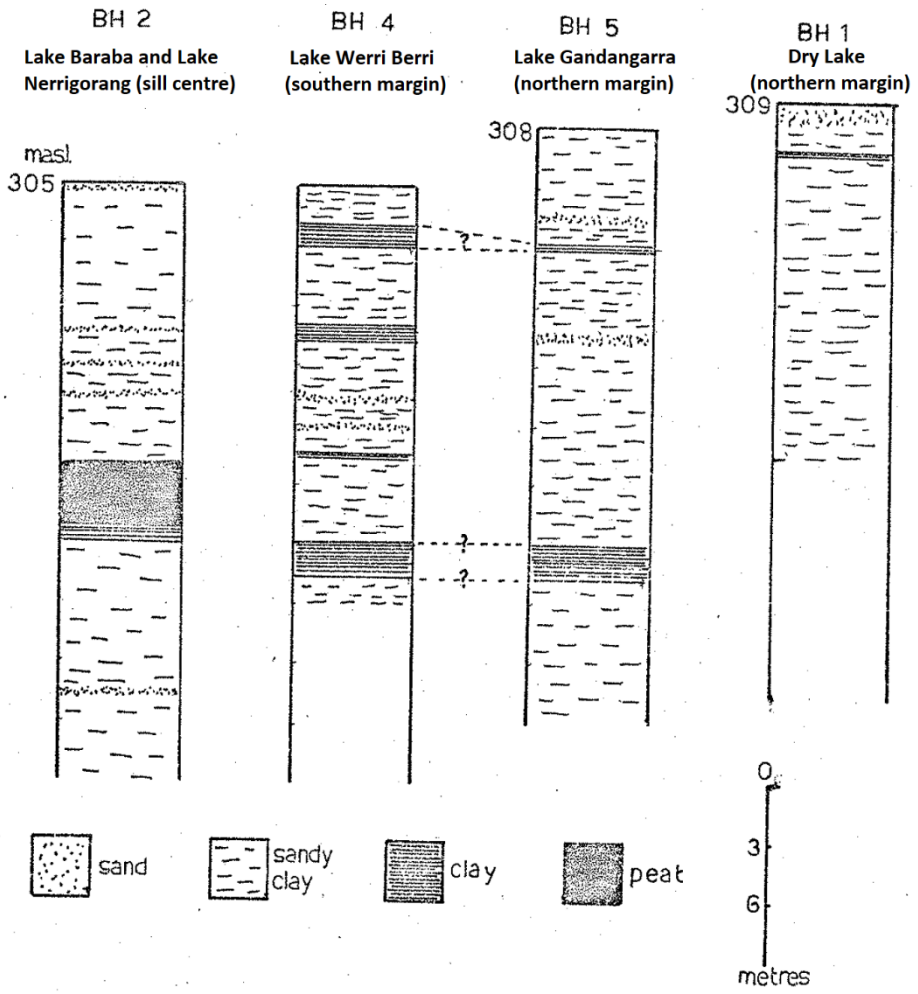

Figure 3.4 Deep borehole stratigraphy of the Thirlmere Lakes. Note that each core was collected from different lakes. From Vorst (1974).

3.3.3 Sedimentation Rates

Sediment accumulation in the Thirlmere Lakes valley most likely began concurrently with uplift and deformation that occurred during the early to mid Cenozoic, as described in Section 3.2.1 (Fanning, 1982, Fergusson *et al.,* 2011). Presently, sediment accreting in the lakes is composed of predominantly mineralgenic peat in the central basins with alluvial hill slope in-wash and fan development at lake margins, creating a mix of in-situ and transported material (Timms, 1992; Rose and Martin, 2007).

Sedimentation rates are relatively slow but have been shown to change through time and vary by an order of magnitude (Black *et al.*, 2006). Sediments in Lake Baraba range from slowly accumulating clays at 0.04 mm/year to Holocene peat at 0.67 mm/year, indicating changing

environmental conditions (Black *et al.,* 2006). Historic (post-European settlement) sedimentation rate is considered to be approximately double that of the pre-European times (Dixon, 1998). Post-European activity is also associated with an increase in the delivery of mineral matter into the lakes by 15 % (Dixon, 1998). However, sedimentation rates just under 2 mm/year were also detected during historic times, which is characteristic of a small and naturally vegetated catchment, possibly reflecting more natural conditions induced by the Thirlmere Lakes becoming dedicated as a reserve and then a national park (Noakes, 1998). An interesting phenomenon at Thirlmere Lakes is the occurrence of floating peat islands, as described by Vorst (1974). These islands are indicative of fluctuating water levels, whereby dried and exposed lake floor peat deposits obtain a degree of buoyancy as lake levels are replenished and are consequently lifted to the surface with the rising water. This process has implications for continuous lacustrine sedimentation as material is redistributed and may not reflect a regular increase of age with depth (Vorst, 1974).

3.4 Climate and Hydrology

Thirlmere Lakes National Park has a warm temperate climate. Average temperatures of 25-33^{o}C are experienced in summer and 5-15^{o}C in the winter (Horsfall *et al.,* 1988). Approximately 806 mm of rain falls annually (nearest rainfall station is at Picton, 6.5 km away from the Thirlmere Lakes) with bimodal wet periods occurring during January – March and June (OEH, 2012). North-easterly winds prevail during the summer months, with winter winds prevailing from the west-south west (BOM, 2017).

3.4.1 Lake Hydrology

Thirlmere Lakes is essentially a hydrologically closed system (Fanning, 1983), however, during wet periods the lakes overtop and drain south-west via Blue Gum Creek. Bowler (1981) developed a hydrologic classification of Australian Lake Basins, utilising lake morphology (catchment area and lake area) and climate (precipitation, evaporation and run-off coefficients) to categorise lakes. Within this classification, Thirlmere Lakes plots on the boundary between permanent and ephemeral conditions, but on the left side (the 'wet' side) of the hydrologic threshold line (Fig. 3.5). This implies Thirlmere Lakes are climatically and morphologically positioned to experience largely perennially wet conditions, yet they may also intermittently dry. The morphometric variables for Thirlmere Lakes were derived from

lake and catchment area estimates (0.46 km^2 and 4.5 km^2 respectively) made by the Thirlmere Lake Inquiry (OEH, 2012) while the climate variables were derived from BOM (2017) data collected at Picton weather station.

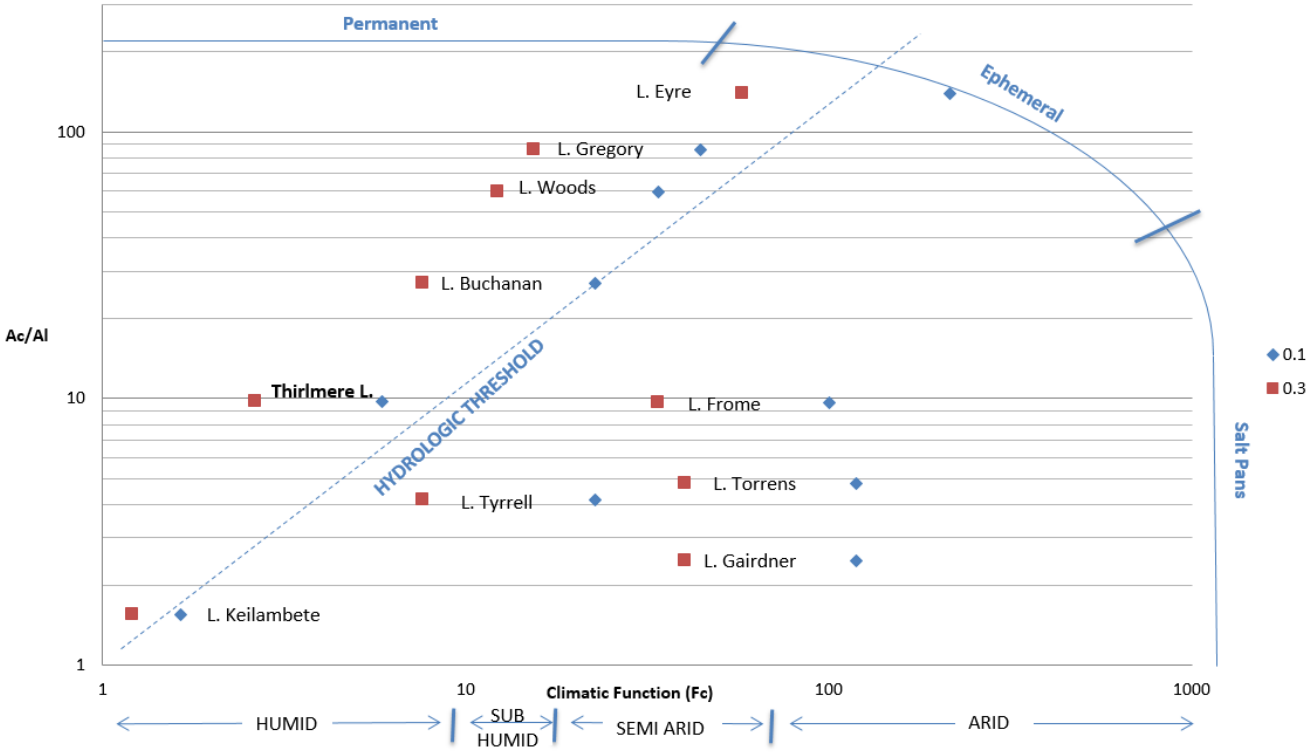

Figure 3.5 Lake classification showing the characteristics of Thirlmere Lakes by comparison to other major Australian Lakes (after Bowler 1981). The Y-axis indicates catchment morphology, where Ac = Catchment Area, Al = Lake Area. The X-axis indicates lake Climate Function, where Fc = (0.8E – P/Pf) + 1, where E = evaporation, P = precipitation and Pf = run-off coefficient x P. Note two data points are plotted for each lake using two different runoff coefficients, (0.1 and 0.3). This is because generally Australian lakes basins have a run-off coefficient that rarely surpasses 10%, but during periods of heavy rain the run-off coefficient can achieve 30%. Steady state conditions are defined by the 'hydrologic threshold'.

3.4.2 The Effect of Sills on Lake Hydrology

The elevation of the sills between the Thirlmere Lakes differ, with the lakes becoming sequentially connected as water levels rise (Riley *et al.*, 2012). Lake Gandangarra, Werri Berri and Couridjah become connected when the water level reaches approximately 302.8 m AHD, equivalent to a maximum depth of approximately 3 m within Lake Werri Berri (Riley *et al.,* 2012). The highest sill in the system is between Lake Couridjah and Lake Baraba and exists at 305.86 m AHD, while the floor of Lake Baraba is higher than all the other lakes. When the three upstream lakes (Gandangarra, Werri Berri and Couridjah) reach a level of approximately 306 m AHD (maximum depth approximately 6 m within Lake Werri Berri) they would overflow downstream into Lake Baraba and eventually into Nerrigorgang (Gilbert and Associates, 2012;

Riley *et al.,* 2012). The capacity of the lakes to overflow limits the volume of water that can be stored within the Thirlmere Lakes at a given time. The outflow point between Lake Nerrigorang and Blue Gum Creek is dependent on the height of the terminal fan, which is itself partly controlled by erosion from the discharging lakes. The maximum capacity of the lakes is therefore likely to be dynamic through time.

3.4.3 Limnology of the Thirlmere Lakes

Thirlmere lakes have been classified as a hypereutrophic system. That is, it experiences high productivity, dense algae and macrophytes with limited light in the water column (Change *et al.*, 2014). This classification may reflect recent conditions only (i.e., it may not reflect longer term trophic conditions). For example, Horsfall *et al.*, (1988) previously classed Thirlmere Lakes as meso-oligotrophic, albeit during a period of above average rainfall and visibly clearer water (Schadler and Kingsford, 2016).

Chemical and physical conditions are generally similar between the lakes, however there are some differences. All five lakes are slightly acidic and the water exhibits dark brown tannin staining due to humic acid leaching from the highly organic lake bed peat deposits. Of the five, Lake Couridjah has the darkest colour and the highest degree of turbidity (Horsfall *et al.*, 1988). Oxygen levels are significantly low throughout the year in all the lakes, particularly Lake Nerrigorang which experiences 0 % dissolved oxygen during summer in bottom waters (Horsfall *et al.*, 1988). The lakes experience temperature stratification during the summer months, especially at Lake Nerrigorang, which is the deepest lake with a maximum depth of approximately 7 m (Horsfall *et al.*, 1988). The TN:TP (i.e., total phosphorus to total nitrogen ratio) in the lakes was around 139, indicating phosphorus is the limiting nutrient at Thirlmere Lakes (Chang *et al.*, 2014). The major cations in the water at Thirlmere Lakes, along with most eastern Australian lowland coastal lakes located <100 km away from the ocean, are closer to the world-average seawater ratio than to the world-average freshwater ratio (Chang *et al.,* 2014 see Figure 2). This indicates that the primary source of all salts in the water at Thirlmere Lakes is derived from seaspray.

3.4.4 Rainfall variability and its impact on Lake Levels

Lake levels at Thirlmere Lakes have been shown to strongly correlate to rainfall over a centennial timescale (1890 – 2015) (Kingsford and Schadler, 2016) (Fig. 3.6). Rainfall in eastern Australia is highly variable and therefore so are lake levels (Riley *et al.*, 2012; Kingsford and Schadler 2016). A rainfall deficit (sum of below average rainfall) of 1600 mm over a 5 – 10 year period would cause the lakes to dry (Riley *et al.*, 2012). Low water levels at Thirlmere Lakes during 1937 – 1947 coincided with "World War II drought" (Kingsford and Schadler, 2016), while above average rainfall caused the lakes to overflow in 1974 (Vorst, 1974) (Fig. 3.6). Supporting information is presented in Appendix A, which shows the relationship between lake levels and rainfall at both Lake Couridjah and Baraba since 2012. Not only do water levels at Thirlmere Lakes reflect local rainfall patterns, but they are also thought to respond to regional precipitation by paralleling drought-dominated regimes evident in Lake

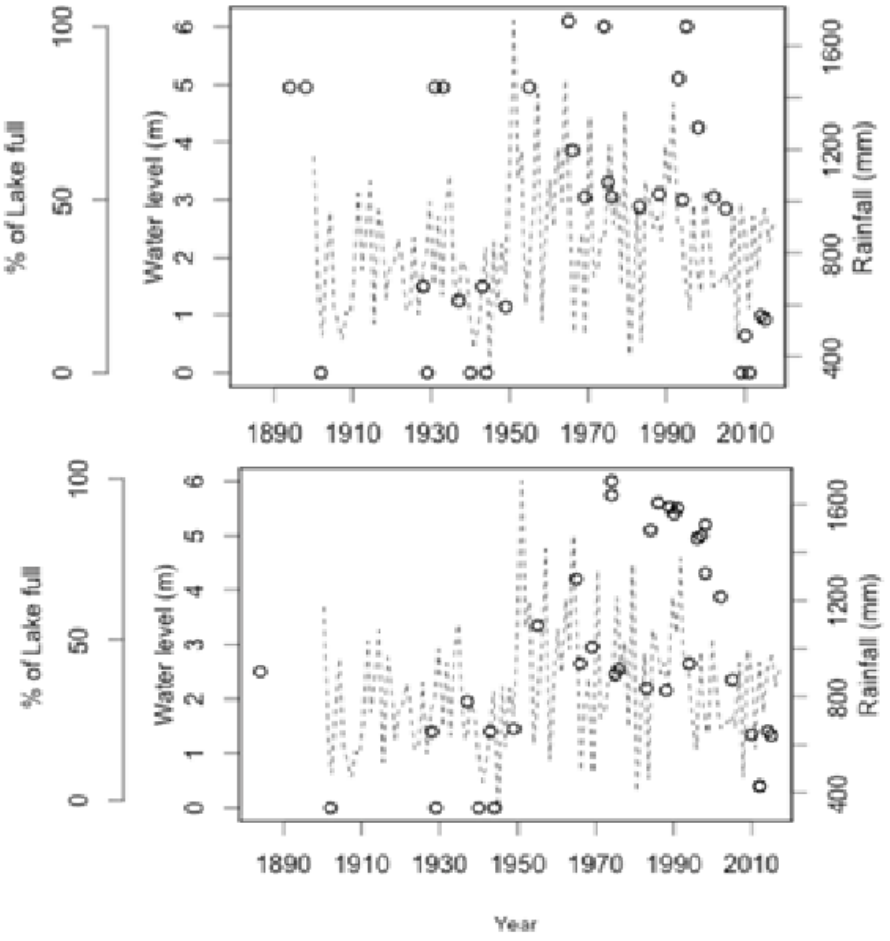

Figure 3.6 Relationship between water level (m) (indicated by the circles), and rainfall (mm) (dashed line) through time in Lakes Werri Berri (top) and Couridjah (bottom). From Kingsford and Schadler (2016) where rainfall data was available from the BOM website, and lake levels were determined directly (measured since 2012 by OEH) and indirectly (through the use of historical photographs and aerial imagery).

George water levels (Riley *et al.,* 2012). Indeed, water levels at Thirlmere Lakes are consistent with the drought- and flood-dominated regimes experienced in south eastern Australia over the past 23 years (Riley *et al.*, 2012). This, however, disagrees with the findings presented in Kingsford and Schadler's (2016) study who statistically analysed long-term rainfall patterns and found that in the years after approximately 1980, a decoupling of the strong correlation between rainfall and water levels occurred at Thirlmere Lakes (i.e., an increasing index of change), and natural variation in climate became less significant in explaining changes in water levels. Analysed changes in the relationship between water levels and rainfall in Kingsford and Schadler's (2016) study was initiated in 1997 at Lake Werri Berri and in 1998 at Lake Couridjah (Fig. 3 6).

3.4.5 Groundwater

Very little is definitively known about groundwater processes at Thirlmere Lakes. Sub-surface water, contained within the alluvial valley-fill, is recharged mainly by rainfall which seeps into the shallow and intermediate groundwater systems in the underlying porous Hawkesbury Sandstone (Riley *et al.*, 2012). Small perched aquifers intermittently occupy the surrounding sandstone ridges and discharge spring flow into the lakes (Russell *et al.*, 2010) (Fig. 3.7). A topographic groundwater divide occurs in the shallow and intermediate aquifers on the far eastern ridgeline of the lakes and influences whether flow will be towards Thirlmere Lakes or east into the adjacent landscape (Russell *et al.*, 2010) (Fig. 3.7). The deep aquifer system occurs in the Narrabeen Group and has no interaction with the hydrology of the lakes. It is divided from the intermediate groundwater system by the Bald Hill Claystone, which is an important regional aquitard and acts to hinder vertical groundwater movement between the Hawkesbury sandstone and Narrabeen Group (Russell *et al.*, 2010). It is presently unclear how deep the Bald Hill Claystone and Narrabeen Group underlie Thirlmere Lakes (OEH, 2016).

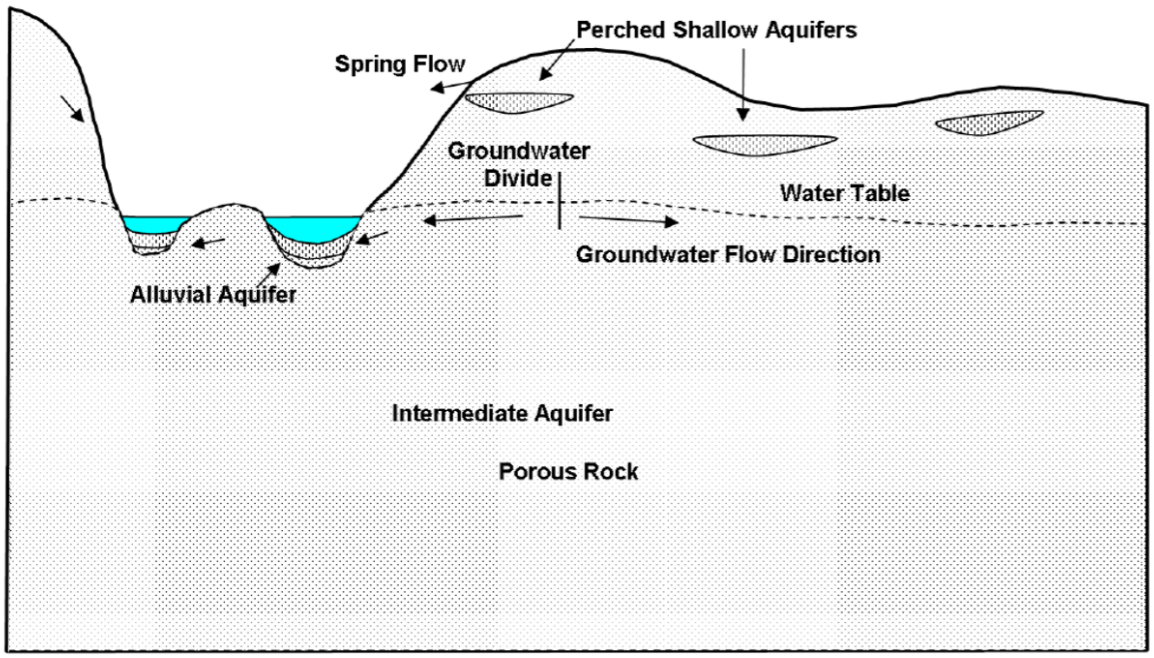

Figure 3.7 Groundwater schematic of the Thirlmere Lakes system. From Russell (2010).

3.5 Flora and Fauna

The flora and fauna of Thirlmere Lakes National Park is generally typical of the Sydney Region. The vegetation of the National Park is predominantly composed of open dry sclerophyll woodland and forest consisting of *Eucalyptus, Casuarina* and *Corymbia* (Black *et al.,* 2006). The Thirlmere Sand Swamp Woodland is unique to the park and occupies approximately 9 ha (0.09 km^2) of the sandy drainage flats of Thirlmere Lakes. It is a low woodland assemblage with an open canopy chiefly comprised of *E. parramattensis* and *Melaleuca linariifolia*, and is particularly prevalent on the eastern side of the lakes and on the adjoining alluvial fan between Lake Couridjah and Lake Baraba (OEH, 2014). Furthermore, the margins of the Thirlmere Lakes often exhibit a particular sequence of vegetation types, those of which are summarised by Rose and Martin (2007) as displayed in Figure 3.8. *Lepironia articulata* (Fig. 3.9), or Grey Sedge, is a freshwater plant presently quite extensive throughout Thirlmere Lakes and could possibly comprise the bulk of the recent peat deposits. The Grey Sedge occupies the lakes in a distinctive pattern. They occur in a rim-like fashion near the edges of the lakes, leaving a border of open water at the lake margins. In other lakes in eastern Australia, the Grey Sedge plays an important role in habitat structure for Lake Biota, and can grow in water up to 5.5 m deep (Marshall and Mcgregor, 2011). Lake Baraba has a distinctive sedgeland of *Lepidosperma Longitudinale* onto which *Melaleuca Linariifolia* is infringing (Rose

and Martin, 2007). Furthermore, *Melaleuca Linariifolia* forests are apparent along the lake margins, particularly on the sill separating Lake Couridjah and Baraba and long Blue Gum Creek (Rose and Martin, 2007).

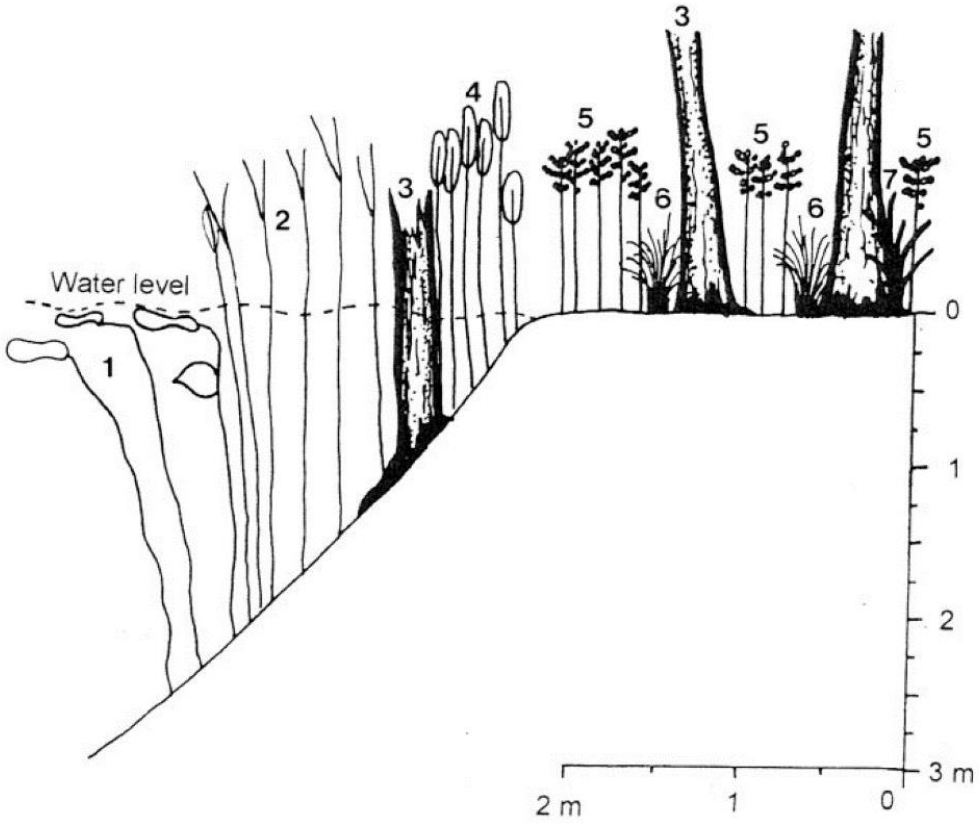

Figure 3.8 - Schematic of general vegetation assemblage on lake margins at Thirlmere Lakes. 1. Brasenia schreberi, 2. Lepironia articulata, 3. Melaleuca linariifolia stump, 4. Eleocharis sphacelata, 5. Lepidosperma longitudinale, 6. Baloskion gracilis, 7. Schoenus brevifolius and S. melanostachys. From Rose and Martin (2007).

The occurrence of a freshwater sponge, *Radiospongilla sceptroides*, in the area has interested previous studies due to its apparent evolutionary adaptation to no longer produce gemmules (biological structures that contribute to the sponge's survival in harsh environmental conditions) (Horsfall *et al.,* 1988; Noakes, 1998). Therefore, their apparent absence may indicate the environmental stability and perennial nature of Thirlmere Lakes over the long term. Likewise, Black *et al.,* (2006) have suggested that this stability encouraged Thirlmere Lakes to act as a refugium for woodland species throughout the Pleistocene and Holocene.

Not only does Thirlmere Lakes hosts at least 10 threatened faunal species including one fish species (Macquarie perch *Macquaria Australasica*), two frog species (Giant burrowing frog

Heleioporus Australiacus, Littlejohn's tree frog *Litoria littlejohni*) as well as a number of vulnerable waterbird species, it also acts as an important link for movement of fauna into the Greater Blue Mountains region (OEH, 2014; Schadler and Kingsford, 2016).

Figure 3.9 View of Lepironia articulata from Lake Werri Berri eastern shore. This freshwater plant can grow up to 2 m in height and presently occupies all of the Thirlmere Lakes.

4. METHODS

4.1 Field Methods

4.1.1 Site Selection and Sub-Surface Data Collection

Lake Couridjah – Lake Baraba Transect (LC-LB Transect)

The majority of fieldwork was undertaken on the sandy alluvial sill that separates Lake Couridjah and Lake Baraba (Fig. 4.1). At this location, alluvial fan sediment from a south-east tributary impinges on the valley floor forming an alluvial sill that separates the two lakes. Cores were obtained across the sill (LC-LB transect) from the Lake Couridjah centre to the Lake Baraba margin. All cores were extracted inside aluminium pipes that had an inside diameter of 74 mm. Accurate core positioning was achieved through real time kinematic (RTK) digital geographic positioning system (DGPS).

Figure 4.1 Exact locations of all cores obtained during this study.

Sill sub-surface characteristics

Sub-surface investigation of the sill itself was undertaken using a hand auger (locations HA1, HA2, HA3, HA4 and HA5) achieving depths ranging from 3 - 7.75 m. Sediment from the auger holes were logged in the field (colour, texture, sorting, and changes in grain size) with samples collected at and within every stratigraphic unit. In addition, a vibracore was used to obtain one core (HA2_CORE) on the sill between Lake Couridjah and Lake Baraba.

Surface Sample Collection

Surface samples were collected at 2-5 cm depth at approximately 5 m intervals along the LC-LB transect, as well as randomly along a small, inactive tributary stream dissecting the alluvial fan adjacent to Lake Couridjah and Baraba (Fig 4.2). The stream generally followed the apex

Figure 4.2 Positions of surface sample collection across the LC-LB Transect and the adjacent alluvial fan.

of the fan, which was previously inferred through LiDAR imagery. These samples were sieved through a 500 µm sieve to remove surface debris before they were analysed for grain size as described in section 4.2.3. Furthermore, small clippings of living plant samples were collected for isotopic analysis, along with surface soil samples directly underneath the selected plant. The living vegetation samples included the species *Lepironia Articulata, Lepidosperma Longitundinale, Melaleuca Linariifolia* and *Acacia Longifolia* due to their presence along the LC-LB transect, and because they approximately occurred in a sequence similar to the generalised lake margin vegetation zonation for Thirlmere Lakes, as inferred by Rose and Martin (2007) and shown in Chapter 3, Figure 3.9. The living vegetation and modern soil samples were dried and crushed for further analysis.

Lake and Lake Margin Coring

One lake centre core and four lake margin cores were extracted using either the vibracore, a percussion corer or by a non-mechanical push-core method. LC2 was taken from the centre of Lake Couridjah and was 6.8 m in length. This core was extracted using the vibracore, deployed from a 3 m quadrapod and operated from within a small, unmotorized boat (Fig. 4.3). A 9 m length aluminium pipe was slowly vibrated into the lake sediment with manual rotations to assist shearing from the outside sediment. LC2 was carefully extracted and drained of excess water once taken back to shore, then cut into 1.5 m lengths, capped, taped and frozen that subsequent afternoon. LC1 was taken from the contemporary southern margin of Lake Couridjah and reached a depth of 6.2 m. LB1 was extracted from the eastern margin of Lake Baraba, using a combination of the vibracore and percussion corer to achieve a depth of 1.7 m. Due to the extremely dense, cohesive clay beneath Lake Baraba, coring was limited to only 1.7 m as the equipment was not able to achieve a greater depth.

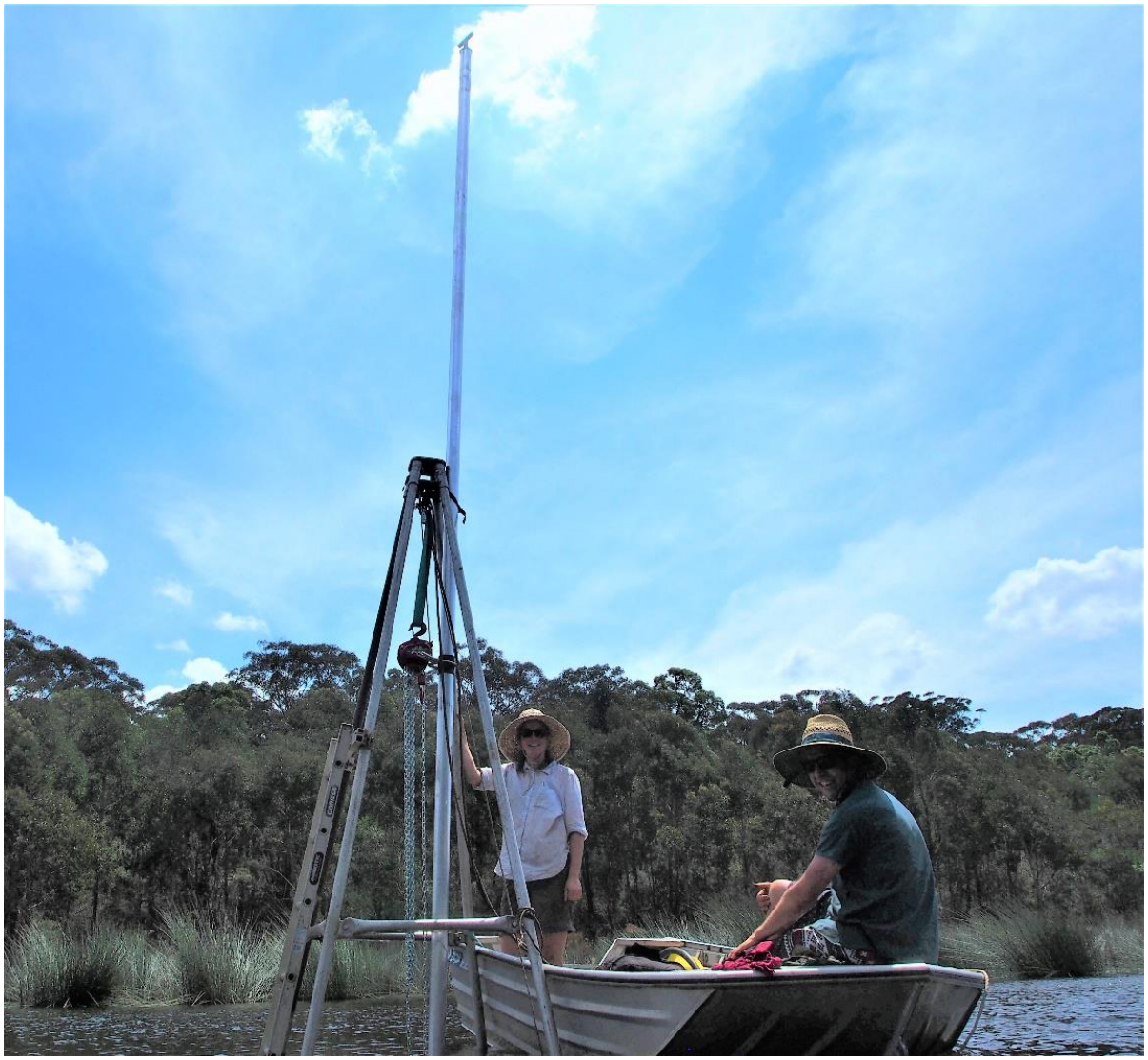

Figure 4.3 Set-up used for the extraction of LC2 (Lake Couridjah core) before it was lowered and taken to shore.

Core Compaction

Core compaction occurred in the cores LC2, LC1, LC1.1, LB1, and LB1.1, and ranged from 60 – 8 cm, representing 4.8 - 21.4 % of the total core lengths (Table 4.1).

Table 4.1 – Details of the cores in this study. The cores are listed according to their positioning northeast to southwest along transect LC-LB.

Core Code	Easting	Northing	Surface Elevation (m AHD)	Method	Core Length (m)	Core Compaction (m), percent of total core length
LC2	0273710	6209399	300.9	Vibracore	6.8	0.6, 8.8%
LC1	0273699.553	6209210.156	301.49	Vibracore	6.2	0.3, 4.8%
LC1.1	0273699.553	6209210.156	301.49	Push Core	1.17	0.25, 21.4%
HA3	0273683	6209188	303.78	Hand Auger	3	N/A
HA2	0273679	6209170	305.26	Hand Auger	4.55	N/A
HA2_CORE	0273679	6209170	305.26	Vibracore	4.55 - 7	0.15, 6.12%
HA1	0273676	6209159	306.5	Hand Auger	6.6	N/A
HA5	0273646	6209151		Hand Auger	7.75	N/A
HA4	0273609	6209145	305.45	Hand Auger	3.3	N/A
LB1	0273566	6209113	305.12	Vibracore and Percussion Corer	1.7	0.11, 6.5%
LB1.1	0273566	6209113	305.12	Gauge Auger	0.8	0.08, 10%

4.2 Laboratory Analyses

Surface and sub-surface samples were analysed both at UOW and externally.

4.2.1 Subsampling

The cores LC2, LC1, HA_CORE and LB1 were all subsampled for approximately 1 cm^3 of sediment at 5 cm intervals. These samples were bagged, labelled and placed in cold storage at approximately 4^oC until further analysis.

4.2.2 Loss-on-Ignition (LOI) Analysis

LOI analysis was performed on the cores LC2, LC1, LB1 and HA1 to obtain the percentage of organic content. The process involved oven drying approximately 1 cm^3 samples at 100^oC for at least 12 hours. After drying, samples were then crushed with an agate mortar and pestle and placed in a muffle furnace for at least 16 hours at 375^oC. Each sample was weighed to four decimals places at each stage in the process. Specific details of the LOI procedure used is detailed in Appendix C.

4.2.3 Methods of Grain Size Determination in Lacustrine Sediments

The Malvern Mastersizer 2000 at the University of Wollongong (UOW) School and Earth and Environmental Science (SEES) was used to determine the grain size distribution of the minerogenic material within samples by adding a small but representative portion into a mixing beaker to attain adequate beam obscuration. Five grain size distributions, as well as an averaged result, were then subsequently achieved through laser diffraction. Between each measurement the instrument was flushed clean with tap water and the background was measured to re-calibrate the machine. However, minerogenic material from very fine, cohesive and organic-rich lacustrine sediments is traditionally hard to measure as all organic material must first be removed (Murray, 2002; Vaasma, 2008). In the core LC2, some samples were exceedingly organic or clay rich. For this core, two different pre-treatment methods (see below) were conducted to check for reproducible results. A comparison of the results derived from the different pre-treatments is presented in Chapter 5, section 5.1.1 and again in Appendix B.

Pre-treatment A: Post-LOI

This method was used for the cores LC2, LC1 and HA1. These samples were firstly crushed and then combusted in a muffle furnace, as described in section 4.2.2, to remove organics. Afterwards, samples were run through the Malvern Mastersizer 2000 to obtain a grain size measurement. While this proved a suitable method for the cores LC1 and HA1, some of the organic and clay rich samples from the LC2 core cemented into sand-sized aggregates and thus were incorrectly measured as fine sand. The affected samples from LC2 were then saturated with tap water after combustion and placed in an ultrasonic bath for at least 2 hours to disaggregate the clay particles that cemented together. Samples seemingly 'not-affected' by the LOI post-combustion cementation, i.e. that were measured as clay and silt, also underwent ultrasonic diffraction as a control measure.

Pre-treatment B: Hydrogen Peroxide Digestion

As an alternative to the post-LOI method, digestion by hydrogen peroxide (H_2O_2) to remove organics was conducted. This method was only used for the LC2 core. The LC2 core was sub-sampled for 1 cm^3 samples approximately every 30 cm. These samples were pre-treated with 60 mL of 15 % H_2O_2 in order to oxidise organic material. The samples were left for

approximately 3 days until there were no visible signs of reaction, and then subsequently put through the Malvern Mastersizer for grain size analysis.

4.2.4 Elemental composition

The elemental composition of LC2 was determined through the ITRAX micro X-ray Fluorescence (XRF) core scanner housed in the Environmental Radioactivity Measurement Centre at ANSTO, Lucas Heights. An optical high-resolution image and radiographic image at a resolution of 500 µm was obtained for the core. X-ray Fluorescence (XRF) scans were performed using a molybdenum tube set at 30 kV and 55 mA with a dwell time of 10 s. A step size of 1000 µm (1 mm) was selected to capture elemental variations occurring in laminations observed in the radiographic image. Furthermore, ratios of incoherent and coherent scattering measurements (Mo Inc/Coh) were produced by the core scanner, which can be used as a proxy for the organic matter content. The data was evaluated using Q-Spec 15.1.

4.2.5 Stable δ13C and δ15N Isotopes, %C, %N and C: N

Stable δ13C and δ15N Isotopes, %C, %N and C: N were determined 136 bulk sediment samples from the core LC2, as well as 10 modern soil, and 6 living vegetation samples, along the LC-LB transect (Fig. 4.2) at the University of Adelaide, Department of Earth Sciences in the Isotope Mass Spectrometry Facility. LC2 was subsampled every 5 cm for 1 cm^3 samples which were dried at 60^oC for two days and then manually crushed with an agate mortar and pestle to homogenise the material. Some comparative samples were acidified, whereby 2 mg of sample was weighed into silver cups and moistened with a single drop of DI water. The samples were then placed into a vacuum desiccator with 12 M HCl in the bottom and fumigated for 4 hours in order to remove carbonate material. Afterwards, samples were dried in a 40^oC oven for 72 hours. Both acidified and non-acidified samples were transferred in covered tin cups and placed into a 40^oC oven before analysis. Both sample sub-sets were then combusted in a EuroVector Elemental Analyser (EA), in conjunction with constant flow to a Nu Horizon isotope ratio mass spectrometer (IRMS). Glutamic acid, glycine, TPA and USGS-42 was used to calibrate samples at the start and end of every run. Every nine samples, glycine standards were checked and one repeat sample was analysed. This same method was undertaken for the modern soil and living vegetation samples, however there were no duplicate acidified samples.

4.2.6 Accelerated Mass Spectrometry (AMS) Carbon-14 Dating

A total of 10 samples at selected depths, containing charcoal fragments, charred material or bulk organic content, were dated to obtain approximate chronologies of the LC2 core and of the sill sediment. Analysis was undertaken by either Beta Analytic Inc. (USA) or University of Waikato, Faculty of Science and Engineering Radiocarbon Dating Laboratory (NZ). All analysed charcoal and charred material samples were pre-treated with an acid/alkali/acid method; samples were firstly cleaned then washed in hot HCl, then rinsed and treated with multiple hot NaOH washes. The NaOH insoluble fraction was treated with hot HCL, filtered, rinsed and then dried. Samples of organic sediment firstly had visible contaminates removed and then washed multiple times with acid. All samples were then dated using Accelerator Mass Spectrometry (AMS). For a detailed description of AMS dating, refer to Beta Analytic Inc. (2018). Complete radiocarbon dating reports are presented in Appendix D.

5. RESULTS

5.1 Core Descriptions and Sedimentology

In this section, the core descriptions, LOI analysis and grain size data is detailed for three primary cores; LC2 representing the centre of Lake Couridjah, LC1 representing the southern margin of Lake Couridjah and HA1 representing the sill. All other secondary cores, apparent in Figure 5.1 and including the surface sediments of the alluvial fan near Lake Couridjah and Lake Baraba, will be subsequently described in lesser detail. Additional information is provided in Appendix B, which details the core logs of each core. Furthermore, loss-on-ignition (LOI) data is presented in Appendix C and the raw grain size data, as well as particle distribution analysis and a comparison of methods for grain size determination for the core LC2, is detailed in Appendix F. Interpretation of grain size and sorting was assisted using Folk (1974, pg. 40 – 48) and Blott and Pye (2001, Table 1).

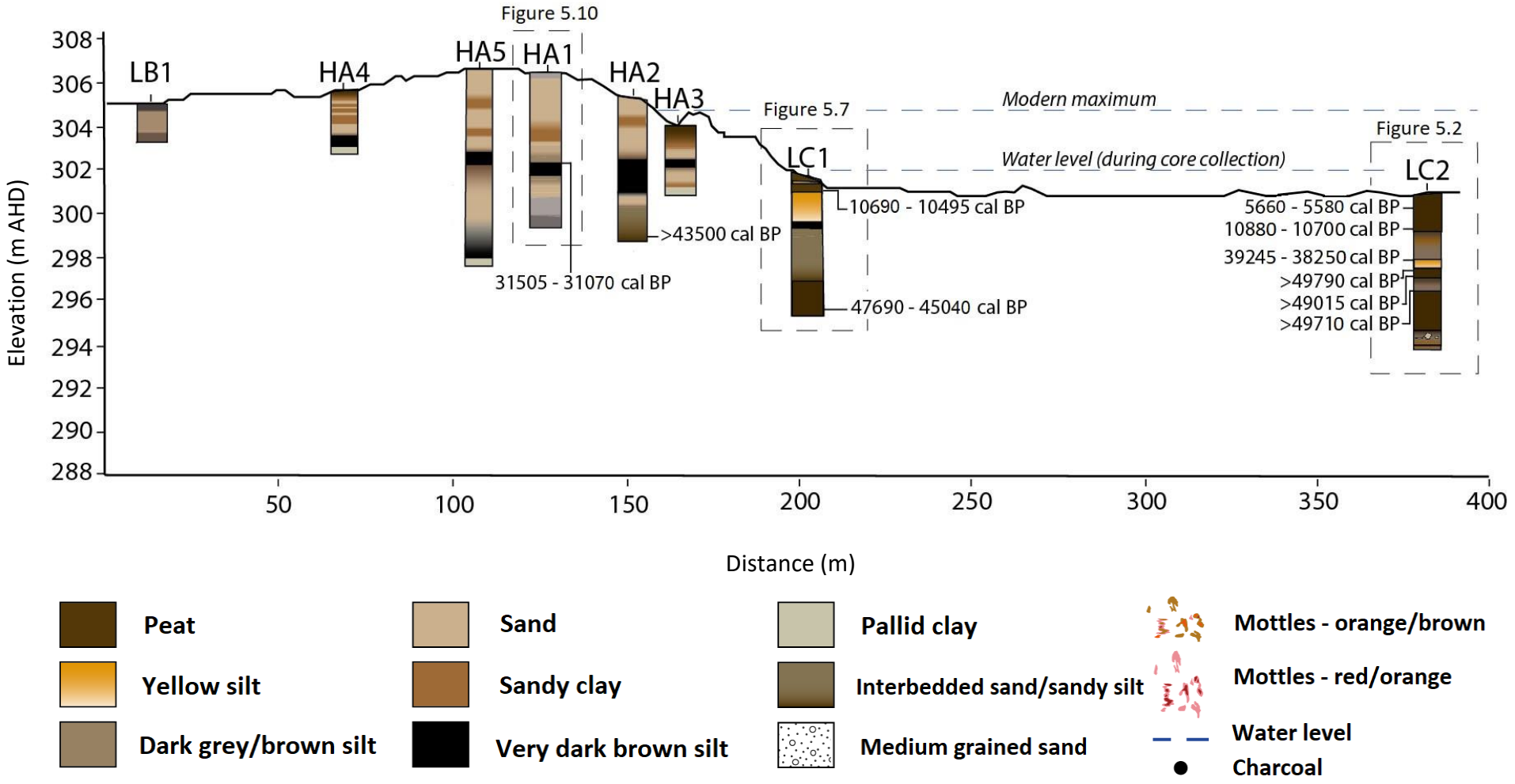

Figure 5.1 Illustration of the stratigraphic findings of all cores in this study, depicted on the LC-LB Transect topographic profile. Radiocarbon dates are shown at their respective depths (Table 5.3). Furthermore, the water level of Lake Couridjah at the time of core collection is noted, as well as the modern maximum as inferred by a shift from Thirlmere Sand Swamp Woodland to a sedgeland dominated by Lepironia Articulata; a species that preferentially resides in saturated environments. Note the legend at the bottom of the figure indicates the general sedimentary characteristics of the core logs.

5.1.1 Primary Cores

LC2 – Lake Couridjah centre core

LC2 was a 6.8 m continuous core taken from the centre of Lake Couridjah with 8.8% core compaction (Figure 4.1; 5.2; Table 4.1). Firstly, the grain size for LC2 will be presented, comparing the results from two different pre-treatment methods (pre-treatment A: post-LOI and pre-treatment B: post hydrogen peroxide digestion) outlined in Chapter 4, section 4.2.3. This grain size information will then be incorporated into the subsequent LC2 core description. All particle size distributions graphs detailed in the core description of LC2 were derived from the pre-treatment B dataset. Note; the grain size data related to all other primary cores was achieved through pre-treatment A, which will be subsequently described.

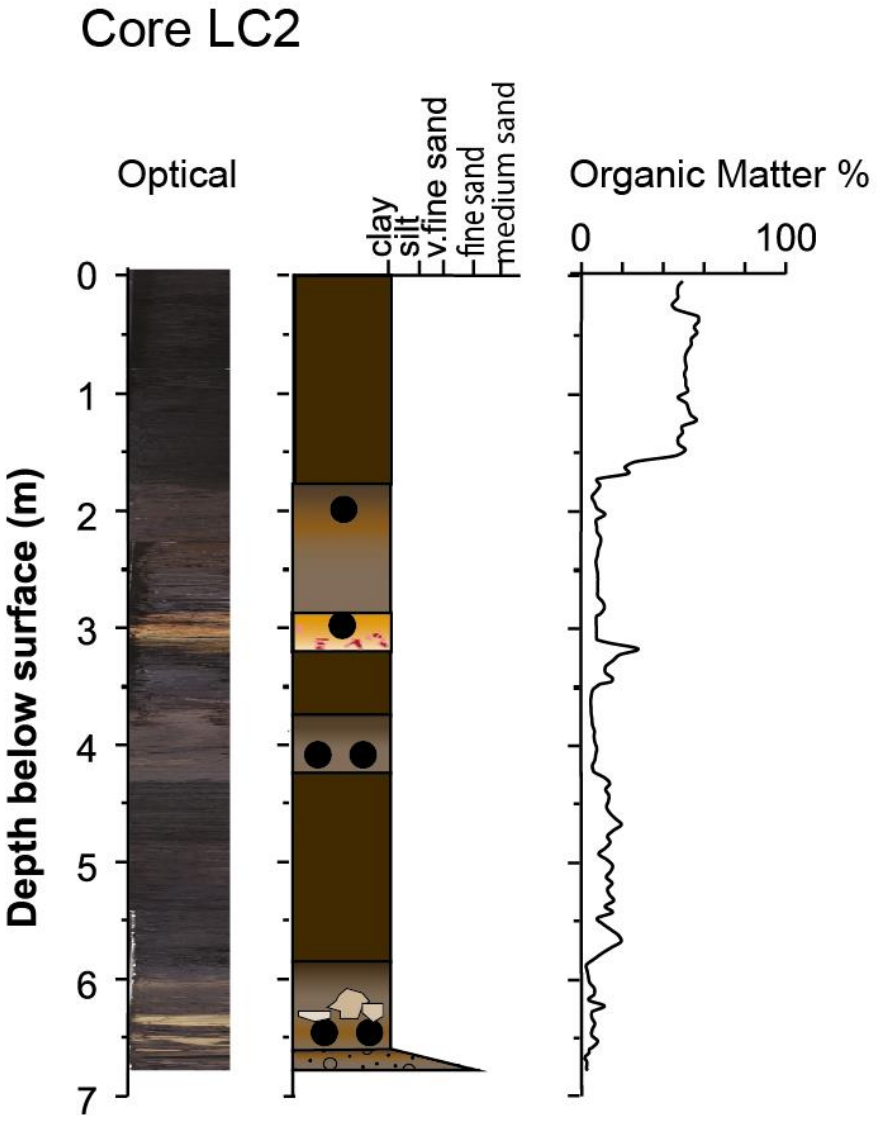

Figure 5.2 Sedimentary details of the core LC2. The left hand panel shows a photograph of the core. The second panel displays the interpreted stratigraphy of the core (refer to the legend provided in Figure 5.1). The LOI results is also included in the right hand panel. LC2, as presented here, is uncorrected for core compaction.

Grain size determination

Two different pre-treatment methods were used for the core LC2 in order to remove organic material before subsequent grain size analysis. Pre-treatment A used LOI to combust the organic material followed by laser particle size analysis. However, in some clay rich samples in LC2, (e.g. between 2.85 – 4.25 m, Figure 5.2), small sand-sized aggregates formed during combustion. All affected samples, as well as some 'unaffected' samples as a control (i.e. samples that were consistently fine silts), then underwent ultrasonic diffraction to disaggregate them. The results of pre-treatment A are shown in Figure 5.3 (A).

Pre-treatment B involved digesting the organics in samples with 60 mL of 15 % hydrogen peroxide before they underwent grain size analysis. The results of pre-treatment B are shown in Figure 5.3 (B).

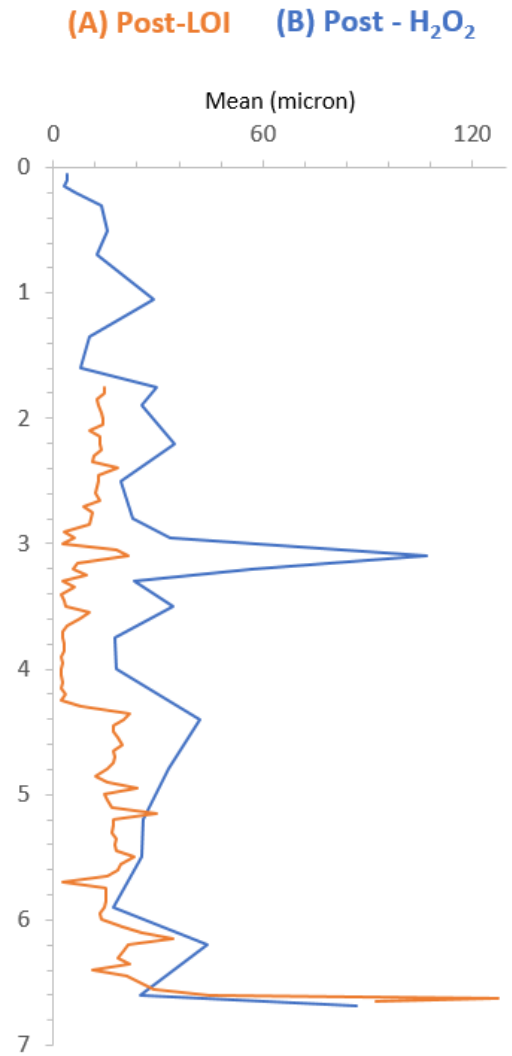

Figure 5.3 (A) Shows the grain size results for pre-treatment A, using combustion to remove organics. Note; after combustion of the highly organic samples in the upper 1.75 m, not enough material was left over for accurate beam obscuration during grain size analysis, so there is no data for this region. (B) shows the grain size for pre-treatment B, which used digestion by hydrogen peroxide to remove organics.

Figure 5.3 shows that while grain size in the LC2 core is generally a fine to coarse silt (~4 – 30 µm), there are increases in grain size at 3.1 m, 4.3 m and 6.8 m depth. These increases are generally represented by both pre-treatment methods, however pre-treatment B (post-H_2O_2) appears to over-represent grain size compared to pre-treatment A (post-LOI). This is interesting considering pre-treatment A was thought to over-represent grain size due to clay cementation during combustion. Furthermore, while the majority of 'unaffected' (control) samples from pre-treatment A remained unchanged after ultrasonic displacement, one sample from 5.7 m depth appeared significantly finer (Appendix B), suggesting that region of core may be finer-grained than presented in Figure 5.3. The reasons and implications of this are further discussed in Chapter 6, section 6.6. In the meantime, the grain size results for pre-treatment B will be used for subsequent core description of LC2, due to the completeness of data compared to pre-treatment A (i.e. missing upper 1.75 m).

LC2 Core Description

0 – 1.75m

The upper 1.75 m of core LC2 mostly consists of homogenous organic material (peat) (Fig. 5.4), containing the fibrous remains of macrophytes which become more humified with

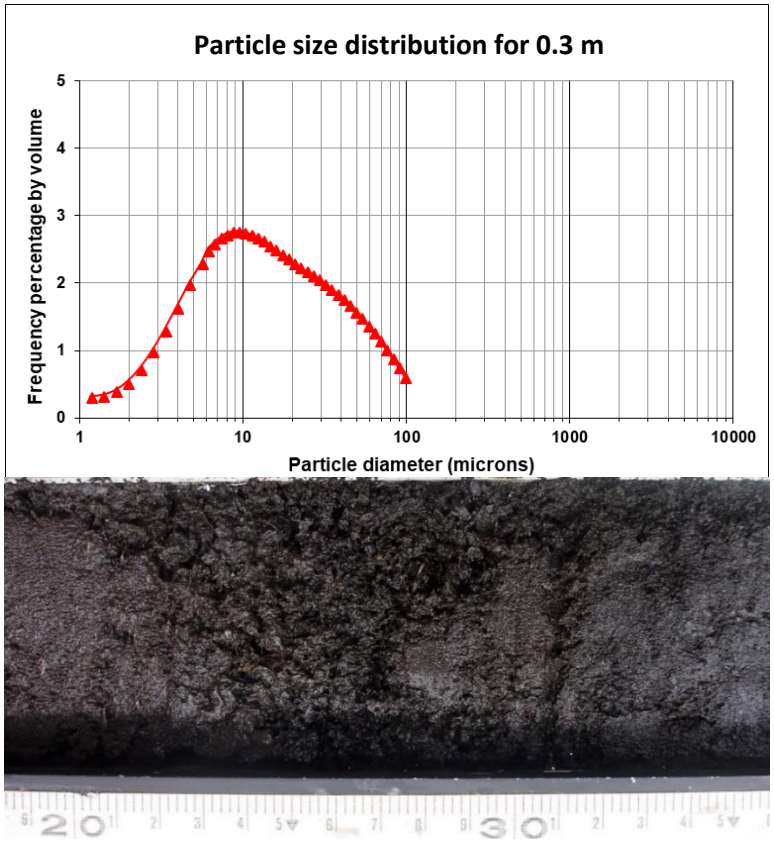

Figure 5.4 The upper panel shows the particle size distribution for 0.3 m depth, which is generally representative of the particle size distribution of the entire peat unit. The lower panel shows a core photograph at the corresponding depth. Notice the change in peat texture between 0.2 – 0.29 m.

depth. This sediment is high in organic matter content, ranging from 44 – 58 % (Fig. 5.2). Within this peat, a change in texture occurs between 0.2 – 0.29 m, whereby the peat becomes less cohesive and condensed into small (>0.5 cm^3) angular clumps (Fig. 5.4). Grain size values reflect a medium silt, ranging from 5 – 30 µm, with a unimodal distribution at ~9 µm (Fig. 5.4).

1.75 – 2.86 m

At 1.75 m there is a gradual transition from peat into inorganic dark grey/brown silt. This silt contains numerous charcoal fragments and olive yellow mottles. Organic matter content ranges between 5.1 – 11.5 % through this unit and grain size reflects a medium to coarse silt (Fig. 5.2 - 5.3).

2.86 – 3.19 m

An abrupt transition occurs at 2.86 m to light yellow silt with bright orange mottles (Figure 5.5). There is abundant charcoal at both the 2.86 m and 3.19 m boundary of this unit. Grain

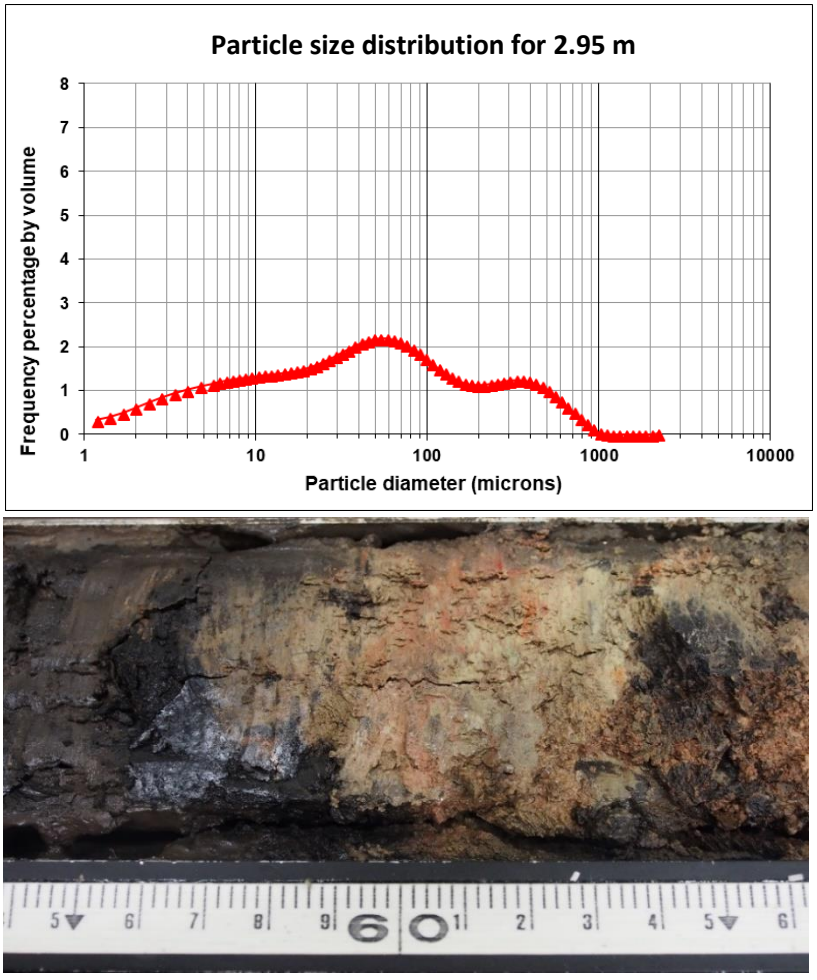

Figure 5.5 The upper panel shows the particle size distribution for 2.95 m depth, which is generally representative of the particle size distribution of the entire light-yellow silt unit. The lower panel shows a core photograph at the corresponding depth (indicated at 65cm on the photographed scale).

size increases to a very fine sand and has a bimodal particle distribution with major modes at 50 µm and 250 µm (Fig. 5.5).

3.19 – 3.66 m

LC2 gradually transitions by 3.19 m into very dark brown sediment. This transition is marked by an abrupt increase in organic matter content from 7.5% to 27.8% and a decrease in grain size to a coarse silt (Fig. 5.3). This dark organic sediment then grades into dark grey/brown silt at 3.66 m depth.

3.66 – 4.24 m

The dark grey/brown silt continues until 4.24 m and is characterised by abundant charcoal and consists of low organic matter content (4.5 – 7.5%) and medium silt.

4.24 – 5.77 m

After 4.24 m depth, the core grades into a dark organic unit similar to that occurring between 3.19 and 3.66 m depth, however, the unit below 4.24 m depth is bedded with thin laminations of lighter coloured material. Here, there is variable organic matter content ranging from 7.7 – 19.6 % (Fig. 5.2) which approximately corresponds to the variations in colour, with the lighter material being inorganic. There is also a slight increase in grain size to a very coarse silt at this depth (Fig. 5.3)

5.77 – 6.8 m

Between 5.77 m depth and the base of the core at 6.8 m depth, dark grey/brown clay occurs, containing intermittent zones of pallid clay, charcoal fragments and variable but low organic matter. At 6.68 m depth a prominent medium grained sand layer occurs, with a unimodal distribution at 350 µm (Fig. 5.6).

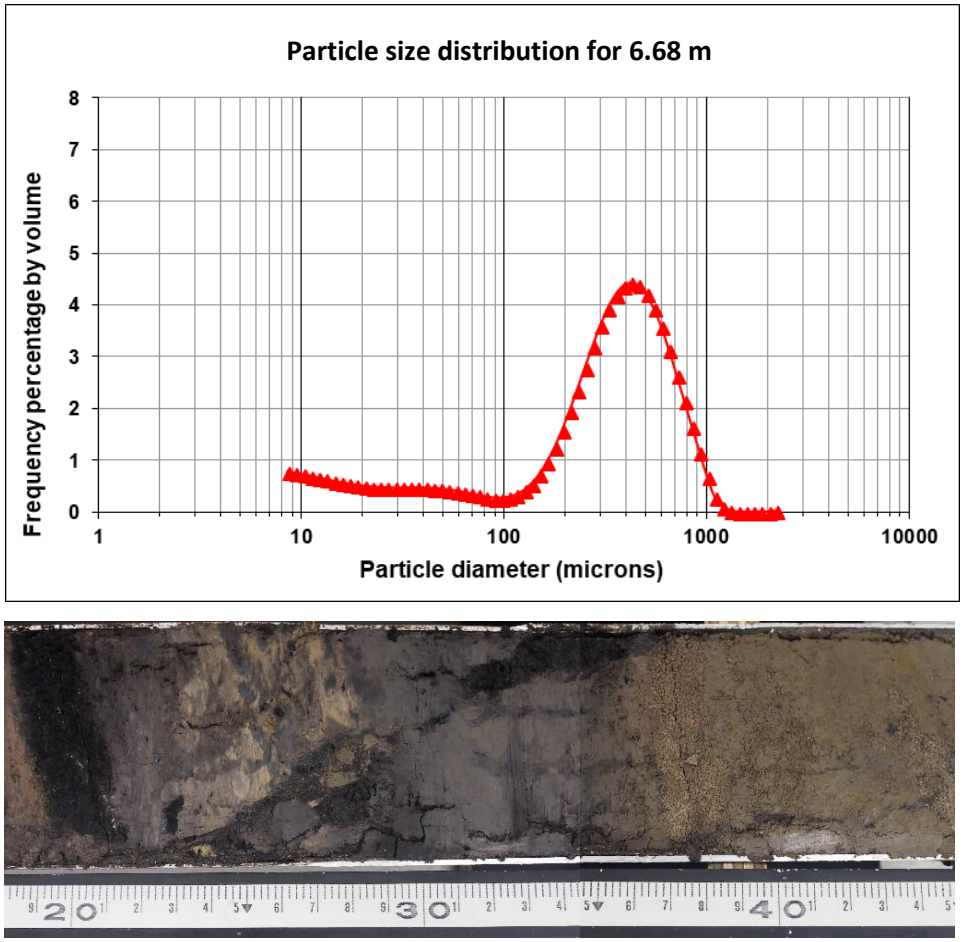

Figure 5.6 The upper panel shows the particle size distribution for 6.68 m depth, which is only indicative of the sand lens within dark grey/brown clay unit. The lower panel shows a core photograph at the corresponding depth (indicated at 38cm in the photographed scale). Notice the complex changes in texture and colour throughout this unit.

LC1 – Lake Couridjah margin core

LC1 was a 6.2 m core taken from the southern margin of Lake Couridjah with 4.8% core compaction (Figure 4.1; 5.7 and Table 4.1).

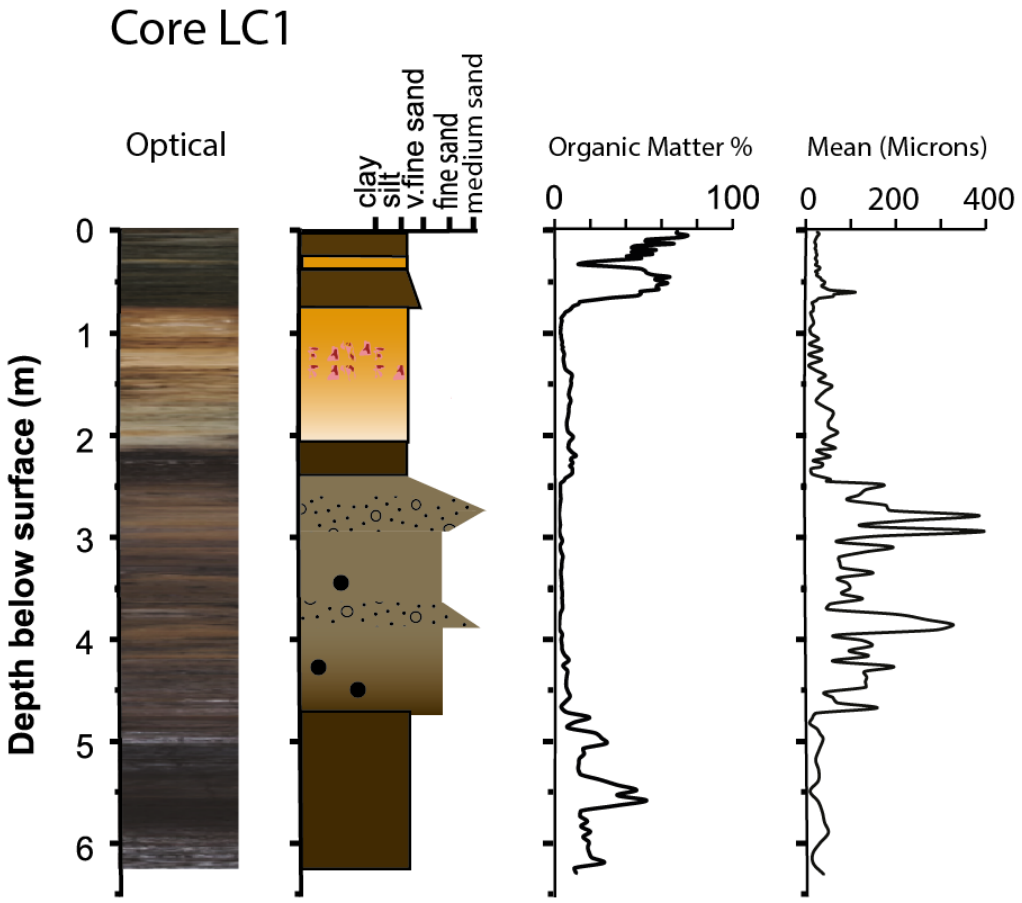

Figure 5.7 Sedimentary details of the core LC1. The left hand panel shows a photograph of the core. The second panel displays the interpreted stratigraphy of the core (refer to the legend provided in Figure 5.1). The LOI results (third panel) and mean grain size (micron) (right hand panel) is also included. LC1 presented here is uncorrected for compaction.

0 – 0.8 m

The upper 0.8m of LC1 consists of generally homogenous peat made up of unimodal and poorly sorted coarse silt with a small peak to very fine sand at 0.6 m depth (Figure 5.7; Appendix F). A minor lens of light yellow silt occurs between 0.33 – 0.335 m depth, implying subaerial exposure of this layer. Organic matter content peaks at 74% just below the surface, decreasing to 11.7% at the light yellow silt lens, then increasing again to 63.2% at 0.8 m depth.

0.8 – 2.13 m

From 0.8 – 2.13 m depth there is then an abrupt transition to a light yellow medium grained silt containing occasional red/orange mottling. This unit is marked by a rapid decrease in organic matter content (<4 %) and alternates between a cohesive to a blocky and 'crumbly' structure, while the colour gradually becomes more pallid down core (Fig. 5.8).

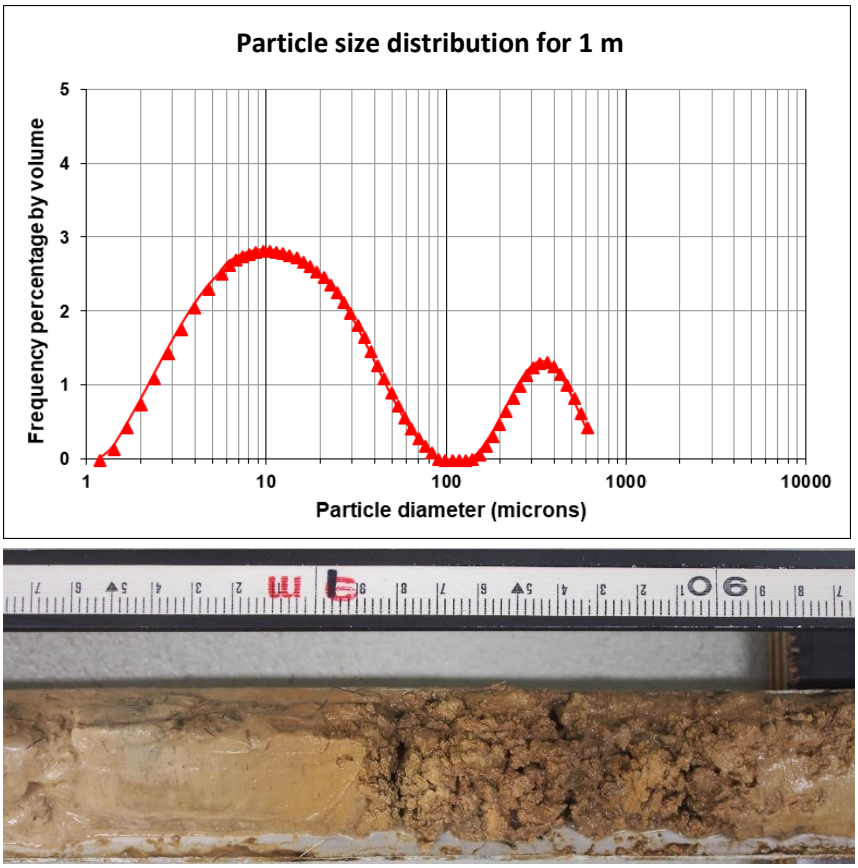

Figure 5.8 The upper panel shows the particle size distribution for 1 m depth, which is generally representative of the particle size distribution of the entire light-yellow silt unit. The lower panel shows a core photograph at the corresponding depth. Notice the change between cohesive and 'crumbly' structure.

2.13 – 2.43 m

At 2.13 m depth there is then a clear transition to a very dark brown unit, which continues until 2.43 m depth. Organic matter content only increases slightly to 9.9 % in the unit, while grain size decreases slightly to a medium silt.

2.43 – 4.7 m

LC1 then grades into a thick layer of medium to coarse grained, very poorly sorted sand interbedded with grey/brown sandy silt with charcoal fragments becoming increasingly abundant. Organic matter was very low (0.3 – 6.5 %) and grain size is highly variable, ranging between ~70 µm in the sandy silt to >300 - 400 µm in the sand (Figure 5.9). In some sand interbeds, granules of quartz, up to 3000 µm in diameter, existed.

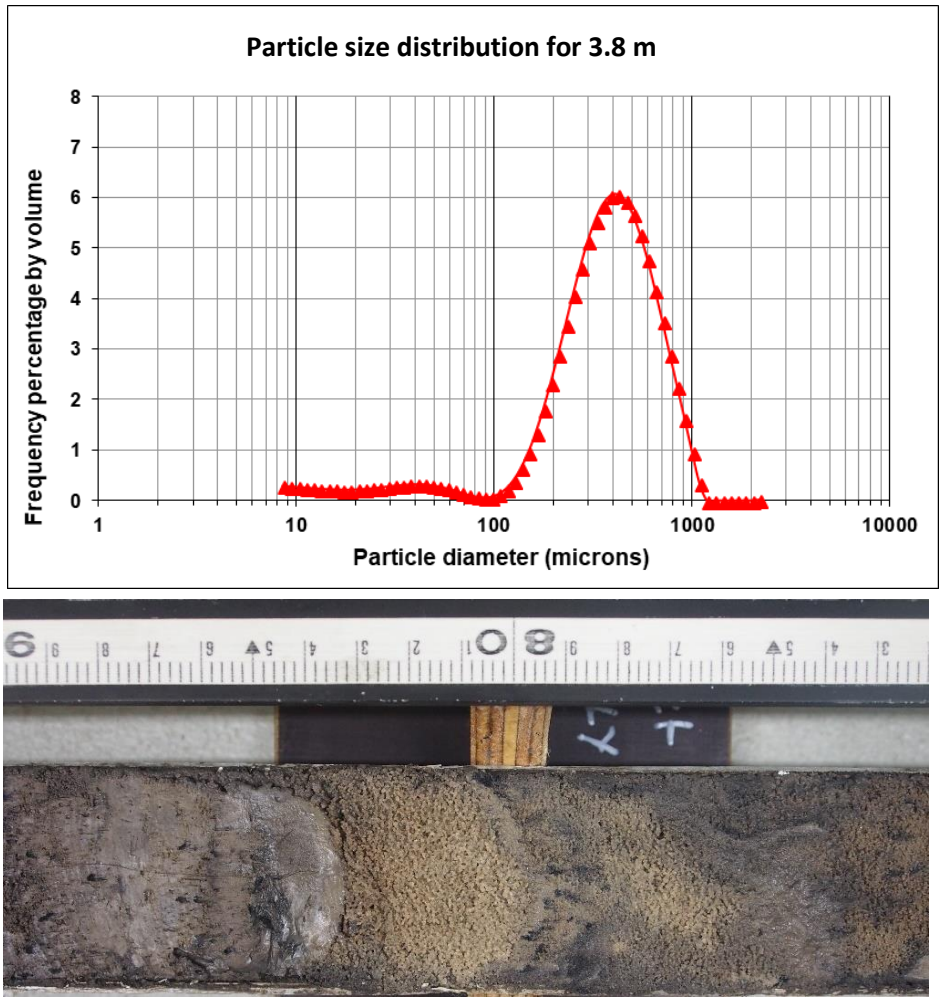

Figure 5.9 The upper panel shows the particle size distribution for 3.8 m, which represents the typical particle size distribution of the interbedded sand. The lower panel shows a core photograph at the corresponding depth (labelled as 80 cm in the photographed scale). Notice the abrupt transitions between the sand and clay interbeds.

4.7 – 6.2 m

At 4.7 - 6.2m depth a very dark brown organic sediment occurs with subtle laminations, demarcated by a lighter grey/brown colour. Organic matter increases with a significant peak to 50 % at 5.5 m depth, and grain size greatly decreases with slight variability between medium silt to very fine sand (~11 – 52 µm).

HA1 – sill core

HA1 is a 6.6 m augured core taken from on top of the sill and is predominantly sand which abruptly alternates with more organic sandy silt (Figure 5.1; 5.10).

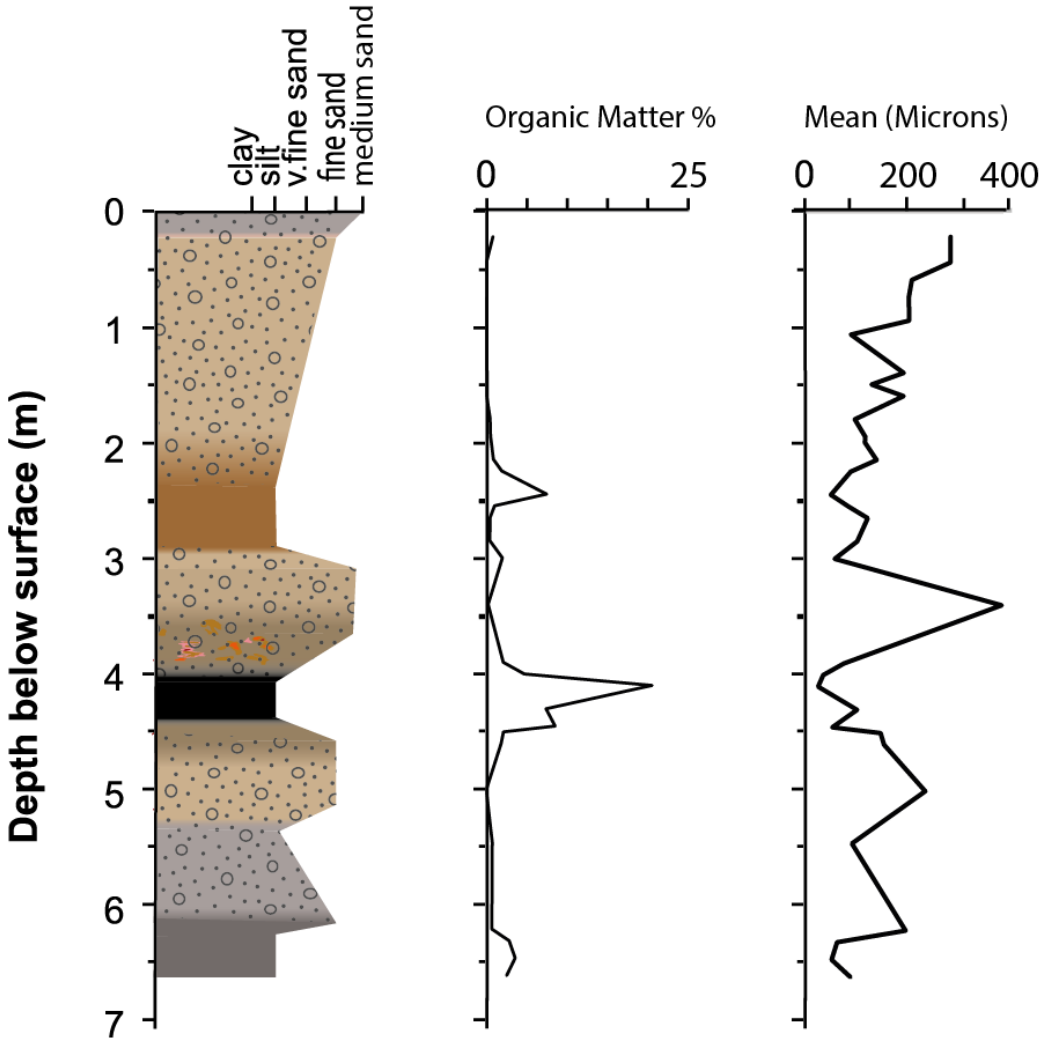

Figure 5.10 Sedimentary details of the HA1 auger hole. The left hand panel displays the interpreted stratigraphy of the core (refer to the legend provided in Figure 5.1). The LOI results (centre panel) and mean grain size (micron) (right hand panel) is also included.

0 – 2.3 m

The upper 2.3m of HA1 is composed of clean, medium grained sand that gradually grades to a very fine orange-brown sand at 2.3 m depth. This upper 2.3 m of sand is generally poorly to very poorly sorted, and most samples exhibited a multimodal grain size distribution with a major sand mode at 350 – 500 µm and minor silts peaks at 7 µm and 15 µm (Figure 5.11; Appendix F).

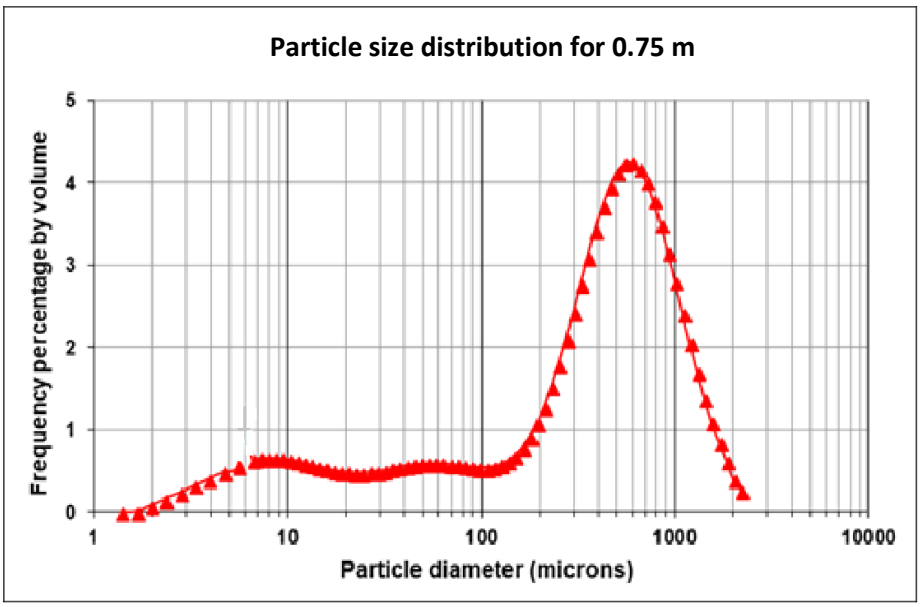

Figure 5.11 Shows the particle size distribution for 0.75 m, which is generally representative of the particle size distribution of the entire unit of sand above 2.3 m.

2.3 – 4.1 m

Between 2.3 – 3m there is a sandy silt unit (organic matter ≤7 %, Fig. 5.10), which is distinctly darker grey-brown and more mottled than both the underlying and overlying sand. At 3 m depth medium grained sand occurs and contains mottles which becoming more prominent with depth and containing wood and charcoal fragments after 3.9 m depth.

4.1 – 6.6 m

There is then an abrupt boundary at 4.1 m into a mottled, very poorly sorted and very dark brown organic sandy silt to coarse (organic matter 5 – 20 %) that extends to 4.45 m (Fig. 5.12).

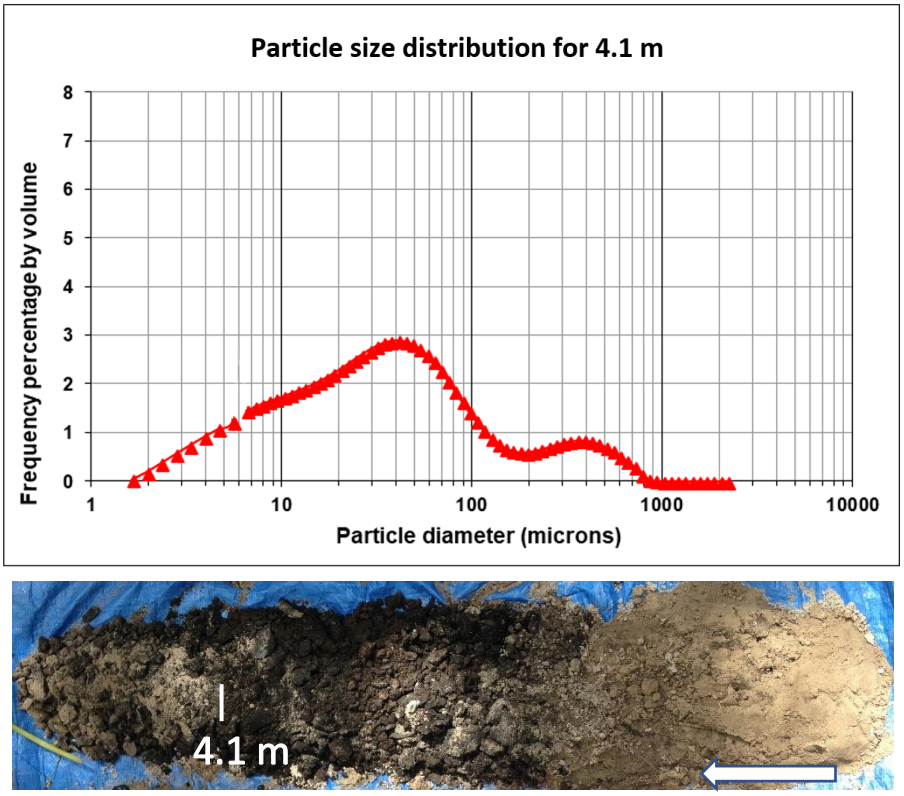

Figure 5.12 The upper panel shows the particle size distribution for 4.1 m, which is generally representative of the particle size distribution of the entire very dark brown sandy clay. The lower panel shows a photograph of the augured material at the corresponding depth.

At 4.45 m depth an abrupt change occurs to a fine grained, very poorly sorted pallid sand, which gradually becomes darker and more clay-rich to 6.2 m depth. From 6.2 – 6.6 m there was dark grey silty sand that became saturated after the water table was encountered at 6.3 m.

5.1.2 Secondary Cores

LB1 – Lake Baraba margin core

LB1 was a 1.7 m core from the eastern margin of Lake Baraba with 6.5 % core compaction (Figure 4.1; Table 4.1). The upper 0.36 m of LB1 consisted of saturated homogenous peat (organic matter 3.3 – 32 %), containing the fibrous remains of macrophytes which became more humified with depth. At 0.36 m depth there was an abrupt boundary into a drier and denser brown clay, containing distinct orange mottling and the remnants of plant roots. This clay gradually became darker and less mottled with depth, with organic matter generally just

below 5 %. A clear boundary occurs at approximately 1.3 m to a grey/brown clay, with a slight decrease in organic matter to 2.3 % that extends to 1.7 m.

HA2, HA3, HA4 and HA5

Complete core logs of HA2, HA3, HA4 and HA5 (Fig. 5.1) are presented in Appendix B. These cores, all taken from the sill between lakes Couridjah and Baraba, displayed predominately poorly to very poorly sandy deposits alternating with sandy silt.

HA3 was taken lower on the sill and closer to Lake Couridjah than the other sill cores (Fig. 5.1), and the upper 0.35 m consisted of reasonably dry, fibrous peat deposits. The majority of HA3 consisted of medium-coarse sand, interbedded with a distinct very dark brown sandy silt between 1.5 – 1.83 m. Another interesting feature in HA3 was the occurrence of a pallid yellow clay at 2.75 m. The core sediments at this location became progressively saturated from approximately 2.3 m onwards as the water table was encountered. Interestingly, the pallid clay appeared reasonably dry despite total saturation of the above sediments.

HA2 was a 7 m auger plus percussion core hole and consisted of poorly sorted medium-coarse sand in the upper 3 m, becoming increasingly darker brown/grey with depth. This sand (organic matter 0.6 – 3.7 %) was bimodally distributed (major sand mode at ~500 µm and

Figure 5.13 The upper 4.55 m of the HA2 core. Note the mottled sandy clay and distinct black to very dark brown sandy clay. These types of sediments were common throughout the Lake Couridjah – Lake Baraba sill. Approximate depths were measured at the time of sediment extraction and thus not displayed in this figure. The water table was reached at 4.55 m depth.

minor silt mode at ~49 µm, Appendix F) and had a region of highly mottled orange/brown sandy clay between 1 – 1.25 m. At approximately 3 m depth, an abrupt transition into black to very dark brown, very poorly sorted and slightly mottled sandy silt occurs (Fig. 5.13). This dark unit was quite organic, increasing to 22.2 % at 3.9 m depth. After 4.55 m, poorly sorted sand prevailed and progressed into interbedded sand and sandy silt until the end of the core at 7 m depth.

HA5 was a 7.8 m auger hole in the middle of the sill and consisted largely of medium to coarse grained, poorly sorted sand. This core had four interbedded units of sandy silt, with each unit of sandy silt becoming visibly darker and more organic with depth. The sandy silt units contained mottles, with the lower three units containing charcoal and wood fragments. Pallid yellow silt occurred at 7.5 m in HA5 and, like HA3, seemed reasonably dry despite the above sediments being more saturated.

HA4 was taken close to the Lake Baraba margin and the upper 0.5 m consists of a sandy peat. The rest of the core sharply alternated between sand and sandy silt, with each alternation occurring roughly every 0.1 – 0.2 m in the upper 1.3 m of HA4 and every 0.5 m in the lower section.

5.1.3 Alluvial fan surface sediments

A total of 11 surface sediment samples were taken from the alluvial fan adjacent to Lakes Couridjah and Baraba. This was undertaken in order to gain an understanding of the origin of the sandy surface deposits encountered in cores HA1, HA2 and HA5, as well as the sand units encountered at depth within all the sill cores. Theoretically, if similar grain sizes and distributions are found in the sill along the LC-LB transect and on the alluvial fan, this would be suggestive of similar origin and transportation processes of the material.

Generally, grain sizes were poorly to very poorly sorted sands. In the upper part of the fan, the majority of grain size distributions were bi-modal with a major mode at ~400 - 500 µm and minor mode at ~50 - 60 µm. In the mid-fan, the majority of samples had more uniform distributions, with a major mode at ~500 - 600 µm. In the lower fan, the samples were also uniformly distributed, with major modes ranging between ~400 – 600 µm (Appendix B). It is important to note that because all alluvial fan surface samples were sieved using a 500 µm sieve, clastic material above ~600 µm was not captured in grain size analysis. The implications

of this are discussed in the 'Limitations' section (Chapter 6, section 6.6) and all supporting data is presented in Appendix B.

5.2 Radiocarbon Dating

A total of ten samples were dated using radiocarbon in order to constrain ages of stratigraphic units within Lake Couridjah and the Lake Couridjah – Lake Baraba sill (Table 5.1, Figure 5.1). Within Lake Couridjah, the LC2 core was dated at six different depths, using either organic sediment, charred material or charcoal. At the Lake Couridjah margin, the LC1 core was dated at two different depths, using either organic sediment or charred material. Within the sill, charred material from cores HA1 and HA2 was dated. All ages have been calibrated using the high probability density range method (HPD) and the SHCAL13 calibration curve. Radiocarbon dating reports are presented in Appendix D and summarized results are presented in Table 5.1.

In the centre of Lake Couridjah, within the core LC2, sediments below approximately 3.20 m depth are all >49,000 cal. yr BP, as shown by dates Wk – 47246, Wk – 47247 and Wk - 47248 (Table 5.1). These dates are all beyond the limit of radiocarbon and consequently all sediments below 3.2 m within the lake centre cannot be dated using radiocarbon. Within the core LC1 on the lake margin, a finite age of 47,690 – 45,040 cal. yr BP was returned at a depth of 6.05 m.

In the centre of Lake Couridjah (core LC2), the boundary between light yellow silt and overlying dark grey/brown silt, which occurred at 2.86 m depth (Figure 5.2), was dated to 39,245 – 38,250 cal. yr BP. The onset of the upper peat deposits within Lake Couridjah was dated at the lake margin (at 0.71 m depth) and lake centre (at 1.69 m depth), returning ages of 10,690 – 10,495 cal. yr BP and 10,880 – 10,700 cal. yr BP respectively. At 0.7 m depth in the centre of Lake Couridjah (core LC2), the peat returned an age of 5,660 – 5,580 cal. yr BP. These dates are relatively consistent with previous studies within Lake Couridjah which found that 0.7 m depth was dated from 4,160 cal. yr BP and 1.754 m depth was dated from 10,390 cal. yr BP (Gergis, 2000).

Within the sill at, a depth of 4 m (core HA1) was dated to 31,505 – 31,070 cal. yr BP. This depth marks the approximate boundary between the very dark brown sandy silt unit and overlying sand. At 6.4 m depth in the sill (core HA2), a date of >43,500 cal. yr BP was returned.

Table 5.1 Summary of radiocarbon results for Lake Couridjah and the Lake Couridjah – Lake Baraba sill. All samples were dated using the Accelerator Mass Spectrometry (AMS) standard delivery and calibrated using the SHCAL13 calibration curve.

Location	Core	Core Depth (m)	Dating Material	Age (cal BP)	Conventional ^{14}C Age (BP)	Probability	pMC	Lab Code
Sill	HA1	4	Charred material	31505 - 31068	27500 +/- 140	95.40%	3.26 +/- 0.06	Beta - 482186
	HA2	6.4	Charred material	> 43500	-	-	< 0.44	Beta - 482187
Lake Couridjah Margin	LC1	0.71	Charred material	10691 - 10495	9400 +/- 30	94.60%	31.03 +/- 0.0012	Beta - 482189
		6.05	Organic sediment	47690 - 45039	42960 +/- 640	95.40%	0.48 +/- 0.04	Beta - 482188
Lake Couridjah Centre	LC2	0.70	Organic sediment	5661 - 5579	4910 +/- 30	86.50%	54.27 +/- 0.20	Beta - 490295
		1.69	Charred material	10883 - 10703	9580 +/- 30	48%	30.34 +/- 0.11	Beta - 488207
		2.86	Charred material	39244 - 38248	34230 +/- 220	95.40%	1.41 +/- 0.04	Beta - 490296
		3.21	Organic sediment	>49790	-	-	-	Wk - 47246
		3.56	Charcoal	>49015	-	-	-	Wk - 47247
		4.25	Charcoal	>49712	-	-	-	Wk - 47248

5.3 Lake Couridjah trace element geochemistry

Elemental counts were analysed at 1000 µm resolution for LC2 using an ITRAX core scanner. This provides continuous *in situ* elemental count data through the core. The results of this analysis are presented in the following sections. Key elements are summarized in Figure's 14 and 15, and the raw data is presented in Appendix F.

5.3.1 Catchment erosion proxies

Delivery of sediment

The elements Al, Si, K, Ti, Rb and Zr are commonly used to assess the influx of detrital material into a lake from the surrounding catchment (Moreno *et al.* 2008; Kampf *et al.*, 2012; Davies *et al.* 2015). Ti does not function in biological processes, and is mainly present in weathering-resistant silicate minerals such as rutile (Kylander *et al.*, 2013). Ti is therefore a useful indicator for temporal changes in silicate mineral input to the lakes. Given that the Thirlmere Lake's catchment is primarily composed of quartz-rich Triassic sandstone, Si could also be considered an appropriate indicator for detrital input. However, there can also be significant biogenic Si production in lakes, which will be discussed in a subsequent section.

In the Lake Couridjah sediments (core LC2), Si correlates with K (R^2 = 0.70), Al (R^2 = 0.69), Rb (R^2 = 0.57) and Zr (R^2 = 0.62), and there is high correlation between K and Al (R^2 = 0.76) (Appendix F). This implies similar behaviour of these elements (Moreno *et al.*, 2008).

The down core detrital element; Si, Al and Ti (Figure 5.13), have low counts in the upper 1.75 m of the core. Below this depth their counts increase sharply, but also become more variable. Below 1.75 m there are several regions of LC2 where there is depletion in detrital elements. These occur between 2.27 – 2.35 m, and at 4.24 m, where the decline in Ti is particularly noticeable, and also between 4.80 – 5 m (Fig. 5.13). After 5.77 m, vales generally increase until the end of the core where there is very high variability in all detrital elements (i.e. Si, Al and Ti).

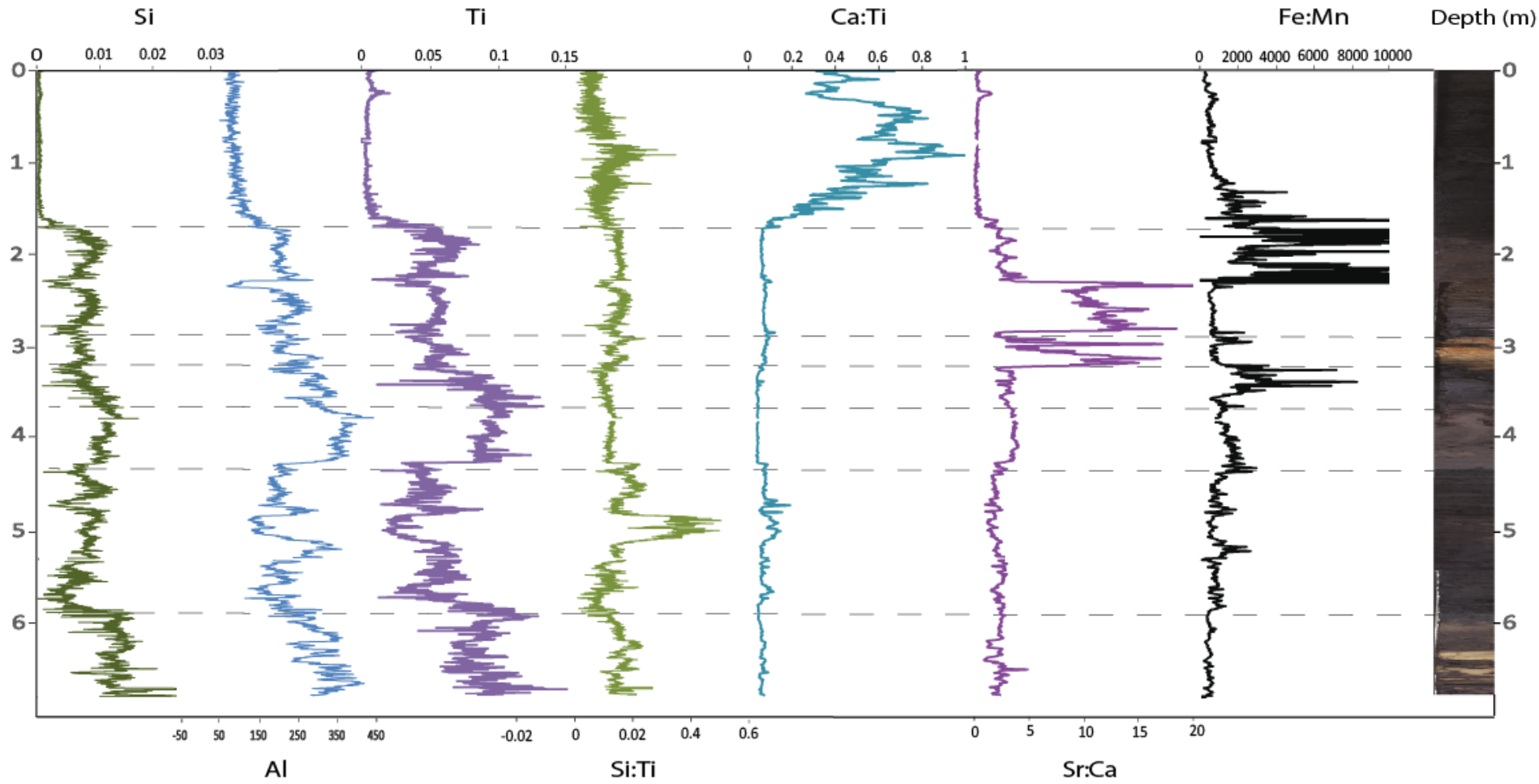

Figure 5.14 Elemental analysis of LC2 including single geochemical profiles of Si, Al, Ti, as well as ratios of Si:Ti, an estimate of biogenic silica, Ca:Ti, a proxy for lake productivity, Sr:Ca, a proxy for lake salinity and Fe:Mn, a proxy for changing redox conditions. Anomalous data was recorded at the core ends where the data was viewed as being a product of the core barrel itself, and was therefore excluded. This occurred at 3.7 m, 5.3 m and 6.8 m depth for all elemental profiles. Also, data was excluded that was >10 times that of the above and below values. This occurred in the Si:Ti, Sr:Ca and Fe:Mn ratios at ~0.77 m depth.

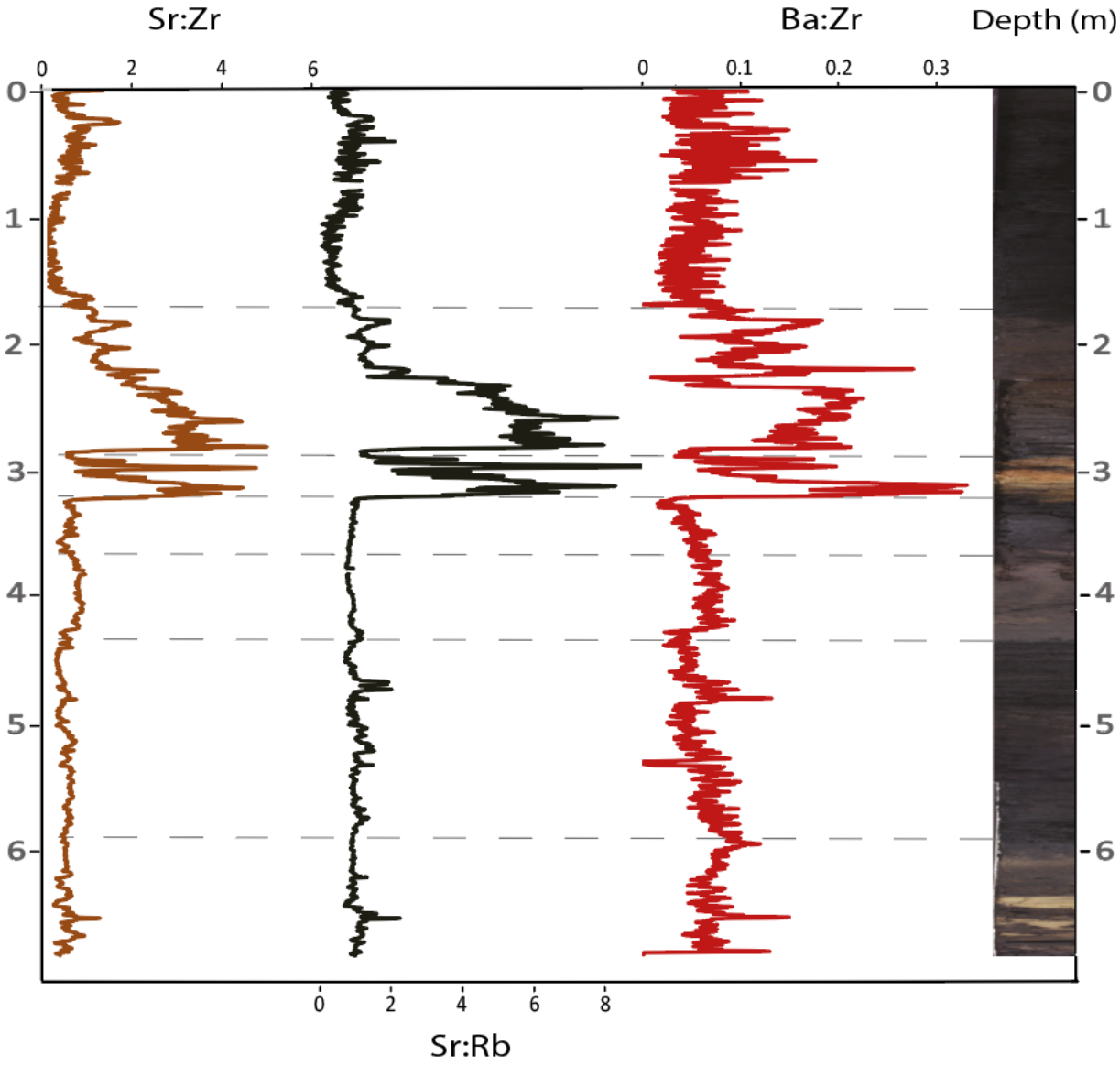

Figure 5.15 Elemental analysis of LC2 including ratios of Sr:Zr, Sr:Rb and Ba:Zr, representing proxies for weathered material. I. In all these ratios, anomalous data points were excluded at ~0.77 m and ~3.7 m depth.

Weathering

The ratios of Sr:Zr, Sr:Rb and Ba:Zr can be used to infer the degree of weathering of minerals (e.g., Kamber *et al.*, 2005). This is because soluble elements (including Sr, Rb and Ba) are hosted by minerals susceptible to weathering, e.g. feldspars, while by contrast, the abundance of less soluble elements (e.g. Rb) or elements hosted by very stable minerals, e.g. zircon in the case of Zr, remain unaffected by weathering. Therefore in weathered sediments the loss of Sr or Ba would result in a relative decrease in the ratio of Sr:Zr, Sr:Rb or Ba:Zr. In the case of Lake Couridjah, that is, an increase in these ratios indicates a decrease in the effects of weathering on the mineral grains. In this context, this can be interpreted as a

decrease in the amount of time between erosion of sediment from host rocks and its subsequent deposition in a lake basin. Conversely, low values indicate the delivery of more weathered material to the lake basin, implying this material has spent more time within the catchment undergoing weathering and/or more favourable conditions for chemical weathering, i.e. wetter conditions and/or a well vegetated catchment. Alternatively, because they are soluble, Sr and Ba can be mobile with sediments, e.g. they are mobile within terrestrial peats, which experience variable water tables (Marx *et al.*, 2011). Therefore, these elements can potentially suffer drying/rewetting of LC2 sediment.

Within LC2, the ratios of Sr:Zr and Sr:Rb apparent in Figure 5.14 indicate generally low values in the upper 1.7 m of the core LC2, except for a small increase at 0.26 m depth. The Ba:Zr ratio is far more variable in the upper 1.7 m (Fig. 5.15). Below 1.7 m, all ratios show greater variability and generally increase. At ~2.84 m depth, values for all the ratios drastically decrease and the increase again at ~3.15 m. Below this depth there is then an abrupt shift to lower values at ~3.2 m depth for all the ratios which persist until the end of the core at 6.8 m depth (Figure 5.15).

5.3.2 Changing hydrological and chemical conditions inferred from elemental data

Lake productivity

Although Si was used as an indicator for detrital input, Si content can be derived from siliciclastic and biogenic components (Davies *et al.*, 2015). The biogenic silica (BSi) contribution can be assessed by the Si:Ti ratio, which provides an uncalibrated estimate of BSi (Brown *et al.*, 2007). This assumes the ratio of Si to Ti remains constant in the catchment and therefore a significant increase in the ratio would imply increased BSi production. Similarly, changes in Ca can result from both carbonate weathering in the catchment and authigenic precipitation of CaCO3 and so normalizing to Ti removes the influence of catchment mineral input to the lake (Kylander *et al.*, 2013). Ratios of Si:Ti and Ca:Ti are displayed in Figure 5.13.

In the core LC2, the Si:Ti ratio has a large but relatively stable range in the upper 1.75 m, after which the range decreases and values remain consistent until at approximately 4.24 m, where there is a significant shift into higher Si:Ti values (Fig. 5.14). Between 4.8 – 5 m there is an abrupt increase in Si:Ti values, mirroring the decrease in detrital influx at that depth. From 5 – 6.8 m, values are generally variable; initially decreasing at 5.75 m and then subsequently

increasing at 6.2 m until becoming highly variable at 6.7 m (Fig. 5.14). The Ca:Ti ratio has markedly higher values in the upper 1.75 m than in the remainder of the core, with a particularly significant peak at 0.8 – 0.9 m depth (Fig. 5.14). Below 1.75 m, the Ca:Ti ratio is fairly low and consistent but shows some variation between 4.3 – 5.8 m depth.

Redox conditions

During anoxic conditions in lakes, i.e. at the sediment-water interface, a significant portion of Mn oxides become reduced and are released into the water column. This results in a decrease of Mn in lake sediments (Davies *et al.*, 2015). The reduction of iron oxides, however, does not particularly increase in anaerobic conditions, and thus there is more Fe relative to Mn within lake sediments (Davies *et al.*, 2015). Therefore, Fe:Mn profiles can indicate whether there may have been changing redox conditions through time. Such changes, i.e. an increase in redox conditions, may be attributed to a) increased stratification in deeper water or b) a decrease in windiness and therefore less mixing of lake water (Haberzettl *et al.*, 2007; Moreno *et al.*, 2007; Davies *et al.*, 2015).

Within the Lake Couridjah sediments, Fe and Mn weakly correlate (R^2 = <0.35) to the detrital elements Si, Al and Ti (Appendix F), suggesting that the presence of Fe and Mn generally reflects lake internal Fe and Mn cycling (Metcalf *et al.*, 2010; Kampf *et al.*, 2012). The plot of Fe:Mn with core depth (Figure 5.14) shows that in the upper 1.2 m there are relatively low values. Between 1.2 – 2.35 m, there is a shift to generally high values and increased variability, which then abruptly decreases at 2.35 m (Figure 5.14). There are then subsequent increases in the Fe:Mn ratio between 3.2 – 3.5 m, 4 – 4.3 m and some variability between 5.1 – 5.8 m depth.

Evaporation

During significant periods of evaporation, there is potential for precipitation of evaporatives such as $CaCO_3$ (calcium carbonate) and $CaSO_4$ (gypsum). Therefore, Ca can be a potentially useful proxy for fluctuating water levels in some situations, where high values indicate drier climatic periods (Brown *et al.*, 2011; Davies *et al.*, 2015). Furthermore, the Sr:Ca ratio may reflect changing salinity, and therefore changing water levels, as Sr precipitates in diminished lake levels (Lui *et al.*, 2014). In this way, a high Sr:Ca ratio can indirectly reflect decreased lake levels.

The Sr:Ca ratio shown in Figure 5.14 have low and consistent values in the upper 1.7 m of the core LC2, except for a small increase in values at 0.25 m depth. Below 1.7 m, there is a steady increase in values before a more abrupt increase at 2.3 m depth. Very high and variable Sr:Ca ratios are then maintained from 2.3 – 3.2 m depth, after which values decrease and are generally consistent until the end of the core at 6.8 m (Figure 5.14).

5.4 Stable carbon ($\delta^{13}C$) and nitrogen ($\delta^{15}N$) isotopes from Lake Couridjah

This section presents the results of $\delta^{13}C$, $\delta^{15}N$, C:N, percentage of C and N analysis conducted on, firstly, 136 bulk sediment samples from the LC2 core, and then secondly, 10 modern surface samples and 6 living vegetation samples from along the LC-LB transect. For the LC2 core analysis, the results show considerable variability in some parameters suggesting variability in the palaeo-environmental factors that influence these isotopes and elements within Lake Couridjah (Fig. 5.17).

In the core LC2, $\delta^{13}C$ values generally increase with core depth, ranging from -34.23 ‰ to -24.92 ‰ with an overall mean of -28.92 ‰ (Fig. 5.17). $\delta^{15}N$ is slightly more variable, also showing a general increase down core and ranging from -0.93 ‰ to 6.9 ‰ with an overall mean of 2.35 ‰. Conversely, %C and %N decrease with depth, ranging from 1.07 % to 35.94 % (overall mean = 10.88 %) and 0.06 % to 2 % (overall mean = 0.57 %), respectively. The overall C:N ratio shows increased variability down core and ranges from 6 to 52.95 with an overall mean of 23.67 (Fig. 5.17).

The percentage of C and N are highly correlated in the core ($r^2 = 0.95$). The y-intercept for the regression line was close to zero (-0.02) (Fig. 5.16*b*), implying inorganic N is minimal (Calvert, 2004; Woodward *et al.*, 2017). $\delta^{13}C$ and $\delta^{15}N$ are also significantly correlated, although to a lesser extent ($r^2 = 0.68$). These data show a distinct zone of $\delta^{13}C$ and $\delta^{15}N$ depleted samples between -30.67 ‰ and -34.23 ‰ for $\delta^{13}C$ and 0.72 ‰ and -0.79 ‰ for $\delta^{15}N$ (Fig. 5.16*d*), clustered in between 0 – 1.75 m depth (Fig. 5.17). When C:N versus $\delta^{13}C$ scatterplots are used, it is commonly to infer sources of organics in sediments (Woodward *et al.*, 2012; Ma *et al.*, 2012; Woodward *et al.*, 2017). The C:N versus $\delta^{13}C$ scatterplot (Fig. 5.16*b*) shows a similar zone of depleted $\delta^{13}C$ samples as in Figure 5.16*d.* This zone of samples ranges between -34.20 ‰ and -30.67 ‰ for $\delta^{13}C$ and 16.65 – 23.67 for C:N, and also cluster between 0 – 1.75 m depth. None of the presented data are influenced significantly by inorganic carbon as samples that were pre-treated with hydrochloric acid to remove carbonates showed minimal differences compared to samples with no pre-treatment (Appendix E).

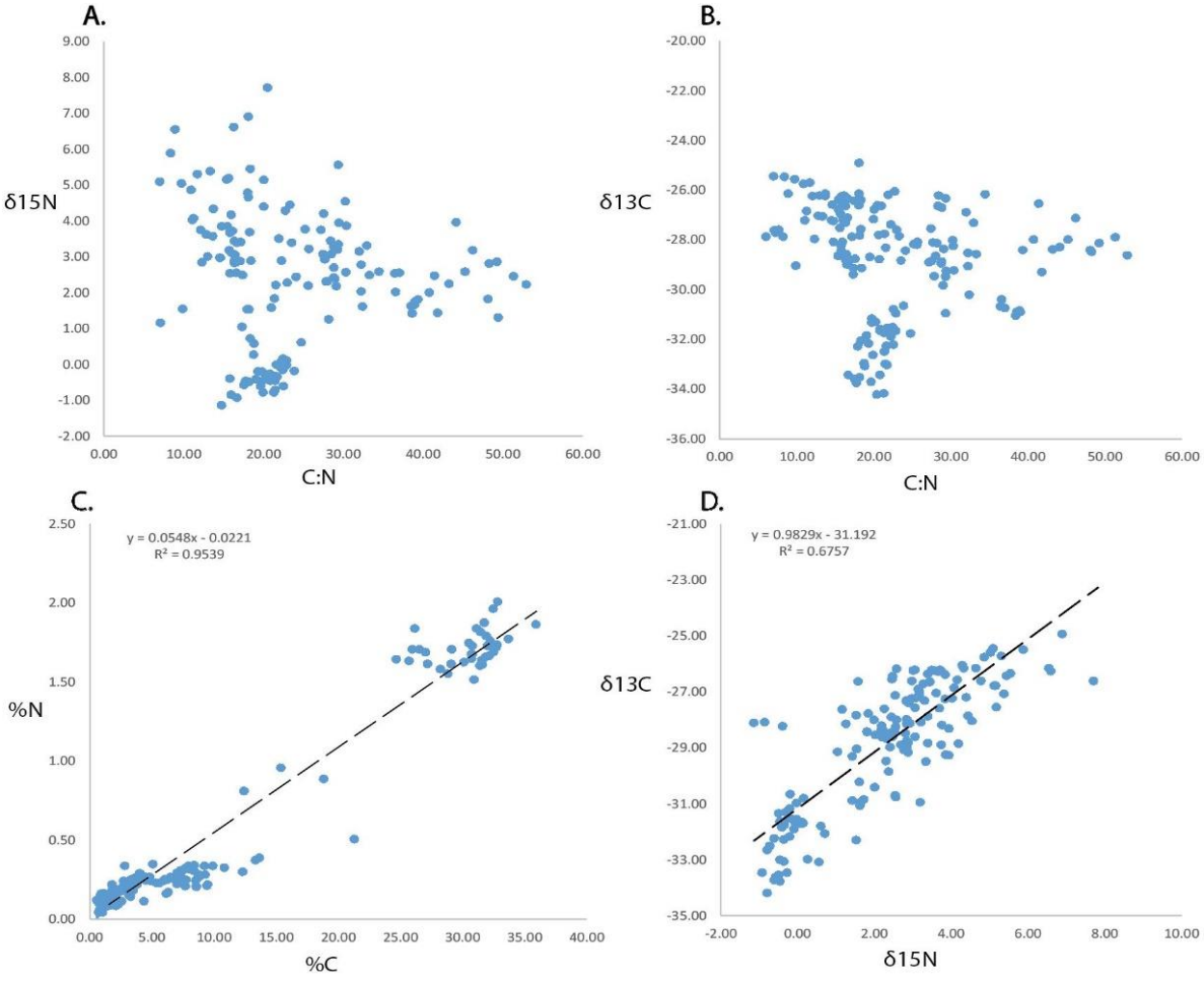

Figure 5.16 Shows scatterplots A. $\delta^{15}N$ vs C:N, B. $\delta^{15}C$ vs C:N, C. %N vs %C and D. $\delta^{15}C$ vs $\delta^{15}N$ from the Lake Couridjah dataset.

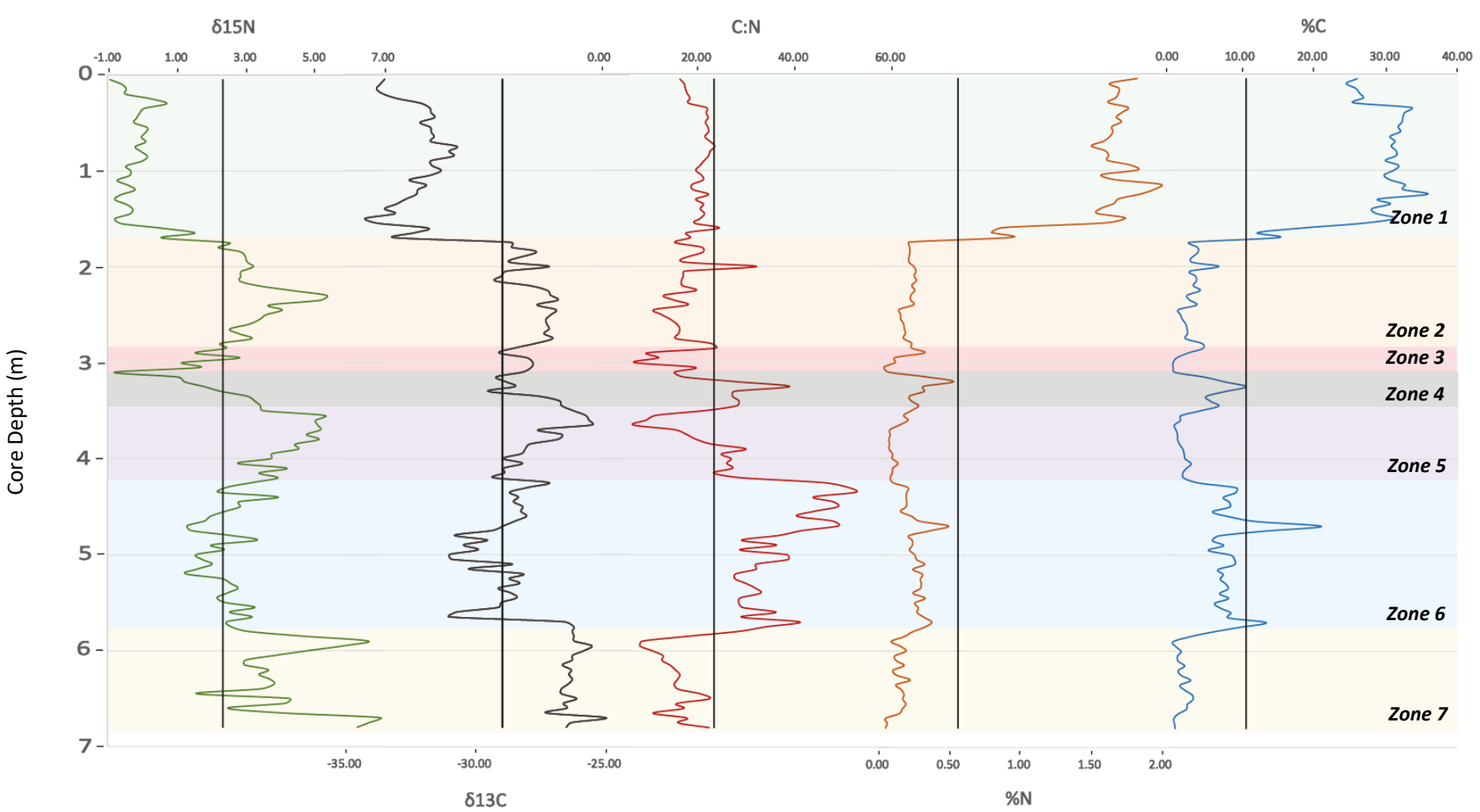

Figure 5.17 Stable isotope data for Lake Couridjah with plotted $\delta^{15}N$, $\delta^{13}C$, C/N, %N and %C against LC2 core depth. Vertical black lines represent overall means for the dataset and background colours separated the different zones.

The $\delta^{13}C$, $\delta^{15}N$, C/N, %C and %N data displayed clear regions down core, and consequently the core was divided into seven zones based on the stable isotope data. These are;

Zone 1, occurring from 0 –1.75 m depth, is characterised by low $\delta^{13}C$ and $\delta^{15}N$ values, ranging between -34.2 ‰ to -30.67 ‰ (mean = -32.18 ‰) and -0.95 ‰ to 0.72 ‰ (mean = -0.07 ‰) respectively (Fig. 5.10). Between 1.1 m and 1.7 m there is a distinct region of depletion in $\delta^{13}C$. Both C and N are the highest in Zone 1 out of the entire record, and range from 26 % to 35.95 % (mean = 28.25 %) and 1.51 % to 2 % (mean = 1.59 %) respectively. The C:N ratio is relatively low and displays little variability, ranging from 16.65 to 23.85 with a mean of 20.86.

Zone 2 (1.75 – 2.85 m) there is an abrupt shift into higher $\delta^{13}C$ values from -29.2 ‰ to -26.78 ‰ (mean = -27.72 ‰) and a more gradual shift to a significant peak in $\delta^{15}N$ at 2.3 m depth, with an overall range between 2.21 ‰ and 5.37 ‰ (mean = 3.27 ‰). Conversely, %C and %N abruptly decrease and remain consistently low, ranging between 1.8 % and 7.11 % (mean = 3.47 %) and 0.15 % to 0.26 % (mean = 0.22 %) respectively. C:N ratio becomes slightly more variable, with a range between 12.83 to 32.49 and a mean of 17.94.

Zone 3 (2.85 – 3.1 m) is characterised by decreases in C:N, %N and %C, as well as small peaks in $\delta^{13}C$ and $\delta^{15}N$. $\delta^{13}C$ and $\delta^{15}N$ range from -28.92 ‰ to -27.75 ‰ (mean = -28.20 ‰) and -0.79 ‰ to 2.84 ‰ (mean = 1.48 ‰) respectively. The C:N ratio quickly decreases from 23.67 to 7.26 (mean = 14.81) and then rises again to 19.78. %N and %C range from 0.33 % to 0.08 % (mean = 0.16 %) and 4.97 % to 0.79 % (mean = 1.95 %) respectively.

Zone 4 (3.1 – 3.45 m) exhibits distinct increases in C:N, %N and %C. Conversely, $\delta^{13}C$ and $\delta^{15}N$ both decrease, with $\delta^{15}N$ sharply decreasing to -0.79 ‰ right on the 3.1 m boundary and $\delta^{13}C$ more gradually decreases to -29.47 ‰ by 3.3 m. The C:N ratio increases from 15.51 to 39.34 at 325cm and then decreases to 28.39. %N and %C both sharply increase to 0.54 % and 10.88 % respectively at 3.25 – 3.3 m, before a more gradual subsequent decrease.

In *Zone 5* (3.45 – 4.25 m), C:N shows an initial sharp decrease to 7.04 at 3.65 m, but is overall variable with a range between 7.04 – 30.26 and a mean of 23.04. %N and %C also decrease but are far less variable, ranging between 0.09 – 0.29 % (mean = 0.14 %) and 1.19 – 7.07 % (mean = 2.56 %) respectively. $\delta^{13}C$ and $\delta^{15}N$ both increase initially to -25.45 ‰ and 5.31 ‰ then gradually decrease to -27.14 ‰ and 3.19 ‰.

Zone 6 (4.25 – 5.75 m), both $\delta^{13}C$ and $\delta^{15}N$ decrease and surround the overall mean, varying between -30.96 ‰ to -27.14 ‰ and 1.26 ‰ to 3.95 ‰ respectively. In this zone, the C:N ratio is entirely above the overall mean and displays a series of peaks ranging between 28 and 52.95. %N and %C both increase and display significant peaks at 4.70 m and 5.70 m. %C increases more significantly than %N and ranges between 5.65 % and 21.28 % (mean = 8.79 %). %N ranges between 0.1 6% and 0.50 % (mean = 0.27 %).

Zone 7 (5.75 – 6.8 m) shows a sharp increase in $\delta^{13}C$, and establishes a new mean of -26.25 ‰, ranging between -27.23 ‰ and -24.92 ‰, of which is the highest in the entire record. $\delta^{15}N$ also initially increases to 6.55 ‰ at 5.9 m but then rapidly decreases again and is highly variable, ranging between 1.57 ‰ and 6.90 ‰ (mean = 4.17 ‰). Both $\delta^{13}C$ and $\delta^{15}N$ peak at 6.7 m, depicting the highest values of both in the whole sequence. C:N, %N and %C all significantly decrease and remain relatively low until the cessation of the core at 6.8 m. In this zone, C:N initially sharply decreases to 8.41 and then slightly increases again to 23.67. %N and %C decrease to a range of 0.06 % to 0.23 % (mean = 0.16 %) and 0.87 % to 3.51 % (mean = 2.52 %), with both low values directly corresponding to the peak in $\delta^{13}C$ and $\delta^{15}N$ occurring at 6.7 m.

5.4.1 Stable carbon ($\delta^{13}C$) and nitrogen ($\delta^{15}N$) isotopes from modern soil and living vegetation

A total of 10 modern soil samples and 6 living vegetation samples from the LC-LB transect were also analysed for $\delta^{13}C$, $\delta^{15}N$, C:N, percentage of C and N in order to provide a modern context for the LC2 core stable C and N isotope analysis. These results will be synchronously presented and discussed in the subsequent discussion chapter (Chapter 6, Fig. 6.2). Raw data is presented in Appendix E.

Generally, there was a degree of variation between the $\delta^{13}C$, $\delta^{15}N$, C/N, %C and %N data between the modern soil and living vegetation samples. For $\delta^{13}C$, modern soil values ranged from -26.34 - -28.76 ‰ and living vegetation values were lower, ranging from -27.69 - -31.45 ‰ (Fig. 6.2). $\delta^{15}N$ values ranged between -0.04 – 3.37 ‰ for the modern soil samples, but were far more variable in the living vegetation samples, ranging between -1.78 – 4.39 ‰ (Appendix E). The percentage of C was far higher in the living vegetation (42.64 – 50.19 %) than the soil samples (5.69 – 24.43 %), and the percentage of N was generally consistent

between the two groups (~1 %) (Appendix E), and therefore the C:N ratio of the living vegetation was much higher than that of the modern soil samples (Fig. 6.2).

6. DISCUSSION

Analysis of the stratigraphy, elemental composition and stable C and N isotope record imply that Lake Couridjah has undergone significant hydrological change in the past. This chapter will explore these results; firstly at face value, discussing the stable C and N isotope dataset, chronology and stratigraphic relationships and then collectively, discussing facies interpretation and lake connectivity. This will then be broadly placed within the context of south eastern Australia.

6.1 δ13C values and C:N ratios

During CO_2 fixation, plants preferentially uptake the lighter ^{12}C isotope rather than the heavier ^{13}C isotope, forming organic matter that is ^{13}C depleted compared to the atmosphere (Lamb *et al.*, 2006). The analysis of δ13C values and C:N ratios of bulk organic lake sediment has the ability to inform about sources of organic matter, as distinct sources of organic matter can reflect distinct δ13C values and C:N ratios in organic sediments (Lamb *et al.*, 2006; Ma *et al.*, 2009; Woodward *et al.*, 2012) (Fig. 6.1). However, δ13C values and C:N ratios in the soil organic matter depart from the corresponding signal in the parent vegetation due to

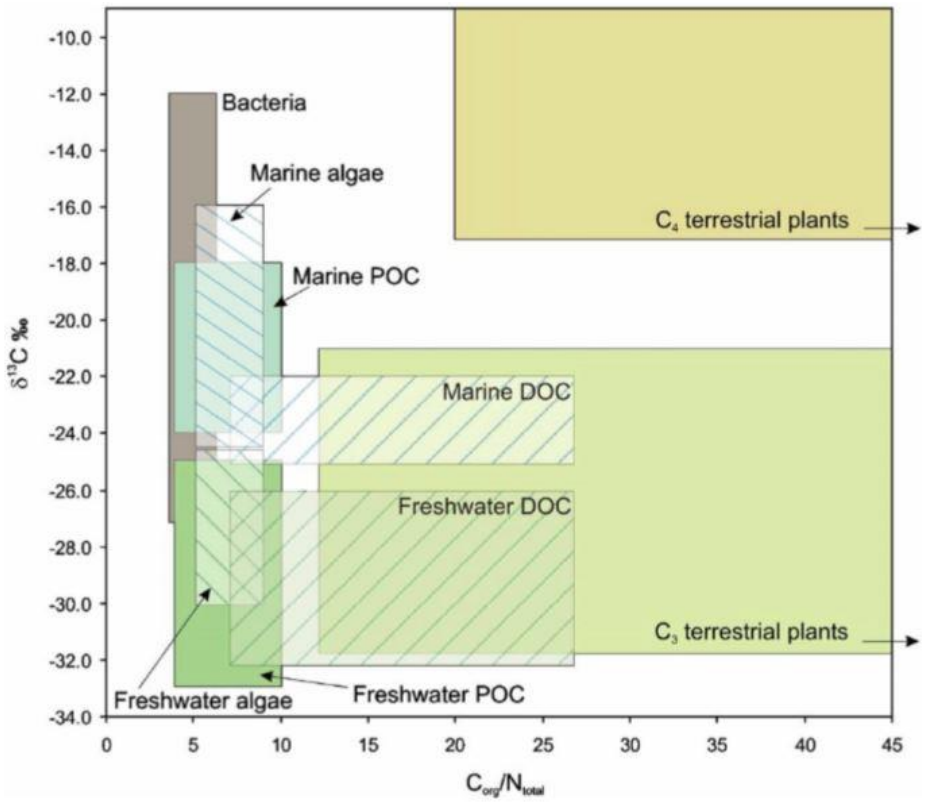

Figure 6.1 General ranges of δ13C values and C:N ratios for varying organic sources. This figure was created by Lamb et al., (2006), who compiled numerous sources of data.

decomposition, thereby effectively decreasing the expected C:N ratio (Lamb *et al.*, 2006). Furthermore, for C3 plants, a significant negative correlation exists between water availability and δ13C values (Ma *et al.*, 2012). This is because plants supplement their requirements for CO_2 consumption between photosynthesis and conversion of water by regulating the absorption levels through their stomata. Therefore, increased water availability (precipitation) stimulates an increase in stomatal conductance of CO_2 and thus the plant δ13C value decreases (Ma *et al.*, 2012).

Figure 6.2 shows a scatterplot of the δ13C values and C:N ratios for the core LC2, from the centre of Lake Couridjah, as well as the surface soil and living vegetation samples taken from along the LC-LB transect (running from Lake Couridjah to Lake Baraba). The variability between C isotopes (δ13C and C:N) within the core LC2, living vegetation and surface soil samples is likely explained by three different controls; differing sources of organic matter, decomposition of organics and environmental water stress/availability. The effect of these three controls in the C composition in the results are discussed below.

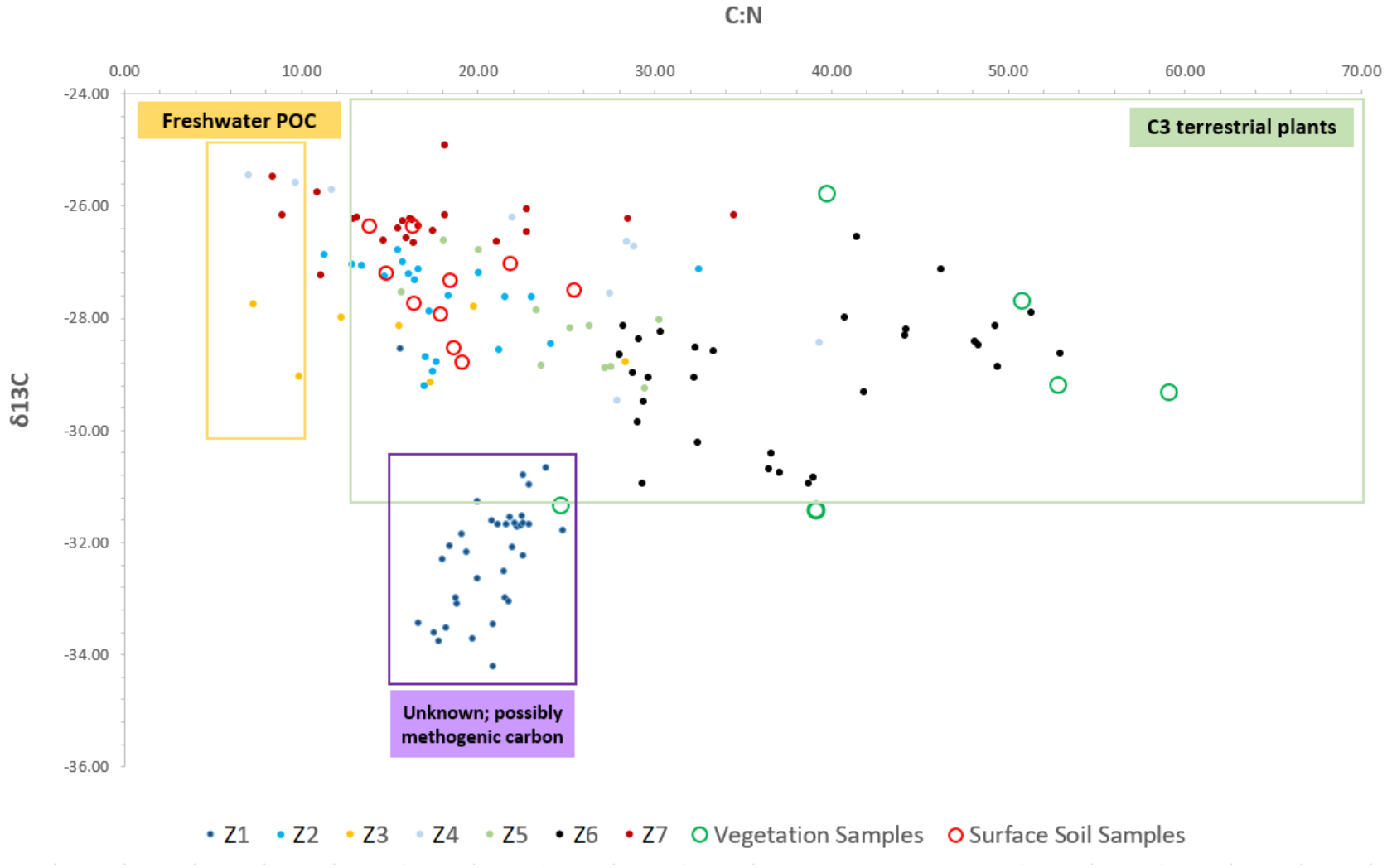

Figure 6.2 The δ13C values and C:N ratios for the sediments within Lake Couridjah (labelled as the zones present in Chapter 5, Fig 5.17, with corresponding colours), the living vegetation samples (open green circles) and the modern surface soil samples (open red circles). The spread of data is categorised, using Figure 6.2, into the suggested sources of organic matter; C3 terrestrial plants, freshwater particulate organic matter (POC) and an unknown source (Lamb et al., 2006).

6.1.1 Sources of organic matter

Most samples, both from within Lake Couridjah (from the core LC2) and the modern soil samples, indicate C3 vegetation as being the source of organic matter (Fig. 6.2). The dominant contemporary peat-forming vegetation within Lake's Couridjah and Baraba is *Lepironia Articulata* and *Lepidosperma Longitudinale* respectively, both of which are C3 cyperaceous sedges.

Furthermore, some samples have δ13C values and C:N ratios which indicate some influence from particulate organic matter (POC), mixing between POC and C3 vegetation (Fig. 6.2).

Interestingly, the lake samples from *Zone 1* (Chapter 5, Fig. 5.17) are significantly depleted in δ13C and don't appear to fit any of the usual sources of organic matter (Fig. 6.1). A possible explanation for this is the production of methane-derived carbon from methane-oxidising bacteria, which characteristically has depleted δ13C values by comparison to organic matter derived from phytoplankton and higher plants (Deines *et al.*, 2007; van Hardenbroek *et al.*, 2012). Biogenic methane is very δ13C-depleted, sometimes as low as -100 to -50 ‰ (van Hardenbroek *et al.*, 2012), and its signature can be retained within higher trophic levels in lacustrine food-webs. For example, the chironomid tribe Chironomini is well known for including the methane-oxidising bacteria into its diet, as chironomid burrows provide favourable conditions for the bacteria's growth (van Hardenbroek *et al.*, 2012). Therefore, the depleted δ13C values of *L1* could be a result of these methogenic-bacterial processes and the assimilation of biogenic methane into the organic matter of sediments by macroinvertebrates.

6.1.2 Decomposition

The decomposition of organic matter can complicate the reliability of using δ13C values and C:N ratios to deduce sources of organic matter in sediments (Lamb *et al.*, 2006). Organic carbon in soil organic matter is lost largely due to microbial breakdown, and therefore C:N ratios affected by decomposition appear lower than expected. Climate (changes in temperature and moisture) and the quality, i.e. chemical composition, of leaf litter can also play a significant role in organic matter decomposition (Bradford *et al.*, 2016).

The spread of C:N ratios in Figure 6.2 could therefore result from differing degrees of decomposition of organic matter through time, whereby high and low C:N ratios represent undecomposed and more decomposed material respectively. The living vegetation samples shown in Figure 6.2 represent undecomposed material, and these can be compared to the core sediments in order to assess potential decomposition. Anoxic bottom waters would be expected to preserve organic matter, and therefore should create sediment δ13C values and C:N ratios that reflects those of the vegetation samples. This seems to be the case for the C signature of sediment in Zone 6 and to a lesser degree, Zone 4, as they have high C:N ratios similar to that of living vegetation (Fig. 6.2). This implies that carbon components in this section of the core were transported relatively rapidly to the lake basin and where they experienced conditions favourable for preservation i.e., anaerobic conditions in the bottom waters of a stratified water column. By contrast the sediments of Zone's 3 and 7 have relatively low C:N ratios, suggesting they experience a greater degree of post depositional decomposition, possibly implying drier or dry periods in the lake and exposure to oxidising conditions. Alternatively and therefore, the level of decomposition may also reflect the rate at which organic matter is being delivered into the lake. The modern soil samples show a degree of decomposition in comparison to the vegetation samples. Therefore if more soil was delivered to the lake, this could also result in sediments with lower C:N ratios.

6.1.3 Water stress/availability

C3 plants are expected to have an enriched signal of δ13C under water stressed conditions and conversely, decreased δ13C values with greater availability of water (Lamb *et al.*, 2006; Ma *et al.*, 2012). Therefore, differences in the δ13C values of the LC2 core samples can indicate the degree of environmental water availability experienced by the parent vegetation. The sediments from Zone 1 were from the upper 1.75 m thick peat unit, indicating perennial waterlogging, and have depleted δ13C values, which supports this interpretation. This implies that the sediments from Zone 6 may have also experienced largely wet conditions, and that the sediments from Zone's 4 and 7 may reflect water-stressed parent vegetation due to their relatively enriched δ13C values (Fig. 6.2). Zone's 2, 3 and 5 may reflect an environment where water was intermittently available.

6.1.4 Summary

The three different controls discussed here, i.e. sources of organic matter, decomposition and water availability, are thought to influence δ13C values and C:N ratios of samples from the core LC2, modern soil and living vegetation (Fig. 6.2). That is, δ13C values and C:N ratios of sediment will produce values reflective of certain organic matter sources, high C:N ratios indicate less-decomposed material and high δ13C values represent water stressed conditions. Furthermore, all three scenarios may simultaneously interact, forming a more complex picture of how these factors influence C isotopes in nature. An indication of which scenario might be more likely is provided by comparison of the C data with the facies interpretation and ITRAX data in section 6.3.

6.2 Chronology and Stratigraphic Relationships

The cores taken along the LC-LB transect have revealed relatively complex stratigraphy, often with significant changes in grain size, organic content, texture and colour. Unsurprisingly, sandy deposits dominate the sill, yet become increasingly diminished towards the centre of Lake Couridjah where peat and organic silts prevail. The margin of Lake Baraba is considerably less organic than the margin of Lake Couridjah, and is predominantly composed of dense clay. The section below discusses an interpretation of the stratigraphic information presented in the results. The nomenclature provided for each unit in Figure 6.3 (e.g., *L1*) will be used for all subsequent unit descriptions.

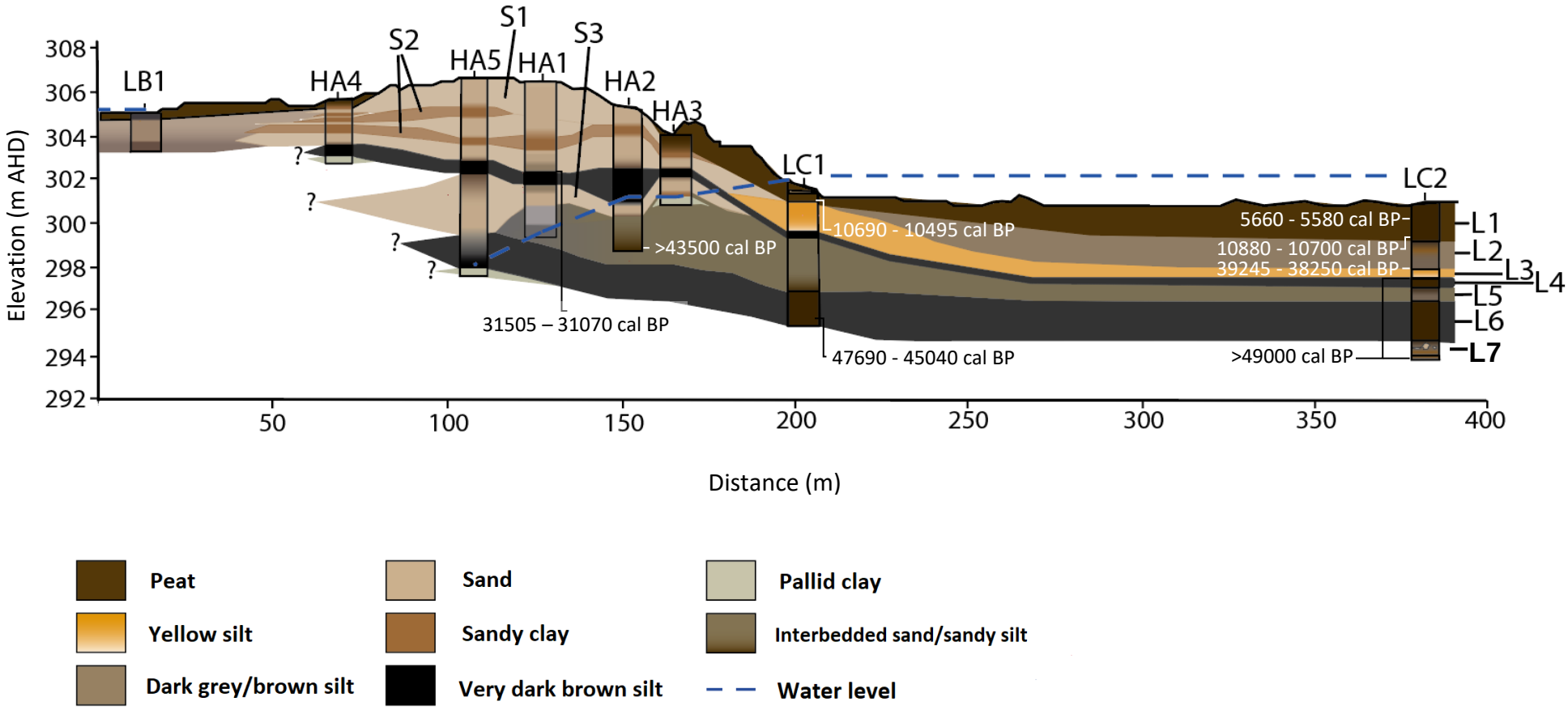

Figure 6.3 Illustration of the stratigraphic interpretation of the core data present in Chapter 5, section 5.1. Each stratigraphic unit is labelled, i.e. L1, L2, etc, as per the facies interpretation in section 6.3. The surface and sub-surface water level (blue dashed line) is shown, representing the water level as it existed at the time of core collection. Radiocarbon dates are also shown at their respective depths.

6.2.1 Sill and lake stratigraphy

The sill is composed predominantly of sand (*S1* and *S3*) and mottled sandy silt (*S3*) deposits which pinch out towards Lake Couridjah and Lake Baraba, becoming replaced by fine-grained lacustrine sediment (Fig. 6.3). The Holocene surface peat (*L1*) and underlying dark grey/brown clay (*L2*) thicken towards the centre of Lake Couridjah, whereas the light yellow silt (*L3*) and the underlying units thin towards the centre. The very dark brown organic sediment (*L4*), apparent as a thin unit underneath *L3* in Lake Couridjah, is present the entire way across the sill and thickens towards the sill centre (Fig. 6.3). *L4* reaches maximum thickness within the HA2 core, and becomes more mottled within HA1, HA5 and HA4. Furthermore, the dark organic sediments (*L6*) that act as the basal unit in Figure 6.3, is apparent at depth at the sill centre, suggesting it too is maintained between the two lakes. No mottling occurs in *L6.*

Therefore, while the sill and lake stratigraphy is characteristically different, two units; *L4* and *L6,* appear contiguous throughout the entire sequence, suggesting the deposition of dark organic sediments occurred between lakes Couridjah and Baraba.

6.2.2 Chronostratigraphy

Within Lake Couridjah, the radiocarbon dates suggest that all the stratigraphic units underlying *L3* are >49 ka, and consequently are beyond the radiocarbon dating range. Within the dates obtained on the sill and within the lake cores, there are some anomalies between the radiocarbon ages and the suggested stratigraphic relationships (Fig. 5.1, 6.3):

- Unit *L3* was dated with charred material within the core LC2 (Lake Couridjah centre) to an age of 39245 – 38250 cal. yr BP. However, the underlying *L4* unit was dated with charred material within the core HA1 (sill centre) and returned a younger age of 31505 - 31070 cal. yr BP. One or both of these ages may well minima, contaminated by younger carbon.
- Similarly, in the core LC1 at the Lake Couridjah margin, unit *L6* was dated to 47,690 – 45,040 cal. yr BP. Yet *L6* also underlies *L3,* implying an age >49 ka. As such, this age is also treated as a minimum.

Until further dating control is provided (e.g. optically stimulated luminescence) for the LC2 core, the basal part of *L2* through to *L6* is simply interpreted as late Pleistocene given the

possibility that samples can be contaminated by either older or younger carbon (Nelson *et al.*, 1988; Wohlfarth *et al.*, 1998).

The most reliable part of the chronology is for the Holocene peats within Lake Couridjah, as these dates are consistent with existing published chronologies. The onset of *L1* is dated to be between 10,690 – 10,495 cal. yr BP at 0.71 m depth (LC1 core) and 10,880 – 10,700 cal. yr BP at 1.69 m depth (LC2 core), agreeing well with the existing chronology by Gergis (2000) where the onset of the peat was dated to 10,390 cal yr. at 1.754 m depth from Lake Couridjah's southern end.

Age-depth model

In light of the above discussion, the chronology for the stratigraphic units within Lake Couridjah and the adjacent sill will be derived from the top three radiocarbon dates of the LC2 core; 5,620 cal. yr BP at 0.7 m depth, 10,790 cal. yr BP at 1.69 m depth and 38,750 cal. yr BP at 2.86 m depth. This approach was chosen due to the greater availability of radiocarbon dates at the Lake Couridjah centre, and the similarity of results between the age-depth model of the present study (Fig. 6.4) and that of another study conducted on Lake Couridjah (Gergis, 2000). However, it is realised that this may only produce dates for the centre of Lake Couridjah

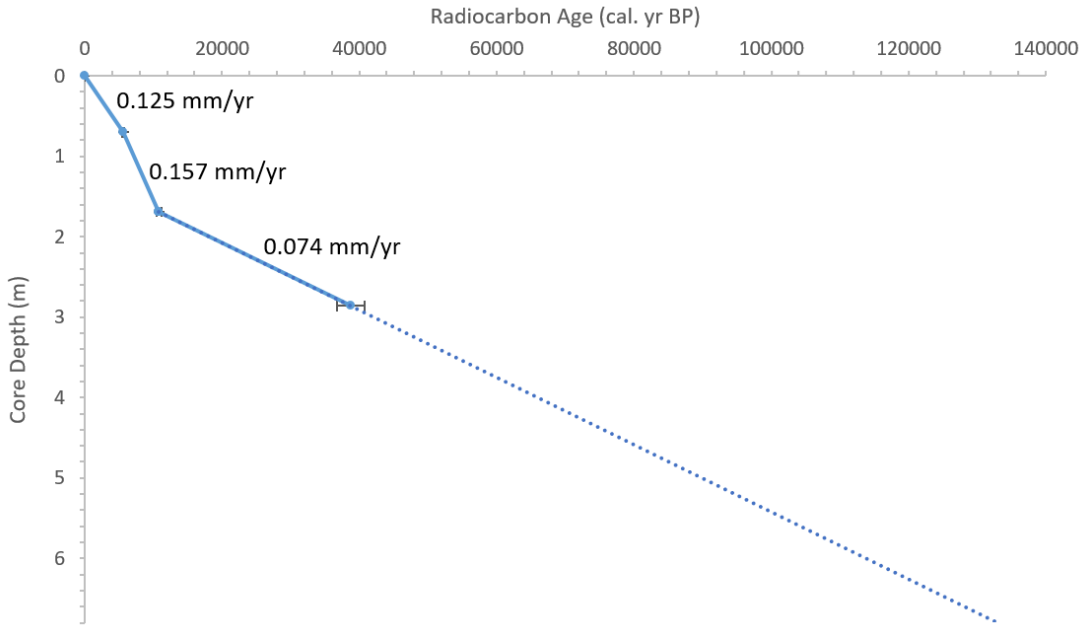

Figure 6.4 Age – depth relationship of the core LC2, utilising the three shallowest radiocarbon dates. Through extrapolation, the base of the core is approximately >120 ka. Two sigma errors were applied; however, these errors were generally smaller than the data point itself.

as sedimentation rates would likely differ on the sill and Lake Couridjah margin due to these regions being complicated by geomorphic position. It is also acknowledged that the age at the boundary of the *L2* and *L3* unit may well be inaccurate due to contamination by younger or older carbon.

This data is presented in Figure 6.4, along with derived sedimentation rates including an extrapolation beyond the last data point. The predicted ages of stratigraphic units in Lake Couridjah are given in Table 6.1.

Table 6.1 Actual and derived ages for the stratigraphic units with Lake Couridjah based on the age model in Fig 6.4. Ages with an asterisk (*) are actual ages.

Unit Code	Unit Description	Depth (m)	Approximate Age (ka BP)
L1	Peat	0 – 1.75	0 – 10.8*
L2	Dark grey/brown silt	1.75 – 2.86	10.8 – 38.7*
L3	Light yellow/brown silt	2.86 – 3.19	38.7 – 50
L4	Very dark brown silt	3.19 – 3.66	50 – 60
L5	Dark grey/brown silt	3.66 – 4.24	60 – 70
L6	Very dark brown laminated silt	4.24 – 5.77	70 - 110
L7	Silt with interbedded sand	5.77 – 6.8	110 - 120

The relative ages presented in Table 6.1, as derived from the LC2 age-depth model, will be used for the subsequent description of all stratigraphic units. The timing of the deposition of the stratigraphic units would suggest (assuming constant sedimentation rates in the bottom half of the core) that the record extends to Marine Isotope Stage 5 (~130 – 74 ka).

No dating was conducted on the Lake Baraba margin (core LB1), and hence the timing of the deposition of the clay and overlying peat cannot be inferred. One study, however, using a core taken from Lake Baraba (approximately 135 m closer towards the lake centre than LB1), deduced the onset of peat deposition at approximately 8.5 ka at 4.1 m depth (Black *et al.*, 2006) and thus the peat at Lake Baraba's margin may have started accumulating at a similar time.

6.3 Facies Interpretation

In the following sections, the sill and lake environments will be divided into facies and their palaeo-environmental context is discussed. Broadly, two primary units are apparent within the sediments existing along the LC-LB transect; these are termed *Primary Unit 1,* composed of sill deposits consisting of three different sill facies, and *Primary Unit 2,* composed of

lacustrine deposits consisting of seven different lacustrine facies. Each sill facies were defined based primarily on sedimentological data, whereas the lacustrine facies were defined based on sedimentological and geochemical data, which are described sequentially below.

6.3.1 Primary Unit 1: Sill Deposits

Sill facies 1 (S1)

Sill facies 1 is composed of poorly to very poorly sorted medium grained sand that physically separates Lake Couridjah from Lake Baraba, and is up to 3 m thick (HA1, HA2, HA3, HA4 and HA5; Fig. 6.3). This sand is thought to be alluvium deposited by small ephemeral streams operating on the alluvial fan that debouches from the adjacent sandstone ridgeline (Russell *et al.*, 2010). A distinct feature within *S1* is the presence of clean, pallid sand anywhere between 7 and 30 cm below the surface. This pallid sand has 'improved' sorting compared to the rest of *S1* (i.e., poorly sorted instead of very poorly sorted) and overlies organic sandy clays (described as sill facies 2 below). In some well-vegetated sandy deposits in Australia, this mantle of clean sand indicates the presence of aeolian processes (Nott *et al.*, 1994) often occurring after bushfires (Bryant *et al.*, 1994). *S1* may therefore represent a mix of fluvially-transported and aeolian sediment and given that its stratigraphic position was most likely deposited in the Holocene.

Sill facies 2 (S2)

Sill facies 2, apparent at approximately 1.5 m and 3 m depth in the augured cores HA1, HA2, HA3, HA4 and HA5 (Fig. 6.3), represents periods of soil development within the sandy deposits of the sill. These paleosols contain higher organic matter than the surrounding units, with increased abundance of wood fragments, charcoal and mottling. This implies that at this time, there was 1) a wetter catchment and Lake Baraba's water levels were high, 2) increased moisture in the sill (i.e. impeded drainage) and 3) relative geomorphic stability, as palaeosols have been interpreted to suggest that catchment sediment delivery was slower than soil formation (Zhou *et al.*, 1994; Lam *et al.*, 2017).

Sill facies 3 (S3)

Sill facies 3, occurring at approximately 5 m depth within the sill and is apparent within the cores HA1, HA2, HA3 and HA5, is composed of 1 – 2 m of very poorly sorted light orange/brown sand. Similar to *S1*, this sand is interpreted as being deposited by fluvial

processes carrying sediment along the alluvial fan. Significantly, *S3* represents the earliest sandy sill deposits encountered in this study, and the deposition of this unit could represent the initial instance of Lake Couridjah becoming separated from Lake Baraba, especially when considering the underlying unit, lacustrine facies 6, is thought to represent a continuous swamp system between the lakes. This will be further discussed under the description of lacustrine facies 5 and 6, and again in section 6.5.

6.3.2 Primary Unit 2: Lacustrine Deposits

Lacustrine facies 1 (L1)

Lacustrine facies 1 in Lake Couridjah consists of a peat unit of approximately 10 – 11 ka. It is characterised by high C and N (Fig. 5.17), a low abundance of detrital elements (Si, Al and Ti) and high Ca:Ti ratios in the sediments (Fig. 5.14). *L1* also has high Fe:Mn ratios in its lower half. Furthermore, Figures 5.14 and 6.2 shows significantly depleted δ13C values in Zone 1 between 0 – 1.75 m of the core LC2, which corresponds to the depth of *L1* and is suggestive of greater water availability for plants during this time. These results suggest that the lake environment in *L1* has been relatively shallow, productive and nutrient-rich enough to encourage widespread growth of swamp vegetation to produce the physical mass of the peat, yet moist enough to cause anaerobic conditions and peat preservation. The low abundance of erosion-derived detrital elements and persistence of relatively shallow water anoxia also indicates climatic stability and minimal wind mixing of lake waters. The current environment of Lake Couridjah closely reflects these conditions, and therefore *L1* provides an analogue for the contemporary depositional environment, implying Lake Couridjah has remained largely unchanged for 10.8 ka. Two interesting features exist within *L1*; a break in peat deposition at the Lake Couridjah margin represented by a small lens of yellow silt between 0.33 – 0.353 m depth, and a section of crumbly, compacted peat occurring at the lake centre between 0.2 – 0.29 m depth. This 'crumbly' peat coincides with small increases in Ti, Sr:Ca, Sr:Zr and Sr:Rb, as well as a decrease in Ca:Ti. These changes all occur for ~0.05 – 0.2 m and are centred around 0.26 m depth. This suggests that the delivery of less weathered (faster delivery of sediment to the lake basin), clastic material increased at a time when evaporation increased, and lake productivity decreased. Therefore, both of these sediments are interpreted to represent lake drying events, with the yellow silt lens indicating subaerial exposure of the sediment during deposition.

Lacustrine facies 2 (L2)

Lacustrine facies 2 consists of slightly mottled dark grey/brown silt that occurred between 1.75 – 2.86 m within the core LC2. Two hypotheses exist for the deposition of *L2*, both of which imply differences in depositional environments, these are:

1. *L2* may be interpreted as representing a lake environment more permanent and significantly deeper than *L1,* in which aquatic vegetation was restricted to the lake margins and fine-grained silts settled out in a low-energy lacustrine environment. This interpretation has been given to similar deposits in other studies at Thirlmere Lakes (Black *et al.*, 2006; Robbie and Martin, 2007). The distinct dark grey/brown colour indicates Fe in its reduced (ferrous) state, suggestive of deep water with anoxic bottoms waters (Davison, Woof and Rigg, 1982). Furthermore, the Fe:Mn ratio is generally high in the upper half of *L2,* reflecting persistent reducing conditions (Fig. 5.14).
2. Alternatively, *L2 could* reflect an environment not persistently saturated enough for the preservation of peat to occur, but instead inorganic clays were deposited in drier conditions than was experienced during the deposition of *L1*. A similar interpretation was previously applied to explain the deposition of clays found at Lake Leake, Marshes Swamp (Dodson, 1975; Dodson and Wilson, 1975, respectively) and Little Llangothlin Lagoon (Woodward *et al.*, 2017) in south east Australia. In the case of Lake Couridjah this interpretation is supported by elevated counts of detrital elements and Sr:Zr, Sr:Rb and Ba:Zr ratios in *L2* (Fig. 5.15), suggesting a significant increase of allochthonous, less weathered material, or, an increase in soluble Sr and Ba, at the lake centre during low water levels. This is further confirmed by some olive/yellow mottling and high δ13C and δ15N values that reflect the increased plant photosynthetic fixation of the heavier isotopes ^{13}C and ^{15}N during times of water stress (Fig. 5.17). Additionally, in the bottom half of *L2,* there are high counts of Sr:Ca, where high values suggest higher lake evaporation, which is supported by low Fe:Mn ratios, suggesting well oxygenated shallow water. The top half of *L2*¸ the Sr:Ca and Fe:Mn ratios decrease and increase respectively, indicating gradual water deepening and the onset of anaerobic conditions (Fig. 5.14). Lastly, there is evidence of drying on the lake margin at the time *L2* was being deposited. That is, the stratigraphic relationships

presented in Figure 6.3 propose that *L3* (which will be subsequently discussed as a unit representing a considerable lake-drying event) occurred synchronously at the Lake Couridjah margin as *L2* was being deposited at the lake centre, as highlighted by the laterally discontinuous nature of *L2.* It is therefore illogical to assume that whilst the margin of Lake Couridjah was undergoing considerable drying, the centre of the lake was depositing deep-water silts.

Overall therefore, *L2* is interpreted as being deposited during conditions that were drier than the peat-forming environment of *L1,* yet still within a shallow water body as indicated by the preservation of the dark grey/brown colour and lack of significant mottling.

Lacustrine facies 3 (L3)

Lacustrine facies 3 consists of yellow silt with bright red/orange mottling and occurs within the core LC1 and LC2 (Figure 6. 3). *L3* is interpreted to represent a distinct shift into dry conditions within Lake Couridjah. This is marked by an increase in grain size (Fig. 5.3), detrital element counts and the Sr:Zr, Sr:Rb and Ba:Zr ratios (Fig. 5.15). Furthermore, there are high values of Sr:Ca and corresponding low values of Fe:Mn (Fig. 5.14). Similar to *L2,* this suggests that coarser grained and less weathered clastic sediment was delivered to the lake floor due to diminished water levels, or that Sr precipitation occurred due to dry conditions. There is also minimal organic content in *L3* as shown by LOI analysis (Fig's. 5.2; 5.7) and low C and N contents in this sediment (Fig. 5.17), suggesting the preservation of organic material was low during this time. Abundant charcoal is preserved both at the onset and cessation of this drying, possibly indicating increased fires and/or an increase in vegetation as water shallowed at the onset and then deepened again as drying ceased.

Lacustrine facies 4 (L4)

The dark and fine-grained sediment of lacustrine facies 4, which was present in all cores except HA4 and LB1, is interpreted as representing an extensive swamp phase, inducing swampy conditions that persisted within Lake Couridjah and across the sill. This is marked by peaks in organic content (Fig. 5.2), C, N and C:N (Fig. 5.17) and increases in the Fe:Mn ratio. Also, counts of detrital elements are relatively high, but there is a significant decrease in the Sr:Zr, Sr:Rb and Ba:Zr ratios (representing an input of more weathered material) (Fig.'s 5.14; 5.15). This represents the input of detrital material that had undergone a significant amount

of weathering in a possibly stable, well-vegetated catchment. *L4* may represent conditions in which Lake Couridjah and Lake Baraba were hydrologically connected. Interestingly, a pallid yellow/grey clay occurred abruptly underneath *L4* in the HA4 core (Fig. 6.3). A possible explanation for this stark change between dark organic sediment and underlying bleached clay is the preservation of the A_1 and A_2 horizon of a podzol respectively, with such deposits previously interpreted as a palaeo A_2 horizon in other settings (Thompson, 1992; Nott *et al.*, 1994). In this way, the humic acid eluviation from the overlying organic sediment bleached the underlying material, creating the pale A_2 horizon.

Lacustrine facies 5 (L5)

The lacustrine facies 5 was present in the cores LC1, LC2 and HA2 (Fig. 6.3), and is interpreted as representing a period of low lake levels, where the influx of detrital elements, particularly Al and Ti, reach the highest counts in the core LC2. Furthermore, δ13C and δ15N values are high (Fig. 5.17), and there is very little organic matter as well as C and N in the sediments. The sediment characteristics within *L5* closely reflect those of *L2*, as both units consist of fine dark grey/brown silt with some mottling low preservation of organic matter. Both units could thus represent similar depositional environments. However, material entering the lake basin at the time *L5* was deposited was much more weathered than the material depositing during *L2,* which may indicate differences in relative stability of the catchment imposed by vegetation.

L5 becomes progressively sandier approaching the margin of Lake Couridjah, with distinctly interbedded sand and clay occurring within the LC1 core. Here, some interbeds of sand are quite thick (>0.2 m) and quartz granules up to 3000 µm in diameter were found, indicating a high energy environment where sand has possibly in-washed from the sill during generally dry conditions with occasional high energy events. Furthermore, the processes that initiated the deposition of the sill (*S3)* physically separated Lake Couridjah from Lake Baraba, which at the time embodied a continuous swamp system (this is further discussed under lacustrine facies 6). The sandy and interbedded nature of the sediments occurring at the Lake Couridjah margin in cores LC1 and HA2 may thus reflect the synchronous deposition of the sill as the continuous swamp system was disrupted and Lake Couridjah consequently shallowed.

Lacustrine facies 6 (L6)

Lacustrine facies 6 exists continuously between Lake Couridjah and the Lake Baraba margin and was present in the cores LC2, LC1 and HA5 (Fig. 6.3). It contains high but variable organic matter content, C, C:N and is relatively low but variable in the composition of detrital elements. Interestingly, a significant increase in the Si:Ti ratio, where high ratios indicate an increase in biogenic silica (BSi), occurs between 4.8 – 5 m depth. This is interpreted as a period of increased lake productivity, and is further confirmed by an increase in the variability of the Ca:Ti ratio, decreases in Al and Ti, as well as relatively unchanged counts of Si at the corresponding depth. Figure 6.2 shows the δ13C values and C:N ratios of *L6* are similar to the δ13C values and C:N ratios of the living vegetation samples. This reflects relatively undecomposed organic matter that was preserved in an anoxic swamp environment. Furthermore, thin laminar alternations between dark sediments and lighter grey/brown silt in the upper section of *L6* roughly correspond with the variations organic matter, with the lighter grey/brown silt being less organic. This indicates the lake may have been transitioning between a saturated peat-depositing system and relatively drier environment. Therefore, *L6* represents a generally swampy, saturated environment where the deposition of peat was intermittently interrupted by the significant lowering of water levels.

Lacustrine facies 7 (L7)

Lacustrine facies 7 was only encountered at the base of the LC2 core (Fig. 6.3). The complex changes in colour, grain size and texture, as well as the occurrence of large charcoal fragments, possibly suggests that this unit was initially sub-aerially exposed in a dry lake, and then became the saturated swamp system reflected in *L6.* In support of this, counts of detrital elements increase from *L6* to *L7* (Fig. 5.14), and δ13C values are high which indicates a decrease in moisture availability for plants (Fig. 6.2). Therefore, overall this period is interpreted as drier conditions with frequent fires occurring.

6.4 Stratigraphy and groundwater and its implications for connectivity between Lake Couridjah and Lake Baraba

The stratigraphic relationships inferred for the Lake Couridjah and Lake Baraba systems, combined with the presence of groundwater, imply the two lakes have experienced differences in connectivity through time. The current water table in the sill was reached at

different depths in the cores HA3, HA2, HA1 and to a lesser extent, HA5 (Fig. 6.3). That is, it was found at greater depths further from Lake Couridjah. This implies that during the time of the present study, Lake Couridjah was losing surface water and effectively recharging the sub-surface groundwater (at least in the sill). Furthermore, abrupt alternations to a relatively dry, pallid yellow silt occurs within the core HA3, HA4 and HA5 (Fig. 6.3), and in all accounts the sediments overlying the pallid yellow silt were far more saturated. This could imply that this pallid yellow silt exerts a form of localised control on sub-surface water movement within the sill.

Assuming the stratigraphic relationships presented in Figure 6.3 are correct, the increase in sediment saturation that caused the development of the palaeosols in *S2* seems to indicate an extension Lake Baraba's surface area, rather than Lake Couridjah's. This is because the palaeosols occur proximal to Lake Baraba's margin, yet only the deepest one remains continuous until apparently grading into the peat deposits at Lake Couridjah's margin (Fig. 6.1), implying that lateral lake development and surface flow on the sill occurred from Lake Baraba to Lake Couridjah as Lake Baraba overflowed, which is against the preconceived 'downstream' flow path. With this in mind, the deposition of *L4* may have occurred in a similar manner, which will be further discussed in section 6.5.

Direct subsurface flow from Lake Couridjah to Lake Baraba or *vice versa* could not be inferred from the findings of this study. However, all the sediments within the core HA4 were essentially dry and crumbly, and the basal clay layers were rigid with only slight plasticity. This was found despite the nearby core LB1 (~55 m away, see Fig. 6.3) being fully saturated at its surface (Fig. 6.1). It is hypothesized that the dense clay found at the Lake Baraba margin may act to hinder water movement between the lakes. That is, the surface water at the Lake Baraba margin may be kept hydrologically separated from Lake Couridjah by this clay aquitard. If this clay is continuous under the whole of Lake Baraba, it may greatly influence the surface hydrology of the lake. It appears that during times of low or decreasing water levels, when the water level drops below the level of the clay, Lake Couridjah and Lake Baraba may act as hydrologically discrete water bodies. During times of higher lake levels when water overtops the clay, Lake Baraba could potentially release water into the sill that may eventually flow into Lake Couridjah. Variations in the hydrologic connectivity between Lake Couridjah and Lake Baraba may influence the propagation of drought-driven responses throughout the

whole system, implicating the general water storage capacity and the systems' resilience in drought periods (Tweed *et al.*, 2009).

6.5 Palaeo-environments and South-east Australian Context

Throughout the Quaternary period, south east Australia experienced alternations between relatively cool to intermediate temperatures as evidenced by changes in sea surface temperatures (Barrows *et al.*, 2007), lake levels and vegetation communities (Cook, 2009) and aeolian depositional phases (Lomax *et al.*, 2011). These oscillations generally coincide with the Marine Isotope Stages (MIS). Broadly, MIS 5 (~130 – 74 ka) and 3 (~60 – 24 ka) were characterised by relatively high effective precipitation, increased river activity and lake levels as well as forest expansion, whereas MIS 4 (~74 – 60 ka) and 2 (~24 – 11 ka) were demarked by diminished forests, decreases in lake levels and increased dune building in central Australia (Harrison, 1993; Kershaw *et al.*, 2007; van Meerbeeck *et al.*, 2009; Webb *et al.*, 2014).

With the lack of accurate dating past 2.86 m depth in the core LC2 at the centre of Lake Couridjah, the lower lacustrine facies, i.e. *L3, L4, L5, L6* and *L7,* are hard to chronologically constrain. However, by extrapolation, the base of the core LC2 could be as old as >100 ka (Fig. 6.4), which sits within MIS 5, an interglacial. MIS 5 is thought to have induced relatively wet conditions throughout south eastern Australia until 100 ka, after which there is a general trend towards a more arid MIS 4 (Webb *et al.*, 2014). This time may be represented in the core LC2 at the centre of Lake Couridjah by *L6,* which was inferred to have been deposited between ~110 – 70 ka and reflects a continuous swamp system between Lakes Couridjah and Baraba (Fig. 6.2). Throughout the upper half of *L6*, there are thin laminar alternations of darker, more organic and lighter, inorganic silt, which indicates the cessation of peat deposition as the swamp intermittently dried. *L5* is interpreted as representing low lake levels and poor preservation of organic matter, and may have been deposited between ~70 – 60 ka (Table 6.1) which coincides with MIS 4 glacial period. Therefore, the sequence from *L6* to *L5,* which represents a shift from wetter to drier conditions, could reflect the transition from the MIS 5 interglacial to the MIS 4 glacial at Thirlmere Lakes. It is also hypothesised that during the period *L6* was being deposited, the synchronous deposition of the sill may have divided the swamp system, consequently disrupting connectivity between Lakes Couridjah and Baraba which further induced drying at Lake Couridjah. Therefore, the drying trend from *L6* to *L5* may have been a product of both climatic and geomorphic influences.

The early last glacial period (~35 – 22 ka) in south eastern Australia coincides with the end of the MIS 3 and beginning of the MIS 2, and was therefore a time of moist conditions with associated high fluvial activity and lake levels that digressed into a cool and dry climate at the onset of the LGM (van Meerbeeck *et al.*, 2009; Petherick *et al.*, 2013). During the LGM, south east Australia experienced a cool climate with enhanced aridity and generally low lake levels (Petherick *et al.,* 2011). The majority of palynological records indicate open steppe grasslands characterised by species such as *Asteraceae, Poaceae* and *Chenopodiaceae* (Petherick *et al.,* 2011). But at Lake Baraba, a pollen record depicts Casuarinaceae community dominance during the late glacial period, suggesting that Thirlmere Lakes may have acted as a refugium for arboreal species during this time (Black *et al.,* 2006). The subsequent glacial – interglacial transition period (~18 – 12 ka) generally exhibited increases in temperature and moisture, although was found to be relatively arid in the Southern Tablelands of NSW (Kemp and Hope, 2014) and lake levels from Lake George were significantly low between 14 – 10 ka BP (Fitzsimmons and Barrows, 2010). This sequence of high effective moisture during the early last glacial period, followed by increased aridity associated with the LGM, and the subsequent more humid deglacial period, approximately aligns with *L4, L3* and *L2* from the Lake Couridjah stratigraphy in core LC2. This suggests that during the MIS 3 and the early last glacial period in south eastern Australia, Lake Couridjah and Lake Baraba were reconnected as a continuous swampy environment which dried sometime during the onset of the LGM. Afterwards, during the deglacial, Lake Couridjah embodied a shallow lake system with intermittent drying and low preservation of organic material.

The onset of the Holocene (~12 ka) is described as a period of increased temperatures and precipitation with generally stable climates (Kemp and Hope, 2014), conditions conducive to the establishment of vegetation and the accumulation of organic sediment in lakes and swamps (Fryirs *et al.*, 2014). This climatic change is represented very well by the geochemical data from Lake Couridjah, showing decreases catchment-derived detritus and increases in lake productivity with the transition into a full peat-depositing system culminating at ~10.8 – 10.5 ka (Figure 5.13, Table 6.1). Furthermore, the greatly depleted δ13C values in the lower part of *L1* (Fig. 6.2) highlights the increased availability if moisture during the early Holocene. This is generally synchronous with lake and swamp development at other sites throughout south-eastern Australia. Mountain Lagoon in the Blue Mountains persisted as a swamp until

becoming a lake at about 10 ka (Robbie and Martin, 2007) and Lake George experienced its highest Holocene shorelines between 10 – 8 ka (Fitzsimmons and Barrows, 2010). Furthermore, mires at Barrington Tops started accumulating peat after 8.6 ka (Dodson, 1987), with alpine soils and peat similarly developing in the Snowy Mountains from this time (Marx *et al.*, 2011; Stromsoe *et al.*, 2016). Interestingly, Lake Baraba started accumulating peats at 8.5 ka (Black *et al.*, 2006), some 2000 years after Lake Couridjah. Dry Lake (situated ~3 km north-west of Thirlmere Lakes) started accumulating peat at ~2 ka, however this was attributed to lake shallowing via sedimentation rather than changes in climate (Rose and Martin, 2007). Nonetheless, this demonstrates that different terrestrialisation or swamp-forming phases throughout the Thirlmere Lakes system can occur at vastly different times, and result from a combination of lake in-filling and climatic changes.

By the mid-Holocene (~6 ka) south-eastern Australia experienced a return to drier and cooler conditions with more pronounced climatic variability, a trend that is widespread in the literature (e.g., Dodson, 1987; Harrison, 1993; Woodward *et al.*, 2014; Tyler *et al.*, 2015). This change is thought to have come about by the onset of modern climate processes such as El Nino Southern Oscillation (ENSO) with a dominate El Nino, which can induce pronounced dry periods in south-eastern Australia (Reeves *et al.*, 2013; Woodward *et al.*, 2014). The margin of Lake Couridjah in core LC1 displays evidence for lake drying at 0.33 – 0.353 m depth, made apparent by a lens of yellow silt. This yellow silt was deposited approximately 4 ka (Figure 6.4), however because this occurred on the lake margin, the accuracy of applying the age-depth model determined for the lake centre to this area is questionable. However, Gergis's (2000) study on Lake Couridjah found distinct increases in Mn:Fe (indicative of oxidative lake conditions) from 6.2 – 3.6 ka, and Black *et al.*'s (2006) study on Lake Baraba found a hiatus in peat deposition and an increase in fungal spores from 6 – 5.2 ka, which similarly indicates a shift to arid conditions during the mid-Holocene.

Furthermore, evidence for climatic variability into the late Holocene is apparent within the Lake Couridjah centre in core LC2 through the occurrence of 'crumbly' peat between 0.2 – 0.29 m depth, dating to ~1.8 – 2.2 ka (Fig. 6.4). This depth coincides with small increases in Ti, Sr:Ca, Sr:Zr and Sr:Rb, as well as a decrease in Ca:Ti (Fig.'s 5.14; 5.15), reflecting the delivery of less weathered (faster delivery of sediment to the lake basin), clastic material at a time

when evaporation increased and lake productivity decreased. This is once again supported by Gergis's (2000) findings of lake shallowing prior to 1.8 ka.

Despite some evidence of hydrological variability throughout the Holocene, Lake Couridjah has remained stable and relatively unchanged for ~10.8 ka. This is significant considering other eastern Australian lakes experienced a significant shift from standing water during the early Holocene to ephemeral wetlands during the mid to late Holocene (e.g. Little Llangothlin Lagoon, Woodward, 2017). Furthermore, Black *et al.* (2006) suggested that Thirlmere Lakes may have acted as a refugium for forest taxa during the late glacial period. Both these findings highlight the general stable nature of the Thirlmere Lakes catchment through time. However, it is also noted that swamp development between Lake Baraba and Lake Couridjah occurred at different times throughout the Holocene, despite no differences in local climate or topography. So, while the Thirlmere Lakes catchment may represent a localised region of stability through time, there is a degree of spatial and temporal heterogeneity in how the different Thirlmere Lakes operate hydrologically and geomorphologically.

6.6 Limitations

LC2 grain size determinations

Both grain size pre-treatment methods, i.e. pre-treatment A (post - LOI) and pre-treatment B (post - H_2O_2) revealed generally synchronous grain size changes in the core LC2 (Chapter 5, Fig. 5.3). However, pre-treatment B revealed consistently higher grain size results than pre-treatment A, and the largest difference between the two methods was 80 µm occurring at ~3.1 m depth. This difference may have been attributed to the grinding of the samples in pre-treatment A as this would have removed any clay aggregates formed during depositional processes. Whereas in pre-treatment B, clay aggregates would have remained and been measured during grain size analysis. Therefore, the cemented clay that formed during the combustion process in pre-treatment A had a lesser effect on grain sizes being 'too large' than previously thought. In general, however, it is unclear which method is more suitable for the grain size analysis of organic-rich sediments.

Alluvial fan grain size

Grain size analysis of the alluvial fan surface sediments revealed no particular trend down-fan, apart from a slight increase in grain size in the lower fan samples. This goes against the well-established view that grain size decreases down-fan. This result was most likely an artefact of the initial sieving of the samples before grain size analysis, consequently removing the coarse fraction.

Chronology

Due to the limitations of radiocarbon dating, all sediments below 2.86 m depth within the centre of Lake Couridjah (LC2 core) were too old (>49 ka) to be dated with radiocarbon. Therefore, the age of the underlying units was approximated via linear extrapolation, implying that each unit below 2.86 m depth was deposited at the same rate. However, the rate at which sediment accumulates in lakes is dependent upon at range of external, i.e. climate and catchment erosion rates, and internal, i.e. lake productivity, factors. Therefore, stratigraphic units formed under different depositional processes are likely to have varying sedimentation rates (Miall, 2014).

7. CONCLUSION

7.1 Summary

This study aimed to assess past hydrological variability within Lake Couridjah in order to put the recent trend of water loss within the Thirlmere Lakes system into a longer-term context of how the lakes respond to change. This was achieved by broadly investigating the palaeo-environments within Lake Couridjah, through examining the sedimentary characteristics and stratigraphic relationships in and between lakes Couridjah and Baraba. This included examining the age, grain size, organic content, elemental composition and C isotopes of the sediments. The results of these analyses were then compared with each other and the literature on palaeo-environments in south eastern Australia. In this regard, the following conclusions can be drawn:

- It is clear from the variability of the sediment characteristics, e.g. texture and colour, elemental data and stable C and N isotope analysis within the core LC2 that Lake Couridjah has undergone significant hydrological change between the MIS 5 (~130 – 74 ka) and the present. During MIS 5, Lake Couridjah and Lake Baraba were hydrologically connected as a continuous swamp system. After this, the formation of the sill acted to physically separate the two lakes. Sometime within MIS 4 (~74 – 60 ka) it is likely that Lake Couridjah became a shallow lake system. A return to wetter conditions is likely to have occurred during MIS 3 (~60 – 24 ka). During this time period lakes Couridjah and Baraba were reconnected as a continuous peat-forming swamp. Significantly, however, during the transition from MIS 3 to the early last glacial period (~35 – 22 ka) Lake Couridjah experienced a considerable drying event, which is interpreted to have occurred During the subsequent LGM and deglacial period (~24 – 12 ka), Lake Couridjah was a shallow lake similar to that of the palaeo-environment experienced during MIS 4.
- While the aforementioned environmental history displays clear evidence of significant drying and hydrological change within Lake Couridjah, it is important to consider that once the climate ameliorated with the onset of the Holocene (~12 – 0 ka), Lake Couridjah generally experienced sustained lacustrine conditions resulting in peat formation. However, there is some evidence for lake drying both at the Lake Couridjah margin during the Mid-Holocene; a period of cooler and drier conditions in

south eastern Australia. In addition, there is also evidence of drying occurring at the Lake Couridjah centre during the Late-Holocene; a time of climatic variability. Both results suggest that Lake Couridjah has experienced relatively recent lake drying events in response to broad climatic changes throughout south eastern Australia. It should be noted that these were not major drying events, unlike the event experienced during the MIS 3 - 2 transition, but rather short lived drying episodes or even periods of very low lake levels, without full drying of the lake.

- The stratigraphic relationships presented in this study reveal that Lake Couridjah has undergone multiple separate phases of predominantly 'swampy' conditions. They are noted to both coincide with, and act separately to, similar conditions within the sill and therefore possibly Lake Baraba. Furthermore, there is a significant difference between the initiation of peat deposition in Lake Couridjah (~10.8 ka) compared to Lake Baraba (~8.5 ka, see Black *et al.*, 2006). Therefore, lakes Couridjah and Baraba appear to have experienced different hydrological and sedimentological processes through time, which suggests that despite their close proximity, these lakes can operate as independent water bodies.

In the context of other peat-forming lakes and swamps within the Sydney Basin, Thirlmere Lakes represents a relatively rare system in that its unique long-term catchment stability has provided excellent preservation of lacustrine sediments, as well as near constant peat deposition for over 10,000 years. In contrast, many upland swamps of the Sydney Basin reflect inter-annual hydrological variability in which the long-term preservation of peat has not occurred (Fryirs *et al.*, 2014). This suggests the Thirlmere Lakes represent a relatively unique palaeo-archive within the Sydney Basin. The Thirlmere Lakes are important ecologically, scientifically and aesthetically, and despite their apparent long-term hydrological variability, Lake Couridjah has remained comparatively hydrologically stable during the Holocene. However, the lakes are still subject to change under regional (south eastern Australia) changes in climate, suggesting the recent trend of water loss from the lakes is not unprecedented if climate is the primary control.

7.2 Future Research

This study has provided some important insights into the palaeo-environmental history of Thirlmere Lakes. However, there is need to further clarify the palaeo-history of the lakes and, in particular, to investigate whether the results found in this study are indeed unequivocal. In regard to this particular study, recommendations for future research are:

1. *Comparative stratigraphy for Lake Baraba*

Further stratigraphic investigation is needed within Lake Baraba to investigate whether (i) the units within the sill, i.e. *L4* and *L6,* are indeed continuous within the Lake Baraba margin and therefore indicative of continuous swamp systems between Lake Couridjah and Baraba, and (ii) to establish the extent and hydrological properties of the dense clay encountered at the Lake Baraba margin. The importance of this clay is that it is considered to act as an aquitard between Lake Couridjah and Lake Baraba and may therefore control the present-day behaviour of the two lake systems, i.e. their hydrological independence.

2. *Establishment of a more robust chronology for Lake Couridjah*

Within the 6.8 m LC2 core from the centre of Lake Couridjah, the radiocarbon dating limit of approximately 50,000 years was reached somewhere between 2.86 - 3.21 m depth. Therefore, the deposition of all stratigraphic units beneath 2.86 m depth was not accurately constrained. Importantly, this includes unit *L3* which indicates a period of considerable drying of Lake Couridjah. Other dating methods, namely, optically stimulated luminescence (OSL), will be required to establish the date of these units.

3. *High precision/accuracy elemental analysis*

While the ITRAX data collected for core LC2 from Lake Couridjah can be used to infer changes in processes such as the influx of catchment-derived material, lake productivity and redox conditions, it cannot be used to accurately quantify geochemical changes within the core LC2. Absolute elemental analysis is required to more accurately understand these results.

4. Understanding the causes of the depleted $\delta^{13}C$ values during the Holocene

Interestingly, all of the $\delta^{13}C$ values and C:N ratios from sediments that were deposited during the Holocene were not suggestive of any 'usual' sources of organic matter. It is hypothesized that this depleted $\delta^{13}C$ signal may have resulted from the increased availability of water for plants, particularly at the onset of the Holocene. Alternatively, some form of methogenic-bacterial process created this depleted $\delta^{13}C$ signal which was subsequently incorporated into the lake sediment through the bacterial uptake by macroinvertebrates, such as the chironomid tribe Chironomini. Therefore, chironomid analysis of these sediments will help explain this depleted $\delta^{13}C$ signal.

REFERENCES

Babechuk, M. G., Widdowson, M., Murphy, M., Kamber, B. S., 2015. A combined Y/Ho, high field strength element (HFSE) and Nd isotope perspective on basalt weathering, Deccan Traps, India. *Chemical Geology*, **396**, 25-41.

Balesdent, J., Girardin, C., Mariotti, A. 1993. Site-Related Delta-13-C of Tree Leaves and Soil Organic Matter in a Temperate Forest. *Ecology*, **74**(6), 1713-1721.

Bałaga, K. 2007. Transformation of Lake Ecosystem into peat bog and vegetation history based on Durne Bagno mire (Lublin Polesie, e Poland). *Geochronometria,* **29**, 23-43.

Barr, C., Tibby, J., Gell, P., Tyler, J., Zawadzki, A., Jacobsen, G. E. 2014. Climate variability in south-eastern Australia over the last 1500 years inferred from the high-resolution diatom records of two crater lakes. *Quaternary Science Reviews,* **95**, 115-131.

Barrows, T. T., Juggins, S., De Deckker, P., Calvo, E., Pelejero, C. 2007. Long-term sea surface temperature and climate change in the Australian–New Zealand region. *Paleoceanography*, **22**(2), 1-17.

Barrows, T. T., Stone, J. O., Fifield, L. K., Cresswell, R. G 2001. Late Pleistocene Glaciation of the Kosciuszko Massif Snowy Mountains, Australia. *Quaternary Research*, **55**(2), 179 – 189

Blair, T. C., McPherson, J. G. 1994. Alluvial fan processes and forms. *Geomorphology of Desert Environments.*

Black, M. P., Mooney, S. D., Martin, H. A. 2006. A >43, 000-year vegetation and fire history from Lake Baraba, New South Wales, Australia. *Quaternary Science Reviews*.

Bloesch, J., Stadelmann, P., Buhrer, H., 1977. Primary production, mineralization, and sedimentation in the euphotic zone of two Swiss lakes. *Limnology and Oceanography*, **22**(3).

Blott, S. J., Pye, K. 2001. Gradistat: A Grain Size Distribution and Statistics Package for the Analysis of Unconsolidated Sediments. *Earth Surface Processes and Landforms,* **26**(11), 1237–1248.

Boehrer, B., Schultze, 2008. Stratification of lakes. *Geophysics*, **46.**

Bragg, O. M., Tallis, J. H. 2001. The sensitivity of peat-covered upland landscapes. *Catena*, **42**, 345-360.

Bridgman, H. A., Timms, B. V. 2012. Australia, Climate and Lakes. *Encyclopaedia of Lakes and Reservoirs.* Encyclopaedia of Earth Sciences Series. Springer, Dordrecht.

Brierley, G. J., Fryirs, K. A. 2005. Geomorphology and River Management: Applications of the River Styles Framework. *Blackwell Publishing*, Oxford, UK.

Brown, E., Johnson, T., Scholz, C., Cohen, A., King, J. 2007. Abrupt change in tropical African climate linked to the bipolar seesaw over the past 55,000 years. *Geophysical Research Letters*, **34**(20), 1-5.

Brugnoli, E., Farquhar, G. D. 2000. Photosynthetic Fractionation of Carbon Isotopes. *Photosynthesis: Physiology and Metabolism*, 399–434.

Bryant, E. A., Young, R. W., Price, D. M., Short S. A. 1994. Late Pleistocene Dune Chronology; near-coastal New South Wales and Eastern Australia. *Quaternary Science Reviews*, **13**, 209-223.

Bureau of Meteorology. 2018. Annual climate statement 2017, rainfall (wet period in 2010 and 2011). viewed 17 March 2018, http://www.bom.gov.au/climate/current/annual/aus/#tabs=Rainfall.

Bureau of Meteorology. 2018. Climate statistics for Australian locations, Wind direction at Camden Airport - http://www.bom.gov.au/climate/averages/tables/cw_068192.shtml.

Bureau of Meteorology. 2016. Average annual, seasonal and monthly rainfall, Mean Australian rainfall. viewed 17 March 2018, http://www.bom.gov.au/jsp/ncc/climate_averages/rainfall/index.jsp.

Bureau of Meteorology. 2016. Average 9am and 3pm relative humidity, viewed 17 March 2018, http://www.bom.gov.au/jsp/ncc/climate_averages/relative-humidity/index.jsp.

Burkitt, L. L. 2014. A review of nitrogen losses due to leaching and surface runoff under intensive pasture management in Australia. *Soil Research*, **52**(7), 621.

Calvert, S.E. 2004. Beware intercepts; interpreting compositional ratios in multi-component sediments and sedimentary rocks. *Organic Geochemistry,* **35**(8), 981-987.

Coventry, R. J. 1976. Abandoned shorelines and the Late Quaternary History of Lake George, New South Wales. *Journal of the Geological Society of Australia,* **23**(3), 249-273.

Cherevichko, A. V. 2009. The Zooplankton of Various Water Reservoirs in the Polistovo-Lovatskaya Upland Swamp System. *Inland Water Biology,* **2**(3), 259-263.

Chimner, R. A., Ewel, K. C. 2005. A tropical freshwater wetland: II. Production, decomposition, and peat formation. *Wetlands Ecology and Management,* **13**, 67-684.

Cohen, T. J., Nanson, G. C., Jansen, J. D., Jones, B. G., Jacobs, Z., Treble, P., Price, D. M., May, J., Smith, A. M., Ayliffe, L. K., Hellstrom, J. C. 2011. Continental aridification and the vanishing of Australia's megalakes. *Geology,* **39**(2), 167-170.

Cook, E. J. 2009. A record of late Quaternary environments at lunette-lakes Bolac and Turangmoroke, Western Victoria, Australia, based on pollen and a range of non-pollen palynomorphs. *Review of Palaeobotany and Palynology*, **153**, 185 – 224.

Cowley, K. L., Fryirs, K. A., Hose, G. C. 2016. Identifying key sedimentary indicators of geomorphic structure and function of upland swamps in the Blue Mountains for use in conditions assessment and monitoring. *Catena,* **147**, 564-577.

Crawford, R. M. M., Jeffree, C. E., Ree, W. G. 2003. Paludification and Forest Retreat in Northern Oceanic Environments. *Annals of Botany*, **91**, 213-226.

Davies, S. J., Lamb, H. F., Roberts, S. 2015. Micro XRF core scanning in palaeolimnology: recent developments. British Antarctic Survey.

Davison, W., Woof, W., Rigg, E. 1982. The dynamics of iron and manganese in a seasonally anoxic lake; direct measurement of fluxes using sediment traps. *Limnology and Oceanography*, **27**(6), 987-1003.

Department of Environment and Energy. 2010. Directory of Important Wetlands in Australia - Information sheet. Thirlmere Lakes NSW091. Viewed 2 November 2018. http://www.environment.gov.au/cgi-bin/wetlands/report.pl

Department of the Environment and Energy. 2016. Australian Wetlands Database, Little Llangothlin Nature Reserve 1996, viewed 28 February 2018, http://www.environment.gov.au/cgi-bin/wetlands/ramsardetails.pl?refcode=47.

Devito, K. J., Hill, A. R., Roulet, N. 1996. Groundwater-surface water interactions in headwater forested wetlands of the Canadian Shield. *Journal of Hydrology,* **181**, 127-147.

Dodson, J. R. 1974. Vegetation History and Water Fluctuations at Lake Leake, South-eastern South Australia. I 10,000 B.P. to Present. *Australian Journal of Botany,* **22**, 719-41.

Donders, T. H., Haberle, S. G., Hope, G., Wagner, F., Visscher, H. 2007. Pollen evidence for the transition of the Eastern Australia climate system from the post-glacial to the present-day ENSO mode. *Quaternary Science Reviews,* **26**, 1621-1637.

Farquhar, G. D., O'Leary. M. H., Berry, J. A. 1982. Relationship between Carbon Isotope Discrimination and the Intercellular Carbon Dioxide Concentration in Leaves. *Australian Journal of Plant Physiology*, **9**, 121-37.

Fitzsimmons, K.E., Barrows, T. T. 2010. Holocene hydrologic variability in temperate southeastern Australia: An example from Lake George, New South Wales. *The Holocene*, **20**(4), 1–13.

Folk, R. L. 1974, 'Petrology of Sedimentary Rocks' Hemphill Publishing Company Austin, Texas.

Freidman, B. L., Fryirs, K. A. 2015. Rehabilitating upland swamps using environmental histories: a case study of the Blue Mountains peat swamps, Eastern Australia. *Physical Geography,* **97**, 337-353.

Fryirs, K. A., Cowley, K., Hose, G. C. 2016. Intrinsic and extrinsic controls on the geomorphic conditions of upland swamps in Eastern NSW. *Catena*, **137**, 100-112.

Fryirs, K., Gough, J., Hose, G. 2014a. The geomorphic character and hydrological function of an upland swamp, Budderoo plateau, southern highlands, NSW, Australia. *Physical Geography*, **35**(4), 313-334.

Fryirs, K. A., Freidman, B., Williams, R., Jacobsen, G. 2014. Peatlands in eastern Australia? Sedimentology and age structure of Temperature Highland Peat Swamps on Sandstone (THPSS) in the Southern Highlands and Blue Mountains of NSW, Australia. *The Holocene,* **24**(11), 1527-1538.

Geoscience Australia. 2012. Australian Stratigraphic database, Hawkesbury Sandstone, viewed 22 March 2018, http://dbforms.ga.gov.au/pls/www/geodx.strat_units.sch_full?wher=stratno=8165.

Habeck-Fardy, A., Nanson, G. C. 2014. Environmental character and history of the Lake Eyre Bason, one seventh of the Australian continent. *Earth Science Reviews,* **132**, 39-66.

Hardenbroek, M. V., Lotter, A. F., Bastviken D., Duc, N. T., Heiri, O. 2012. Relationship between d13C of chironomid remains and methane flux in Swedish lakes. *Freshwater Biology*, **57**(1), 166–17.

Harrison, S. P. 1993. Late Quaternary Lake-level Changes and Climate Changes of Australia. *Quaternary Science Reviews*, **12**, 211-231.

Heathwaite, A. L. 1993. Disappearing peat-regenerating peat? The impact of climate change on British peatlands. *The Geographical Journal*, **159**(2), 203-208.

Helene, M. A. 1998. Tertiary climatic evolution and the development of aridity in Australia. *Proceedings of the Linnean Society of New South Wales*, **119**, 115-136.

Holden, J. 2006. Peatland Hydrology. *Developments in Earth Surface Processes,* **9**, 319-346.

Holden, J., Burt, T. P. 2002. Piping and pipeflow in a deep peat catchment. *Catena*, **48**(3), 163-199.

Hope, G., Nanson, R., Flett, I. 2009. The Peat-Forming Mires of the Australian Capital Territory. *Territory and Municipal Services*, Canberra.

Huang, C., Yao, L., Zhang, Y., Huang, T., Zhang, M., Zhu, A., Yang, H. 2017. Spatial and Temporal variation in autochthonous and allochthonous contributors to increased organic carbon and nitrogen burial in a plateau lake. *Science of the Total Environment*, **603**, 390 – 400.

Inisheva, L. I. 2006. Peat Soils: Genesis and Classifcation. *Eurasian Soil Science,* **39**(7), 699-704.

Jenkins, R. B., Frazier, P. S. 2010. High-resolution remote sensing of upland swamp boundaries and vegetation for baseline mapping and monitoring. *Wetlands,* **30**, 531-540.

Jones, R. N., McMahon, T. A., Bowler, J. M. 2001. Modelling historical lakes levels and recent climate change at three closed lakes, Western Victoria, Australia (c. 1840 – 1990). *Journal of Hydrology,* **246**(1-4), 159-180.

Kalnina, L., Stivrins, N., Kuske, E., Ozola, I., Pujat, A., Zeimule, S., Grudzinska, I., Ratniece, V. 2014. Peat Stratigraphy and Changes in Peat Formation During the Holocene in Latvia, *Quaternary International,* 1-10.

Kamber, B. S., Greig, A., Collerson, K. D. 2005. A new estimate for the composition of weathered young upper continental crust from alluvial sediments, Queensland, Australia. *Geochimica et Cosmochimica Acta*, **69**(4), 1041 – 1058.

Kattel, G., Gell, P., Zawadzki, A., Barry, L. 2017. Palaeoecological evidence for sustained change in a shallow Murray River (Australia) floodplain lake: regime shift or press response? *Hydrobiologia,* **787**, 269-290.

Kemp, J., Hope, G. 2014. Vegetation and environments since the Last Glacial Maximum in the Southern Tablelands, New South Wales. *Journal of Quaternary Science.*

Kershaw, P., McKenzie, M., Brown, J., Roberts, R. G., van der Kaars, S. 2010. Beneath the peat: A refined pollen record from an interstadial at Caledonia Fen, highland eastern Victoria, Australia. *Altered ecologies: fire, climate and human influence in terrestrial landscapes,* 33-48.

Kohlhagen, T., Fryirs, K., Semple, A. L. 2013. Highlighting the need and potential for use of interdisciplinary science in adaptive environmental management: the case of endangered upland swamps in the Blue Moutains, NSW, Australia. *Geographical Research*, **51**(4), 439-453.

Kokfelt, U., Reuss, N., Struyf, E., Sonesson, M., Rundgren, M., Skog, G., Rosen, P., Hammarlund, D. 2010. Wetland development, permafrost history and nutrient cycling inferred from late Holocene peat and lake sediment records in subarctic Sweden. *Journal of Paleolimnology*, **44**, 327-342.

Kolaczek, P., Niska, M., Miroslaw-Grabowska, J., Galka, M. 2016. Periodic lakes-peatland shifts under the Eemian and Early Weichselian climate changes in Central Europe on the basis of multi-proxy studies. *Palaeogeography, Palaeoclimatology, Palaeoecology,* **461**, 29-43.

Kylander, M. E., Klaminder, J., Wohlfarth B., Lowemark, L. 2013. Geochemical responses to paleoclimatic changes in southern Sweden since the late glacial: the Hasseldala Port lake sediment record. *Journal of Paleolimnology,* **50**(1), 57–70.

Lami, A., Marchetto, A., Kaempf, L., *et al.* 2012. Detrital layers marking flood events in recent sediments of Lago Maggiore (N. Italy) and their comparison with instrumental data. *Freshwater Biology*, **57**(10), 2076 – 2090.

Lomax, J, Hilgers, A., Radtke, U. 2011. Palaeoenvironmental change recorded in the palaeodunefield of the western Murray Basin, South Australia – New data from single grain OSL-dating. *Quaternary Science Reviews*, **30**, 723 – 736.

Lui, W., Wu, J., Ma, L., Zeng, H., 2014. A 200-year sediment record of environmental change from Lake Sayram, Tianshan Mountains in China. *GFF*. **136**(4), 548 – 555.

Ma, J-Y., Sun, W., Liu, X-N., Chen, F-H. 2012. Variation in the Stable Carbon and Nitrogen Isotope Composition of Plants and Soil along a Precipitation Gradient in Northern China. *PLoS ONE.* **7**(12).

Macphail, M., Fifield, L. K., Pillans, B., Hope, G. 2016. Lake George revisited: new evidence for the origin and evolution of a large closed lake, Southern Tablelands, NSW, Australia. 2: earliest Pleistocene (Gelasian) environments. *Australian Journal of Earth Sciences,* **63**(4), 453-468.

Martin, H. A. 2006. Cenozoic climatic change and the development of the arid vegetation in Australia. *Journal of Arid Environments,* **66**(3), 533 – 563.

Marx, S. K., Kamber, B. S. and McGowan, H. A. 2005. Provenance of long travelled dust determined with ultra-trace-element composition: A pilot study with samples from New Zealand glaciers. *Earth Surface Processes and Landforms,* **30**, 699-716.

Marx, S. K., Kamber, B. S., McGowan, H. A., Denholm, J. 2011. Holocene dust deposition rates in Australia's Murray Darling Basin record the interplay between aridity and the position of the mid-latitude westerlies. *Quaternary Science Reviews,* **30**, 3290-3305.

May, J. H., Barrett, A., Cohen, T. J., Jones, B. G., Price, D., Gliganic, L. A. 2015. Late Quaternary evolution of a playa margin at Lake Frome, South Australia. *Journal of Arid Environments,* **122**, 92-108.

McGlone, M. S., Moar, N. T., Meurk, C. D. 1997. Growth and Vegetation History of Alpine Mires on the Old Man Range, Central Otago, New Zealand. *Arctic and Alpine Research,* **29**(1), 32-44.

Mee, A. C., McKirky, D. M., Williams, M. A. J., Krull, E. S. 2007. New radiocarbon dates from sapropels in three Holocene lakes of the Coorong coastal plain, southeastern Australia. *Australian Journal of Earth Sciences,* **54**(6).

Meyers, P. A., Ishiwatari, R., 1993. Lacustrine organic geochemistry – an overview of indicators of organic matter sources and diagenesis in lake sediments. *Organic Geochemistry*, **20**(7), 867 – 900.

Miall, A. D., 2014. Updating uniformitarianism: Stratigraphy as just a set of 'frozen accidents'. *Geological Society London Special Publications*, **404**(1).

Mishrat, P. K., Anoop, A., Jehangir, A., *et al.* 2014. Limnology and modern sedimentation patterns in high altitude Tso Moriri Lake, NW Himalaya - implications for proxy development. *Fundamental and Applied Limnology*, **185**(3-4), 329 348.

Mitsch, W. J., Bernal, B., Nahlik, A. M., Mander, U., Zhang, L., Anderson, C. J., Jørgensen, S. E., Brix, H. 2013. Wetlands, carbon, and climate change. *Landscape Ecology*, **28**, 583–597.

Moreno, A., Valero-Garces, B. L., Gonzoalez-Samperiz, P., Rico, M. 2008. Flood response to rainfall variability during the last 2000 years inferred from the Taravilla Lake record (Central Iberian Range, Spain). *Journal of Paleolimnology,* **40,** 943-961.

Moore, P. D. 1984. Classification of Mires: An Introduction. *Academic Press Inc. (London) Ltd.*

Moore P. D. 1995. Biological processes controlling the development of modern peat-forming ecosystems. *International Journal of Coal Geology,* **28**, 99-110.

Morris, P. J., Waddington, J. M., Benscoter, B. W., Turetsky, M. R. 2011. Conceptual frameworks in peatland ecohydrology: looking beyond the two-layered (acrotelm – catotelm) model. *Ecohydrology,* **4**, 1-11.

National Wetlands Working Group. 1997. The Canadian Wetland Classification System Second Edition. *Wetlands Research Centre,* University of Waterloo, Waterloo, Ontario.

Nelson, C. S., Lister, G. S. 1995. Surficial bottom sediments of Lake Taupo, New Zealand: texture, composition, provenance, and sedimentation rate. *New Zealand Journal of Geology and Geophysics*, **38**, 61-7.

Nelson, R. E., Carter, L. D., & Robinson, S. W 1988. Anomalous Radiocarbon Ages from a Holocene Detrital Organic Lens in Alaska and Their Implications for Radiocarbon Dating and Paleoenvironmental Reconstructions in the Arctic. *Quaternary Research*, **29**, 66-71.

Noakes, A. J. 1998. A study of the land use change and fire record of the Thirlmere Lakes area since European settlement as provided by the sediment record. *Hons Thesis, University of Wollongong.*

Nott, J., Young, R., Bryant, E., Price, D. 1994. Stratigraphy vs. pedogenesis; problems of their correlation within coastal sedimentary facies. *Catena*, **23**, 199-212.

Odson, J. R., Wilson, I. B. 1975. Past and Present Vegetation of Marshes Swamp in South-eastern South Australia. *Australian Journal of Botany*, **23**, 123-50.

Office of Environment and Heritage, NSW. 2012. Peat-forming bogs and fens of the Snowy Mountains of NSW. Technical Report. Viewed 10 October 2018, http://www.environment.nsw.gov.au/~/media/FA89572937B24945A9F9C8C926F51138.ashx.

Office of Environment and Heritage, NSW. 2016. The Mysterious Hydrology of Thirlmere Lakes. Viewed 17 July 2017. http://www.environment.nsw.gov.au/~/media/2255E00C3AC74E3A9985DA0202639E88.ashx

Office of Environment and Heritage, NSW. 2014. Thirlmere Lakes National Park Draft Plan of Management, viewed 18 July 2017. http://www.environment.nsw.gov.au/resources/planmanagement/draft/20140091ThirlmereLakesDraft.pdf

Osleger, D. A., Heyvaert, A. C., Stoner, J. S., Verosub, K. L., 2009. Lacustrine turbidites as indicators of Holocene storminess and climate: Lake Tahoe, California and Nevada. *Journal of Paleolimnology,* **42**(1), 103-122.

Page, K., Nanson, G., Price, D. 1996. Chronology of Murrumbidgee River palaeochannels on the Riverine Plain, southeastern Australia. *Journal of Quaternary Science,* **11**(4), 311-326.

Pemberton, M. 2005. Australian Peatlands: a brief consideration of their origin, distribution, natural values and threats. *Journal of the Royal Society of Western Australia,* **88**(3), 81-89.

Petherick, L., McGowan, H., Moss, P. 2008. Climate variability during the Last Glacial Maximum in eastern Australia: evidence of two stadials? *Journal of Quaternary Science,* **23**(8), 787-802.

Petherick, L. M., Moss, P. T., McGowan, H. A. 2011. Climatic and environmental variability during the termination of the Last Glacial Stage in coastal eastern Australia: a review. *Australia Journal of Earth Sciences,* **58**, 563-577.

Petherick, L., Bostock, H., Cohen, T. J., Fitzsimmons, K., Tibby, J., Fletcher, M. S., Moss, P., Reeves, J., Mooney, S., Barrows, T., Kemp, J., Jansen, J., Nanson, G., Dosseto, A. 2013. Climatic records of the past 30 ka from temperate Australia – a synthesis from the Oz-INTIMATE workgroup. *Quaternary Science Reviews*, **74**, 58 – 77.

Phillips, S., Bustin, M. R. 1998. Accumulation of organic rich sediments in a dendritic fluvial/lacustrine mire system at Tasik Bera, Malaysia: implications for coal formation. *International Journal of Coal Geology,* **36**(1-2), 31-61.

Proske, U., Stevenson, J., Seddon, A. W. R., Taffs, K. 2017. Holocene diatom records of wetland development near Weipa, Cape York, Australia. *Quaternary International,* **440**, 42-54.

Reeves, J. M., Barrows, T. T., Cohen, T. J., Kiem, A. S., Bostock, H. C., Fitzsimmons, K. E., Krause, C., Petherick, L. M, Phipps, S., & OZ-INTIMATE-Members. 2013. Global climate variability recorded in marine and terrestrial archives in the Australian region over the last 35 ka: an OZ-INTIMATE compilation. *Quaternary Science Reviews*, **74**, 21 – 34.

Rubensdotter, L., Rosqvist, G. 2009. Influence of geomorphological setting, fluvial-, glaciofluvial- and mass-movement processes on sedimentation in alpine lakes. *The Holocene,* **19**(4), 665–678.

Russell, G. N., Green, R. T., Spencer, J., Hayes, J. 2010. Thirlmere Lakes groundwater assessment. NSW Office of Water. Viewed 27 August 2018. http://www.water.nsw.gov.au/__data/assets/pdf_file/0003/548283/avail_ground_thirlmere_lake_report_draft.pdf

Robbie, A., Martin, H. A. 2007. The History of the Vegetation from the Last Glacial Maximum at Mountain Lagoon, Blue Mountains, New South Wales. *Proceedings of the Linnean Society of New South Wales,* **128**, 57-80.

Schulze, E. D., Nicolle, D., Boerner, A., Lauerer, M., Aas, G., Schulze, I. 2014. Stable carbon and nitrogen isotope ratios of Eucalyptus and Acacia species along a seasonal rainfall gradient in Western Australia. *Trees*, **28**, 1125–1135.

Smith, H. G., Hopmans, P., Sheridan, G. J., Lane, P. N. J., Noske, P. J., Bren, L. J. 2012. Impacts of wildfire and salvage harvesting on water quality and nutrient exports from radiata pine and eucalypt forest catchments in south-eastern Australia. *Forest Ecology and Management,* **263**, 160-169.

Swanson, D. K. 2007. Interaction of mire microtopography, water supply, and peat accumulation in boreal mires. *Suoseura – Finnish Peatland Society,* **58**(2), 37-47.

Stromsoe, N., Marx, S.K., Callow, N., McGowan, H.A. and Heijnis, H. 2016. Estimates of late Holocene soil production and erosion in the Snowy Mountains, Australia. *Catena,* **145**, 68-82.

Tallis, J. H. 1973. The terrestrialisation of Lake Basins in North Cheshire, with Special Reference to the Development of a 'Schwingmoor' Structure. *Journal of Ecology,* **61**(2), 537-567.

The Australian Soil Classification. 2018. The Second Edition of the Australian Soil Classification. Isbell and NCST 2016, Viewed 27 March 2018. http://www.clw.csiro.au/aclep/asc_re_on_line_V2/soilkey.htm

Thompson, C. H. 1992. Genesis of Podzols on Coastal Dunes in Southern Queensland. I. Field Relationships and Profile Morphology. *Australian Journal of Soil Research*, **30,** 593-613.

Thornhill, A. H. 2010. Can Myrtaceae pollen of the Holocene from Bega Swamp (New South Wales, Australia) be compared with extant taxa? *Altered Ecologies (Terra Australis 32)*, 405-427.

Tiffany, M. A. 2011. Epizoic and Epiphytic Diatoms. *The Diatom World*, *Cellular Origin, Life in Extreme Habitats and Astrobiology,* **19**, 195-209.

Tranvik, L. J*. et al.* 2009. Lakes and reservoirs as regulators of carbon cycling and climate. *Limnology and Oceanography,* **54,** 2298–2314.

Tweed, S., Leblanc, M., Cartwright, I. 2009. Groundwater-surface water interaction and the impact of a multi-year drought on lakes conditions in South-east Australia. *Journal of Hydrology*, **379**, 41-53.

Webb, M., Dredge, J., Barker, P.A., Mueller, W., Jex, C., Desmarchelier, J., Hellstrom, J., Wynn, P. M. 2014. Quaternary climatic instability in south-east Australia from a multi-proxy speleothem record. *Journal of Quaternary Science,* **29**(6), 589–596.

Williams, M., Cook, E., van der Kaars, S., Barrows, T., Schulmeister, J., Kershaw, P. 2009. The vegetation history of the last glacial-interglacial cycle in eastern New South Wales, Australia. *Journal of Quaternary Science,* **21**(7), 735 – 750.

Woodward, C. A., Potito, A. P., Beilman, D. W. 2012. Carbon and nitrogen stable isotope ratios in surface sediments from lakes of western Ireland: implications for inferring past lake productivity and nitrogen loading. *Journal of Paleolimnology,* **47**, 167–184.

Woodward, C. A., Shulmeister, J., Zawadzki, A., Child, D., Barry, L., Hotchkis, M. 2017. Holocene ecosystem change in Little Llangothlin Lagoon, Australia: implications for the management of a Ramsar-listed wetland. *Hydrobiologia*, **785**, 337–358.

Young, A. 2017. Upland Swamps in the Sydney Region. *Dr Ann Young*, Thirroul, NSW.

Young, A. R. M. 1982. Uplands swamps (dells) on the Woronora Plateau, N.S.W. *University of Wollongong (Hons) Thesis*.

Huang, C., Yao, L., Zhang, Y., Huang, T., Zhang, M., Zhu, A., Yang, H. 2017. Spatial and Temporal variation in autochthonous and allochthonous contributors to increased organic carbon and nitrogen burial in a plateau lake. *Science of the Total Environment*, **603**, 390 – 400.

APPENDIX A – Rainfall and Lake Level Graphs

Buxton weather station is located ~3 km away from Thirlmere Lakes, capturing local rainfall patterns. Ainslie weather station is located 200 km away from Thirlmere Lakes, and represents regional rainfall.

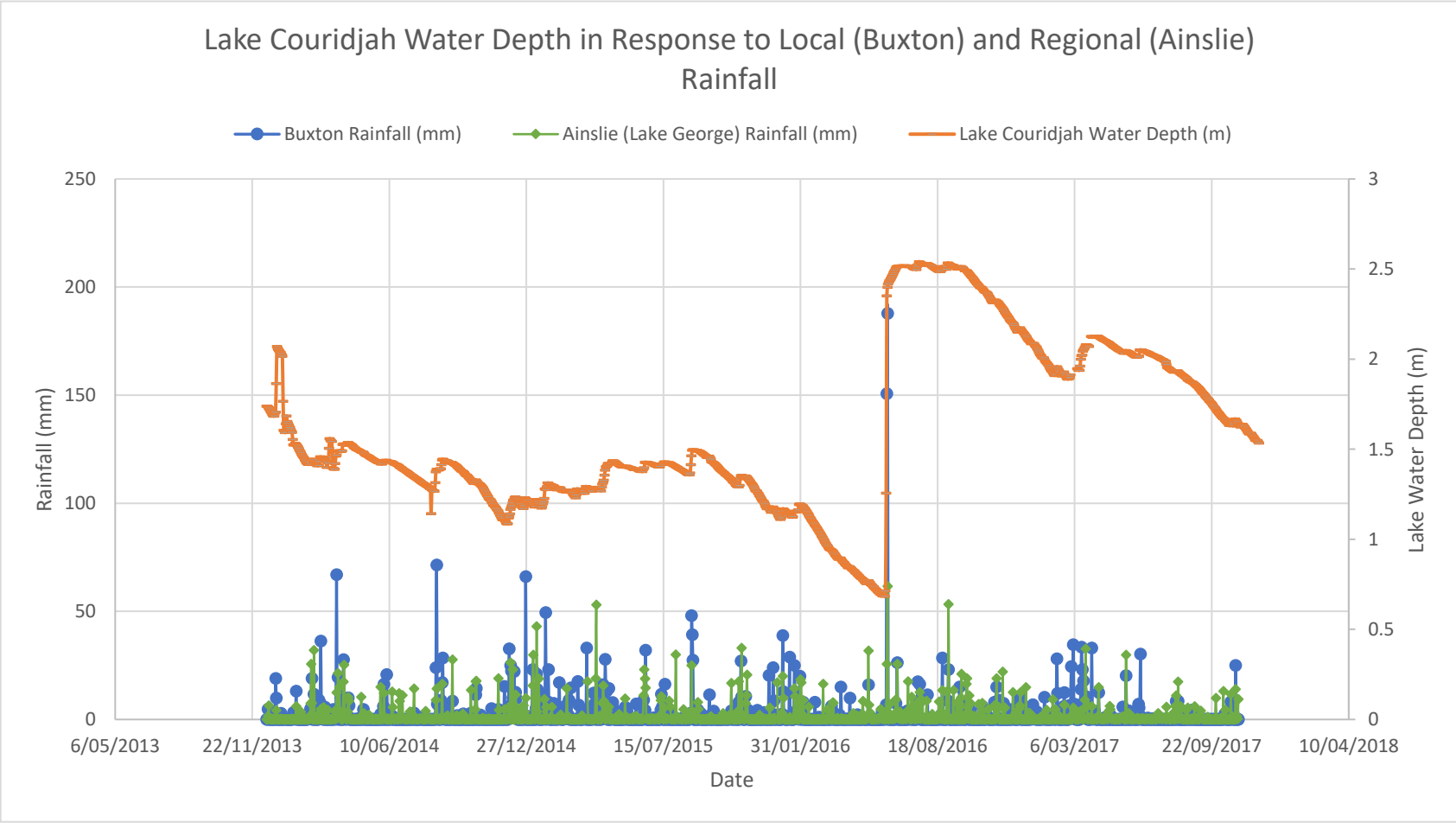

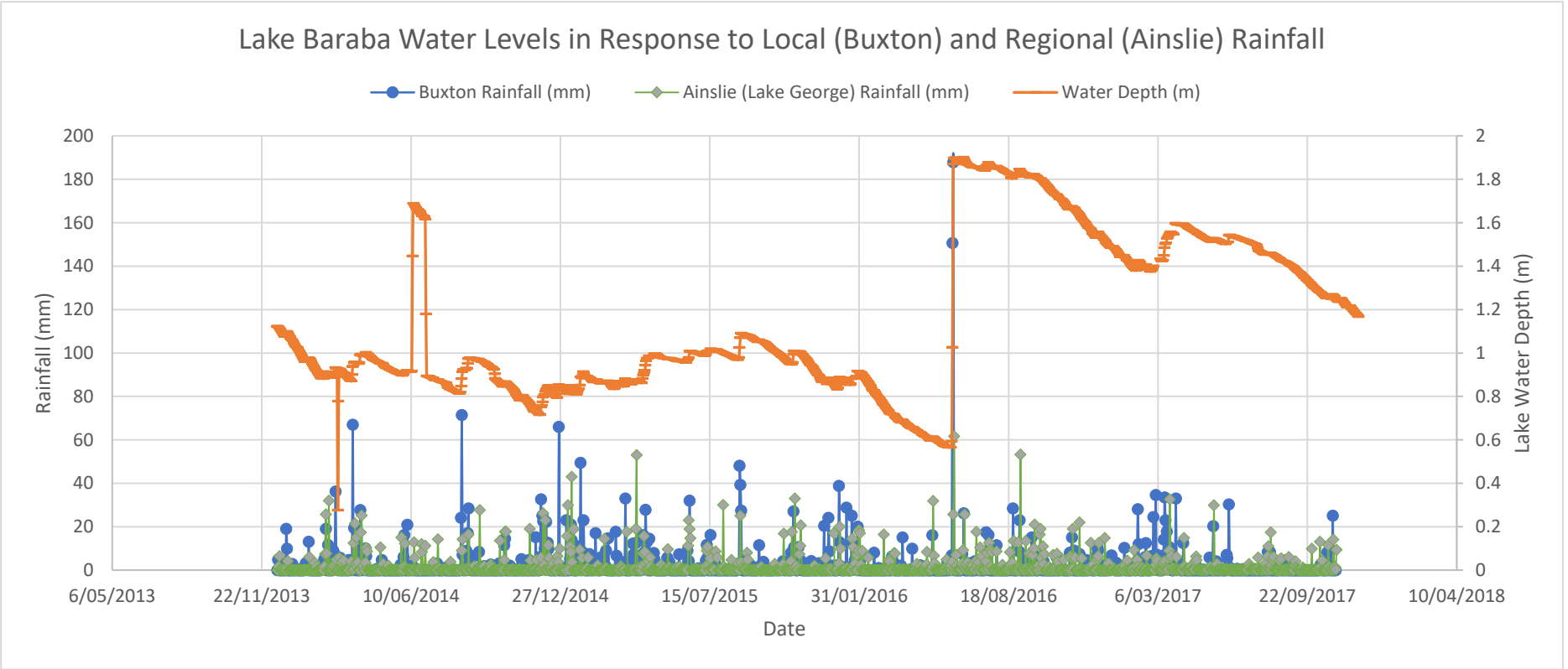
Lake Baraba Water Levels in Response to Local (Buxton) and Regional (Ainslie) Rainfall
Buxton Rainfall (mm)
Ainslie (Lake George) Rainfall (mm)
Water Depth (m)
Rainfall (mm)
Lake Water Depth (m)
200
180
160
140
120
100
80
60
40
20
0
2
1.8
1.6
1.4
1.2
1
0.8
0.6
0.4
0.2
0
6/05/2013
22/11/2013
10/06/2014
27/12/2014
15/07/2015
31/01/2016
18/08/2016
6/03/2017
22/09/2017
10/04/2018
Date

The following appendices (Appendix B – F) can be found on the supporting 'Appendices' followed on the thesis USB:

APPENDIX B – Core logs, grain size data and particle size distribution

APPENDIX C – LOI analysis

APPENDIX D – Radiocarbon dating reports

APPENDIX E – Stable C and N isotope data

APPENDIX F – ITRAX data